INTRODUCTION

1.1 Background of Study

Temperature is one of the important parameters to tell the condition of internal process, material and even quality of the desired output. A qualitative but accurate conclusion can be drawn by observing the temperature profile of any surface. Infrared cameras are such a non-contact type technique which provides a fast, reliable and accurate temperature profile of any surface (according to the field of application), and it can be used to make the world that invisible to human eye come to life [1].

This thesis deals with design and constructs of distinctive IR optical system in order to contribute in building and creating uncooled thermographic camera characterized by efficient, simplicity in the structure, and appropriate for civilian applications. Design and manufacturing of mechanical case in addition to establishment of PC thermal images processing software by using MATLAB programming language represent a complement to the thesis in the construction of hand held uncooled thermographic camera. The integration between IR optical system and thermal detector module through the mechanical case leads to build a thermal camera, addition of thermal image processing software to thermal camera leads to completion of thermographic camera. This camera is suitable for many civilian applications such as early detection of breast cancer as example of medical application, detection of overheated connections, oxidation of high voltage switches, tank level detection, detect of pipework fault, refractory and petrochemical installations, overheated motors, hot bearings, etc. as examples of industrial applications.

1.2 Literature Review

Modern thermal imaging technology evolved in the middle of the last century when the first single-element liquid nitrogen cooled detector and scanning systems which could be put to practical use, began to emerge from research institutions. Germany is leader in IR instruments, IR systems using single lead sulphide (PbS) detectors sensitive up to 2.5μm ware used by the German force as trackers in anti-aircraft searchlights guns. This was followed up with the development of lead selenide (PbSe) detectors sensitive in the 3~5μm, using deposited thin film technology [2].

Considerable efforts were made to design and develop military instruments like infrared search system, communication devices and image converters to enable night vision. Hudson [3], Jamieson et al [4], Wolfe [5], Holter [6], etc., have given a detailed historical background of the subject.

In 1952, the US army built the first thermograph using a 16″ searchlight reflector for optics, a two-axis optomechanical scanner, and a bolometer as detector. This was followed by the first long wavelength forward looking infrared (FLIR) built at University of Chicago in 1956 with the support of American air force. Subsequently, a ground based thermal imagers was designed and developed by Perkin Elmer (PE) Corporation of USA in 1960. Between 1960 and 1974, six different types of thermal imagers were developed and product in bulk, using detector of doped germanium and silicon alloys cooled to 77K. An imager based on mercury doped germanium was the first practical IR system sensitive in 8-14μm. this was followed by the development of mercury cadmium telluride (MCT) detector cooled to 77K for 8-14μm region [2].

Parallely, the Soviet navy launched a missive program to detect ships by means of their thermal signatures. A paper titled *thermal imaging*, essentially a report on coastal thermal direction finders and thermal viewing in industry and medicine, was presented at the 15th Academician D.S. Rozhdestvenskii lectures by M.M. Miroshnikov [7]. This report carried some unique thermal photographs (thermograph) that of the trace left by the prone body of a man on a wooden floor, taken some 30 minutes after the man had left. The thermal trace allowed one to recognize the shape of the man's body. This was achieved by virtue of high sensitivity of thermal viewer equal to 0.03ºC at background temperature of 20ºC.

The method and techniques of designing, developing and utilizing thermal imagers reached a high degree of perfection in 1970s [8].

In order to enhance the number of detector beyond 180 pixels and thereby achieve longer ranges, Hughes (USA) entered into the design and fabrication of hybrid (2D) detectors. Almost parallely, in the beginning of the eighties, second generation IR detectors known as IR focal plane arrays (IRFPA) appeared in France [2]. However, focused efforts for developing second generation detector FPA began in the late eighties with the arrival of MCT detectors having 240×4, 288×4, 440×4 elements developed for the long wave IR (8~12 µm) based on hybrid technology[2]. This opened up the gates for 2nd generation high performance thermal imagers, which have been frequently employed in missile for target acquisitions with new designs for several advance IR seekers. At the same time, medium format 320×240 elements 2D arrays detectors were also being developed for the middle wave infrared (3~5µm). During late eighties in 1994, Honeywell and Texas Instruments introduced uncooled microbolometer and pyroelectric technology, respectively [2]. Thermal camers based on both pyroelectric

and microbolometer technologies are available now for non-military applications. Thus, a new era of thermal technology was born and for the first time thermal imaging has now expanded to be used in firefighting, law enforcement, industrial applications, security, transportation and many other industries.

One way of increasing the range of identification equipment is by increasing resolution and sensitivity of cameras by employing multispectral detection and correlating images in different wavelengths. This is possible with large 2-D FPA using staring array (3^{rd} generation thermal imagers), working with this technology (3^{rd} generation or large format and dual colors imagers) finally become available at a tight ranges around the world as latest technologies in thermal imaging [2].

1.3 Research Problem

Despite the importance and effectiveness the thermal cameras in a large numbers of vitality civilian applications, it's relatively absence from these applications across the country, this is due to the lack of a specialist platform for launching this technology internally. In addition to the price of these cameras when imported from aboard as an integrated system is relatively high and that for the privacy of optical systems (IR optical system) and detectors (thermal detector).

1.4 Objectives of the Research

The focus will be on the design of high performance, compact structure (small volume, light weight) and low cost IR optical system, and then design of simple IR image processing software (PC software) and simple mechanical case to do the main objectives of the research which represented in:

1- Constructing simple and efficient thermal camera to work at night and day with the same efficiency.

2- Adding the PC software to the thermal camera to convert it to thermographic camera for the purpose to read the temperature of any object from its thermographic image at any condition (day, night, and bad weather).

1.5 Research Significance

- The importance of this study comes from features and specification of the IR optical system which was designed (high performance, small size, light weight, simple structure and low cost) and its contribution in the production of a high-performance thermal camera at low-cost, because the IR optical system in addition to thermal detector plays a key role in determining both the performance (quality) and cost of this type of cameras.
- Providing a solution to the problem of night vision.
- Contribute in starting for create local platform to this important and vital technology (thermal imaging).

1.6 Outlines of the Thesis

Chapter one is an introduction of thesis, it presents: the background of study, literature review, problem statement, objectives of research, research significance and outlines of the thesis.

Chapter two dedicated to talk about thermal imaging in general, and elements of thermal imaging camera. The rest of the chapter deals with basics of IR optics, that's because the design of IR optical system is core of this project. IR image-forming optical system, factors affecting the image quality (diffraction& aberrations), performance evaluation of the optical system, special optical surfaces which faced us in this design, IR optical material with focus on optical material which used in this work (germanium), All these topics were covered in the chapter.

The third and fourth chapters are the backbone of the thesis.

Chapter three concentrates on the design of IR optical system which starts by definition of detector module which will be used in construction of the optical system and thermal camera, design criterion to arrive at criteria for an optimum performance, basic design required to the optical design, brief features and definition of the optical design software Zemax which is used in design and construction of the optical system and the steps will followed in design phase of optical system, until arrived to final design phase. In addition to creation of thermal image processing program which is used to convert gray image to pseudo color image and read the temperature of the object from that image, and design and manufacturing of the mechanical case to assemble the components of thermal camera.

Chapter four focuses on dissection and analysis of the results obtained from previous chapter (chapter three). Starts with general specification and evaluation of the constructed optical system, tolerance analysis, solve of defocus treatment, and integration between designed IR optical system (after manufacturing) and thermal detector module through designed and manufactured mechanical case which was designed and manufactured. In addition to IR images processing software which is used to convert the thermal camera to thermographic one by converting thermal images of the thermal camera to thermographic images, and concludes with conclusion and recommendation (future work).

A list of references is shown at the end of the thesis.

BASIC CONCEPTS OF THERMAL IMAGING

2.1 Introduction

This chapter dedicated to deal with basic concepts of thermal imaging, including the thermal and thermographic imaging in general, elements of thermal imaging system. Because the design of high performance, simple structure and low cost of IR optical system is the core of this project then rest of the chapter will be devoted to talking about IR image-forming optical system, factors affecting the image quality with a focus on primary aberration and correction of it because the main task of the optical designer in design of any optical system is reducing the aberration as much as possible, Image quality and performance evaluation to evaluate the optical system and estimate the quality of its images, definition and effect of some special optical surfaces that face us in our design like conic surfaces and plane parallel plate, general overview to some famous and common IR optical materials with focusing on germanium as primary/basic optical material in this project.

2.2 Thermal Imaging

The thermal imaging is the remote sensing and display of the spatial and time varying intensity of infrared radiation emanating from a scene by virtue of temperature and emissivity difference among its constituent. Thermal cameras are based on Infrared (IR) technique, the principle underlying this technique is that every object (all materials) has a temperature above absolute zero (-273°C) emits certain amount of IR energy, even objects that we think of as being very cold such as ice cubic's emit IR radiation and the intensity of this IR radiation is a function of temperature and emissivity, thermal camera records the intensity of radiation in the IR part of electromagnetic spectrum and

converts it to a visible image, because the human eye only responds to radiations extending from 0.4µm to 0.75µm, and is insensitive to infrared radiation and unable to see and extract information about an object encoded in its thermal radiation. The techniques of thermal imaging, like that of the human eye and other sensors like photographic films, plates and photoemissive devices. A suitable optical system is used to capture and focused the radiance, either reflected and/or emitted, by an object or a scene. The optics forms the image of captured radiance filed across a suitable transducer (IR sensor) that convert the radiance to electrical signal. The electrical signals, after suitable processing translate into an image that can be viewed in viewfinder or on a standard video monitor or other screen. A thermal imager, identical in many respects to a home video camera, is capable of capturing this information and converting it into visual images that can be seen by human eye. But the basic difference between the two cameras is that a thermal imager responds to the long wavelength radiation beyond 3µm instead of the short wavelength of the visible light. Therefore, the thermal imagers employ camera optics transparent in thermal bands. The optical glass, which is not transparent to radiation beyond 2µm, is not used as IR optical material. The sensors used are made of material sensitive to infrared radiations [2].

Due to thermal imagers its reliance on variation of self-emitted radiation of scene contents rather than reflected radiation. It is superior to conventional cameras in many respects. They extend vision beyond the visible region by using longer wavelength radiation. They can operate both in day and night conditions and in total darkness. They can operate in poor or bad weather conditions i.e., they can penetrate smoke, dust, fog and light rain. Thermal imagers have much higher detection ranges than low-light-level TV (LLL TV) and image-intensifier-tube based

systems because they are not dependent on external light source and they penetrate atmospheric obscurants better. They can reveal details which the human eye and low-light imagers cannot, e.g., whether a vehicle engine is running or not, whether someone had occupied a chair sometime ago or not, etc. daylight, low-light-level sensors and image-intensifier-tubes based systems can be blinded by searchlight and normal camouflaging possible, in thermal systems camouflaging of temperature and emissivity impact very difficult.

Thermal imaging is generally considered to be in the medium or mid wave IR (MWIR) that extends from 3 to 5µm and in long wave IR (LWIR) that extends from 8 to 12µm in this wavelength bands we are looking at thermal or heat rather than visible light [9].

Today the applications of thermal imagers fall under these main board categories (could expand/increase): military and paramilitary, commercial, medical, remote sensing, astronomical and scientific [8].

The applications of thermal imagers and Their use is limited only by the imagination of the user's and depends on the operator's understanding of principle of heat transfer and their applications in the fields in which they are working. Therefore the applications of thermal imagers could expand/increase depending on user requirements.

2.2.1 Thermographic Imaging

Infrared thermography is the science of transforming an infrared image into a radiometric one, which allows temperature values to be read from the image. So every pixel in radiometric image is in fact a temperature measurement. In order to do this, complex algorithms are incorporated into thermal imaging camera to convert the thermal (gray) image to pseudo (flash) color image depending on the conversion of intensity of IR radiation (amount of temperature) that appears in thermal image to several colors according to the amount of temperature and the amount of

temperature at any point in the target according to the apparent colors will be illustrated and reads from that image [10].

Thus, the thermographic camera is a thermal camera plus thermal image processing software to convert the output of thermal camera (thermal/ gray image) to thermographic image (flash color image) in order to improve visibility and read the temperature to any point in the target which was imaged (depending on application and use of thermographic camera) from the image of it. Therefore IR thermograhy is the temperature profiling of a surface or point. And it can be used to make the world that is invisible to the human eye (thermal world) come to life; basically it's a graphical representation of heat. This technology allows operators to validate normal operations and, more importantly, locate thermal anomalies (abnormal patterns of heat invisible to the eye) which indicate possible faults, defects or inefficiencies within a system or machine asset; this makes the thermographic imaging camera a perfect tool for many civilian applications. An example of these applications:

- Electrical inspections: examples of failures in high-voltage and low-voltage installations and equipments that can be detected with thermographic images are hot/overheated connections, failing components, overloaded circuits, oxidation of high voltage switches, insulator defects, high resistance connections, and corroded connections, internal fuse damage, internal circuit breaker faults.
- Mechanical inspections: examples of mechanical faults that can be detected with thermographic imager are overheated motor, overloaded pumps, hot bearings, suspect rollers, lubrication issues.

These and other issues (electrical &mechanical inspections) can be spotted at an early stage with a thermographic camera. This will help to prevent costly damages and to ensure the continuity of production.

- Pipe work: leakage in pumps, pipes, and valves, insulation breakdown, pipe blockage. All types of leakage, blocked pipes and faulty insulation will clearly show up in the thermal image. And because a thermal image can quickly give an overview of an entire installation, there is no need to check each pipe individually.
- Building: used to make sure from thermal envelope, moisture in roof, air leakage, and roof leaks so as to increase the cooling and heating efficiency in buildings.
- Medical application: the medical application are many such as early detection and identification of breast cancer, measurement of skin temperature, heat therapy, obtaining information about the features of transitional temperature processes, etc.
- Inspection of aeronautical material: predictive maintenance of air craft tires [10].

These are just examples of thermographic cameras applications, and as we have said previously the applications list for thermal and thermographic cameras always depend on the operator's understanding of principle of heat transfer and their application in the field in which they are working.

The following points spell the advantages of using this technique (IR thermography) in general:

- It is a contactless, non-destructive and non-intrusive technique (uses remote sensing). This means keeping the user out of danger, and does not intrude upon or affect the target at all. Therefore, compiles with legislation or insurance requirements.

- It is two dimensional; therefore a large surface area can be scanned in no time. With an IR thermographic camera we are able to measure the temperature on the entire image not at one single spot as thermometers. This means use thousands (exactly equals to the resolution of camera -number of pixel-) of IR thermometers at same time.
- The result of this technique was presents in image format form for analysis. Then the results relatively easy to interpret and it can be stored for later image processing and analysis.
- Requires very little skill for monitoring.
- Identifies and locates thermal anomalies.
- It is real time; enables capture of fast moving targets, and enables of fast changing thermal patterns.
- Due to mobility of most IR cameras they can be made available at any time and at any place.
- Addresses numerous applications.

Disadvantages of IR thermography:

- Cost of instrument relatively high.
- It is unable to detect the inside temperature if the medium is separated by a non-transparent for IR radiation medium such as glass/polythene material or other cover. For this reason it's a surface method to evaluate the results according chosen application [1].

2.3 Elements of Thermal Imaging System

A typical scenario for thermal imager is shown in figure (2.1). It consists from many subsystems each of which processes information differently. With exception of target and atmosphere each of the remaining from figure (2.1), exactly the optics or IR optical system, the thermal detector,

electronics, signal processing, and in sometimes the display represents the subsystems that forming the thermal imaging system itself.

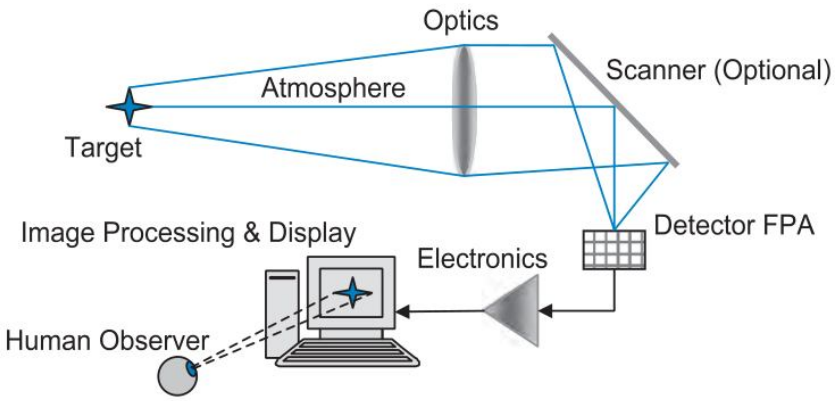

Figure (2.1): Basic element of thermal imaging system [11]

The target is the object of interest; usually the real reason for the existence of the system, the system may be designed to detect the presence of the target, to track it as it moves, to glean information leading to its identity, or to measure its temperature [3].

All bodies above the temperature of absolute zero emit IR radiation energy according to plank's low. A hotter object corresponds to higher electromagnetic or, in this case, optical power emission leaving the object. The emissive surface characteristics of a radiating object determine the spectral emission weighting of the light [12].

Targets (IR sources) of general interest can be classified into four board categories as shown in figure (2.2).

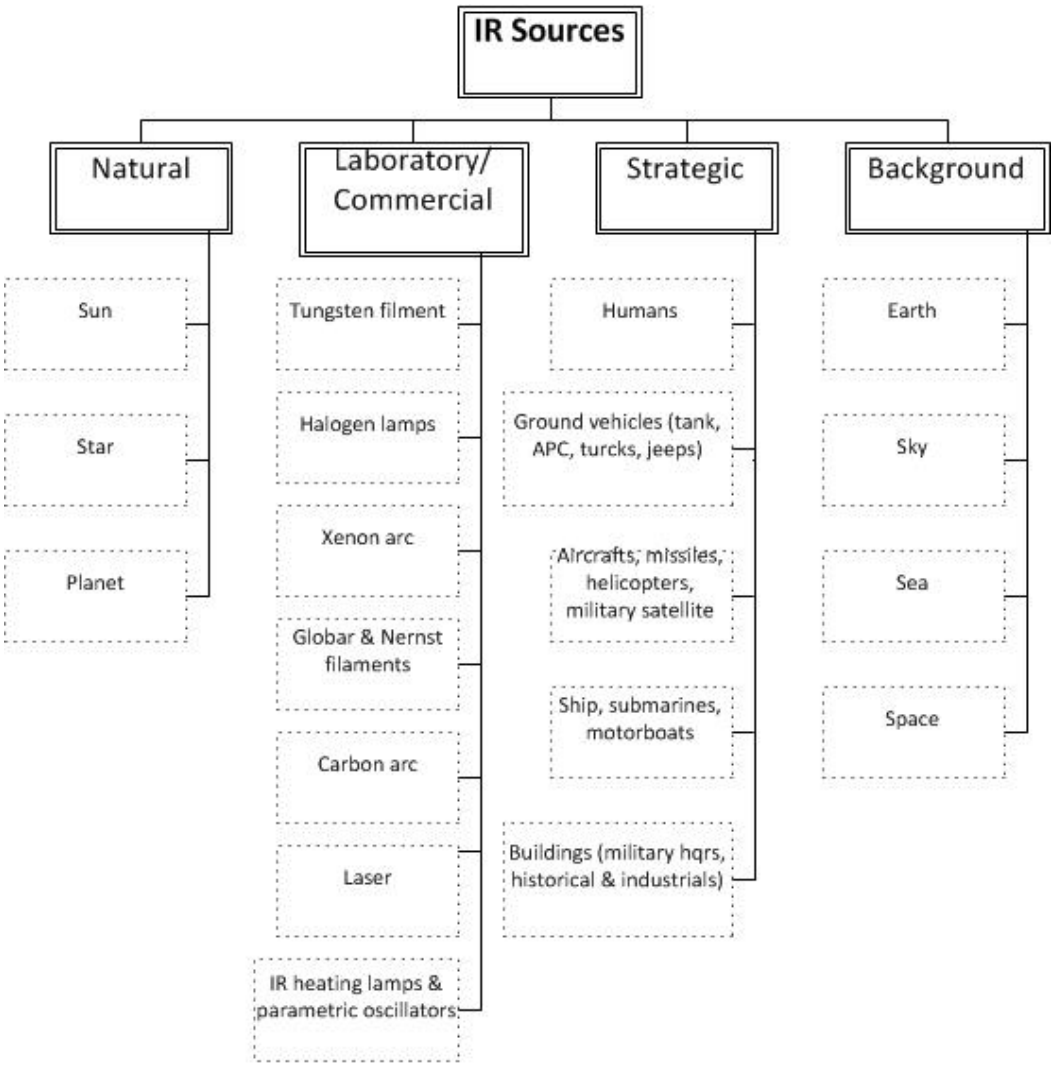

Figure (2.2): Types of infrared sources [2]

The thermal imaging cameras designed to deal with strategic sources as targets to be imaged by thermal camera. And dealing with any type/kind of targets depends on the application of the thermal imager. In thermal imaging the field targets could be classified into five categories depending on the applications of thermal imagers. In figure (2.3) these types of field targets are shown.

The infrared energy emitted from scene (target and background) propagates through the atmosphere. If the radiation from target passes through any portion of earth's atmosphere, it will be attenuated because the atmosphere is not perfectly transparent [3]. It degrades both the amplitude and the phase of IR energy. These effects manifest themselves

as reduction in information content of the signal and then reduce the performance of a thermal imager. In addition, particles in the atmosphere reflect unwanted stray light into sensor. The variation of atmospheric transmission with wavelength is plotted in the lower part of the figure (2.3).

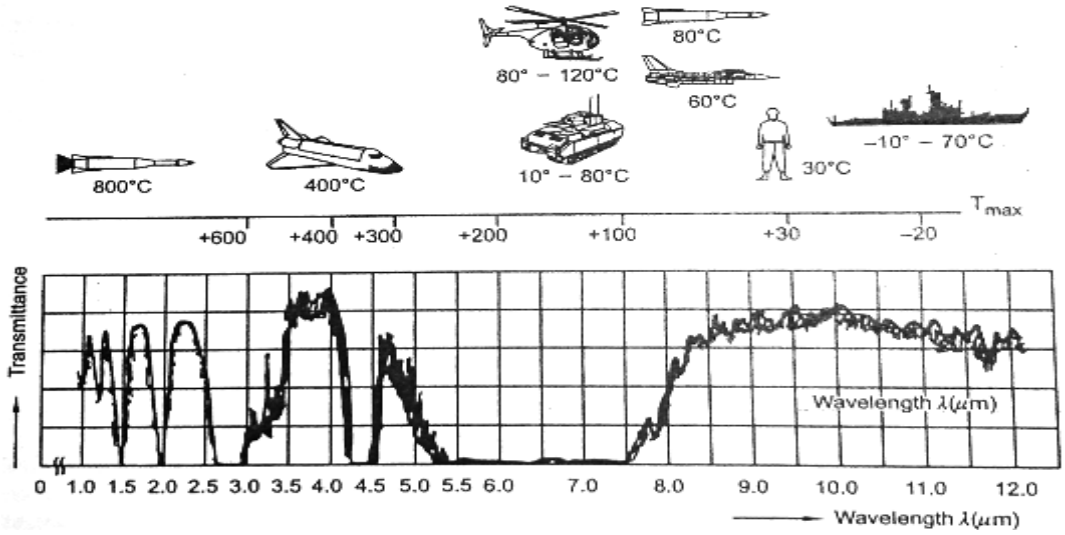

Figure (2.3): Various field/strategic targets [2]

The optics (IR optical system) collects and focused the light (IR energy) that emitted from scene (target, background, and any stray atmospheric) and imaged that scene onto IR detector plane, or it forms the image of captured radiance field across suitable transducer/ IR detector(s).

The detector transforms portion of IR energy into electrical signals that represent the spatial distribution of the flux amplitude leaving the scene. The detector system may be a staring array (FPA), a linear array, or a single detector. The staring array/ FPA is latest technology of thermal imaging detector, it is a tow-dimensional arrangement of detectors (pixels) and it does not require scanner to create an image from any scene, for this reason it so called staring array, and a linear array is a column or a few columns of detectors. In a linear array system, a scanner moves the image across the detectors. For a signal-detector system, a two-dimensional scanner moves the image across the detector in both

the horizontal and vertical dimensions to scan the scene and drop his image on the detector. The detector represents the heart of an imaging system because it converts the scene radiation into measurable electrical signal [8]. All optical design considerations start from the type of detector available to the system designer.

Each detector (pixel) will have its own amplifier to amplify the detector output (electrical signal). The amplifier outputs are multiplexed together and then digitized. The number of channels multiplexed together depends upon the specific design (number of detectors/pixels). System may have several multiplexer and several A/D converters operating in parallel. Signals are digitized because of relative easy to manipulate (process and enhance) digital data which will intervene in the formation of the IR image [2]. Amplification and signal processing after suitable processing creates an image in which voltage differences represent scene intensity difference due to the various objects the field of view.

Then the electronic output signal can then converted/translated into optical signal that can be displayed or viewed in the viewfinder or on a standard video monitor or LCD screen [12]. The monitor may or may not be an integral part of thermal imaging system.

Most or whole of the modern thermal imaging detectors (FPA) today comes accompanied with a number of electronic boards as the form of single module. In other words the detectors (sensitive area/ pixels) and detector electronics (preamplifier, amplifier, signal processing, image reconstruction, etc) comes as single and integrated unit.

2.4 IR Image-Forming Optical System

The purpose of virtually all image-forming optical systems (visible, IR, ...etc) is to resolve a specified minimum-sized object over a desired field of view. The field of view is expressed as the spatial or angular extent in

object space, and the minimum-sized object is the smallest resolution element which is required to identify or otherwise understand the image [9].

In more details there are four basic goals in design of an IR optical system. The 1st goal is to maximize overall system performance. The 2nd goal is to maximize the resolving power for desired task while maintaining good coverage area. The 3rd goal is to increase the amount of radiated energy/image flux that is collected from scene contents (target and background) and project the image of the scene onto system detector array, and the 4th goal is to minimize overall system complexity, cost and weight [12].

The optical systems play a key role in defining some of the overall system parameters like system resolution, system field of view, and system prediction range. For this reason the optical system is one of the most important subsystems in the construction of any camera [12].

IR optical systems has become choice for services and paramilitary forces over Image Intensifier Tube based passive night sights as they offer long ranges and better see through capability [13].

On the one hand designing lenses (optical systems) for infrared region is in some ways easier than working in the visible spectrum, since the wavelengths are longer, the index of refraction of most lens materials is higher, their relative dispersion is lower, and the diffraction limit is ten to twenty times larger in infrared than in the visible region. This generally results in smaller primary aberration [14]. But on the other hand designing of IR optical system featuring by other critical considerations not considered in other design type of optical imaging system such as: pixel size V/s diffraction spot, IR materials of lenses is rare and limited and expensive, vignetting, cold shield efficiency, and thermalization etc,

these additional factors make the design of IR optical system more complex [13, 14].

Optical design remains a rapidly developing field due to the increased performance demands, improved software and computing platforms for modeling, better algorithms, and new technologies for better performance.

2.5 Factors Affecting the Image Quality (Diffraction& Aberrations)

Image quality of any designed optical system is never perfect! It is limited by geometrical aberrations, diffractions, the effects of manufacturing and assembly error, and other factors. While it would be very nice if the image of a point object could be formed by the optical system as a perfect point image, in realty and from optical point of view the quality of the final image degrade by either geometrical aberration and/or diffraction. Figure (2.4) illustrated the situation. The top part of the figure shows a hypothetical lens where you can see that all of the rays do not come to a common focus along the optical axis. Rather, the rays entering the lens at its outer periphery cross the optical axis progressively closer the lens than those rays entering the lens closer to the optical axis. This is one of the most common and fundamental aberrations, and it know as spherical aberration. Geometrical aberration aberrations are due to the failure of lens or optical system to form perfect geometrical image [9].

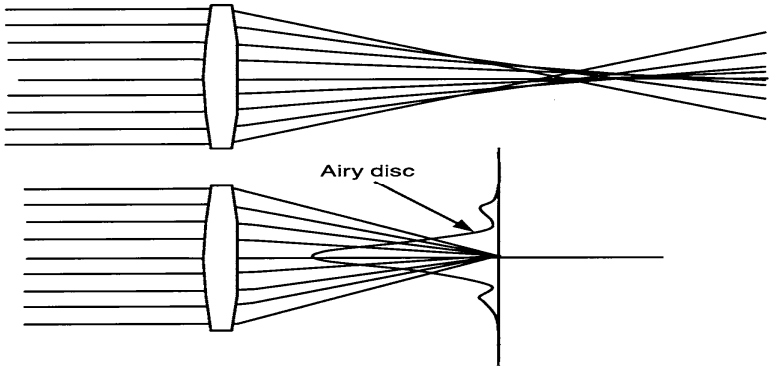

Figure (2.4): Image quality, geometrical aberration (top) and diffraction limited (bottom) [9]

If there were no geometrical aberration of any kind, the image of a point source from infinity is called an Airy disk. The profile of the Airy disk looks like a small Gaussian intensity function surrounded by low-intensity rings of energy as shown in figure (2.4) [9].

If we have a lens system in which geometrical aberrations are significantly larger than the theoretical diffraction pattern or blur, then we will see an imaged dominated by the effect of these geometrical aberrations. If, on the other hand, the geometrical aberrations are much smaller than diffraction pattern or blur, then we will see an image dominated by the effect of the Airy disk. This form of optics is called diffraction-limited optics [9].

Optically (from optical point of view), two processes contribute to the size and position of the blur circle and hence quality of the image formed by any optical system; these are diffraction, which is consequence of wave nature of radiant energy, and aberration, which depend on the geometrical arrangement of the optical surfaces and on the dispersion of the optical materials. Aberrations can be controlled by the optical designer; indeed, his main task in any design to reduce them less than the specific values. Diffraction, on the other hand, is physical limitation over which he has no control because of wave nature of electromagnetic radiation. Even in the absence of aberrations,

diffraction still causes a point to be imaged as blur circle. Such optics are said to be diffraction limited, they represent the ultimate in optical performance [3].

2.5.1 Primary Aberrations

It is the function of a lens (optical system) to collect light from a point on the object and to focus that light to a corresponding point (a conjugate point) on the image. In nearly every case the lens will fail at this task, in that there will some residual error in the precision with which the lens collects, refracts, and focuses that light. Rather than a true point image, the lens will produce a blur circle, i.e., spot. It is the function of the lens designer to ensure that this spot size is sufficiently small to allow the lens to produce the required resolution, or image quality. These errors in the lens's ability to form a perfect image are referred to as lens aberration [15].

In general, the optical aberrations are deviations of an image point from its ideal position or it failures of the optical system to produce a perfect point image of a point object as a consequence of the laws of geometrical optics and not because of faulty optical manufacturing [8]. Or, optical aberrations occur when points in the image do not translate back onto single point after passing through the lens – causing image blurring, reduced contrast or misalignment of colors (chromatic aberration). Lenses (optical system) may also suffer from uneven, radially decreasing image brightness or distortion. All of These factors have a much impact on the final image quality. Then, aberrations are the main factors from optical point of view that affecting the performance of an optical system and then the performance of any imaging devices.

Third-order theory predicts seven types of aberrations, these types' called 3rd order aberrations (primary aberrations)

- Spherical aberration

- Coma
- Astigmatism
- Field curvature
- Distortion
- Axial chromatic aberration
- Lateral chromatic aberration

Once can separate these aberrations by general categories. The first five types (spherical aberration, coma, astigmatism, field curvature, and distortion) listed deal with monochromatic radiation and called *monochromatic aberrations*, occur even though only a single wavelength is involved. The last two (axial chromatic aberration and lateral chromatic aberration) address polychromatic effects and called *chromatic aberrations*, are caused by variation in the index of refraction of the lens material with wavelength. Sometimes the categories are split between on-axis and off-axis aberrations. By this definition, spherical and axial chromatic aberrations are *on-axis aberrations* because they refer to object points located on the optical axis (the system axis of symmetry). The rest (lateral chromatic aberration, coma, astigmatism, field curvature, distortion) are *off-axis aberrations* [14].

Each one of these types of aberrations has quantitative impact on the quality of the image that formed by the optical system, then the relationship between aberration and image quality is very hard; we can improve/enhance optical system and then image quality by correcting/reduce the aberrations. In a well corrected optical system the designer has worked hard to reduce the aberrations so that the imagery will be limited by diffraction. It has been noted that many infrared applications do not need such excellent correction. Recognizing this, the system engineer should insist that the optics not be over designed; correcting each design to the diffraction-limit May satisfying in the

optical designer, but it can play havoc with the project budget [3]. With a well-chosen combination of optical parameters such as lens shapes, diameters of optical element, number of optical elements, and material of optical element, aberration in real optical systems with large ray angle can be reduced to a minimum or may be able eliminated to the level of the diffraction limit or any acceptable level [9]. And this is the main task of any optical engineer/designer.

Because the main task of the optical designer in design of any optical system is to reduce the aberrations as much as possible. And better designed optical system has smaller aberrations, but aberration can never be completely eliminated, just reduced. Therefore we will talk about aberrations under separate subtitle.

By understanding the basic characteristics of these seven primary aberrations, the optical engineer will be better equipped to specify and evaluate the image quality of a lens or an optical system [15]. The following paragraphs will describe the seven primary aberrations and discuss the more important characteristics of each.

2.5.1.1 Spherical Aberration

Spherical aberration is the most important of all primary aberrations, because it affects the whole field of a lens. The name of this aberration comes from the fact that it is observed in most spherical surface, reflecting or refracting [16].

Spherical aberration can be defined as the variation of focus with aperture. Figure (2.5) is a somewhat exaggerated sketch of a simple lens forming an image of an axial object point a great distance away.

Notices that the rays close to the optical axis come to a focus (intersect the axis) very near the paraxial focus position. As the ray height at the lens intersect, the position of the ray intersection with the optical axis (focus) moves further and further from the paraxial focus.

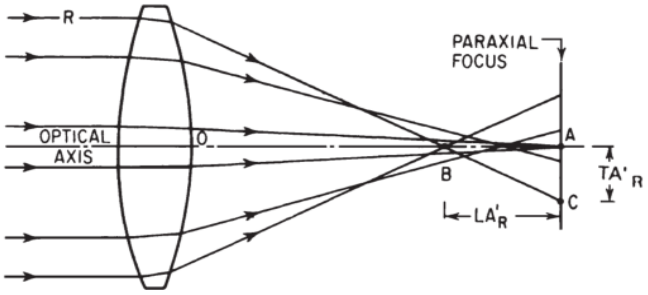

Figure (2.5): Spherical aberration (the rays farther from the axis are brought to a focus nearer the lens) [17]

The distance from the paraxial focus to the axial intersection of ray is called longitudinal spherical aberration. Transverse, or lateral, spherical aberration is the name given to the aberration when it is measured in vertical direction. Thus, in figure (2.5) AB is the longitudinal, and AC is the transverse spherical aberration of ray R [17].

Quantitatively, spherical aberration depends on three factors:

I. Height of the ray in the entrance pupil (aperture).
II. Diameter of entrance aperture for a given focal length.
III. For a given *f/number*, spherical aberration is a function of object distance and lens bending.

Spherical aberration can be controlled in two ways: (a) by bending as shown in figure (2.7) and (b) by splitting the optical power among several elements as shown in figure (2.6). This shows the impact of using larger number of lenses alone.

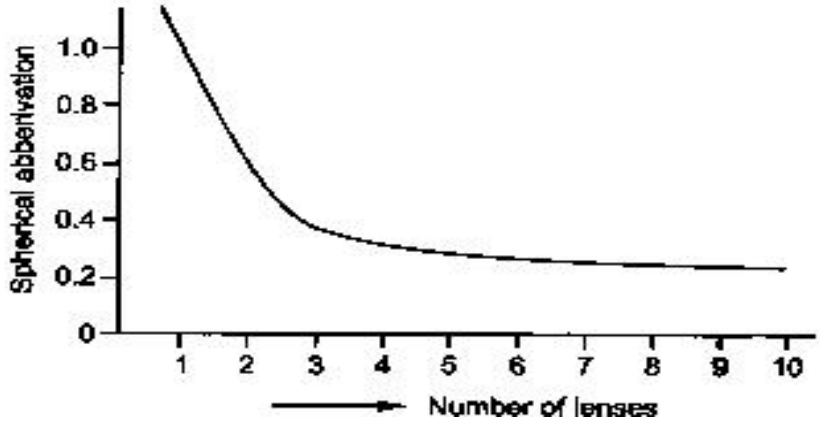

Figure (2.6): Spherical aberration correction using a number of lenses [8]

To control spherical aberration, some of the following steps may be adopted:

1- A single lens give minimum spherical aberration when:

$$s = \frac{2(n^2-1)p}{(n+2)} \qquad (2.1)$$

Where the shape factor $s = R_1 + R_2/R_1 - R_2$, and the position factor $p = (v + u)/(v - u)$.

For an equiconvex or equiconcave lens, $r_1 = -r_2$ and s= 0. For a plane surface, $r_1 = \infty$ and if the second surface is convex or concave, then s= -1. If the second surface is plane s= +1. Similarly, when p = -1, the incident beam is plane, and when p = +1, the emergent beam is plane, when p = 0, u = -v. in other words when either $u = \infty$ or $v = \infty$, the best form is Plano-convex lens and when u=v, the best form is symmetric curvature [8].

The changing of the lens shape is called lens bending. It is a powerful basic tool, because the shape of the lens affects spherical aberration and coma but not its focal length. The dependence of spherical aberration on the shape for a most common IR material [germanium lens (N = 4)] is illustrated in figure (2.7) [14].

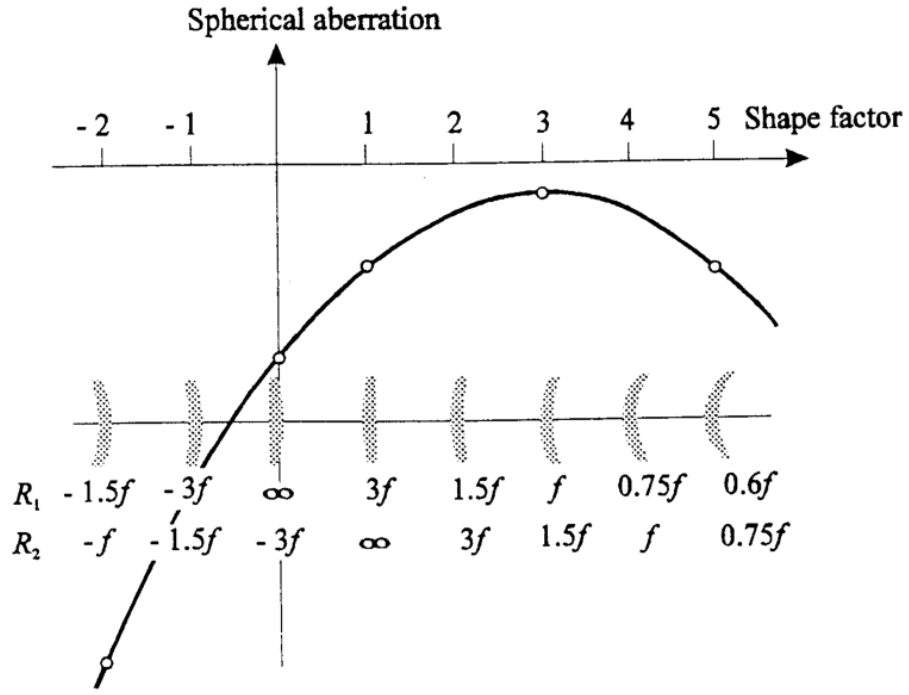

Figure (2.7): Change of spherical aberration with change of lens shape (lens bending) for a germanium lens with index n=4. Minimum spherical aberration is obtained in this case when the first radius of the lens is equal its focal length and the second radius is 1.5 times the focal length (s = 3) [14]

The best shape for singlet lens made from any material to obtained minimum spherical aberration is:

$$R_1 = \frac{2(n+2)(n-1)}{n(2n+1)} f \qquad (2.2)$$

$$R_2 = \frac{2(n+2)(n-1)}{n(2n-1)-4} f \qquad (2.3)$$

Table (2.1) show the minimum spherical aberration for singlet lens made from different optical materials.

Table (2.1): Minimum spherical blur spot sizes for singlet made from different material [14]

Material	**Refractive index (*n*)**	R_1	R_2	**Blur spot size in radian** (β_{spher} *in radian*)
Glass	1.5	*0.583f*	*-3.5f*	$0.0670(f/number)^3$
Zinc selenide (ZnSe)	2.4	*0.885f*	*2.406f*	$0.0187(f/number)^3$
Silicon (Si)	3.4	*0.997f*	*1.649f*	$0.0108(f/number)^3$
Germanium (Ge)	4	*1.0f*	*1.5f*	$0.0087(f/number)^3$

It is easy to remember that the best shaped thin germanium lens (shaped for minimum spherical aberration) has a front radius equal to its focal length and a rear radius is 1.5 times it focal length (see also figure (2.7)). The advantages of using a high-index materials like silicon or germanium is quiet apparent from table (2.1) [18].

2- If the lens material has high refractive index, then the radii R_1 and R_2 of the lens surfaces are taken to be as large as practicable.
3- Lens surfaces can be made aspheric.
4- Lens aperture can be controlled with iris diaphragm.
5- Lens material can be graded index glass
6- Use a combination of lenses such that the separation between the two lenses is equal to the difference in their focal length [2].

2.5.1.2 Coma

When the optical systems form images for object away from the optical axis but within field of view, additional aberrations occur that increase the size of the blur circle. The most important of these is coma [3]. In optical coma can be defined as variation of magnification with aperture. Thus, when a bundle of oblique rays is incident on a lens with coma, the ray rays passing through the edge portion of the lens may be imaged at different height than those passing through the center portion. In figure (2.8), the upper and lower rim rays A and B, respectively, intersect the image plane above the ray P which passes through center of the lens. The distance from P to the intersection of A and B is called the tangential coma of the lens, and is given by:

$$\mathrm{Coma_T} = \mathrm{H'_{AB}} - \mathrm{H'_P} \qquad (2.4)$$

Where $\mathrm{H'_{AB}}$ is the height from the optical axis to the intersection of the upper and lower rim rays, and $\mathrm{H'_P}$ is the height from the optical axis to the intersection of the ray P with plane perpendicular to the axis and passing through the intersection of A and B.

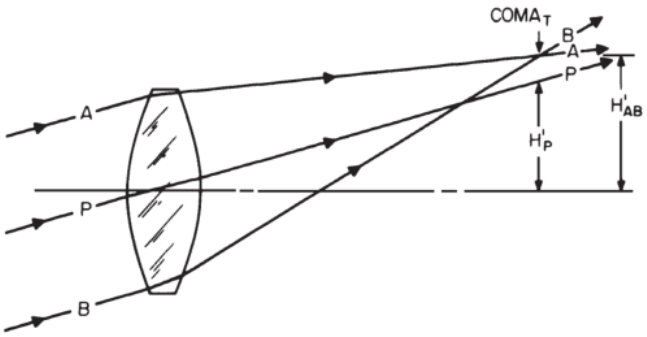

Figure (2.8): In the presence of coma, the rays through outer portions of the lens focus at a different height than the rays through the center of the lens [17]

The appearance of a point image formed by comatic lens in indicated in figure (2.9).

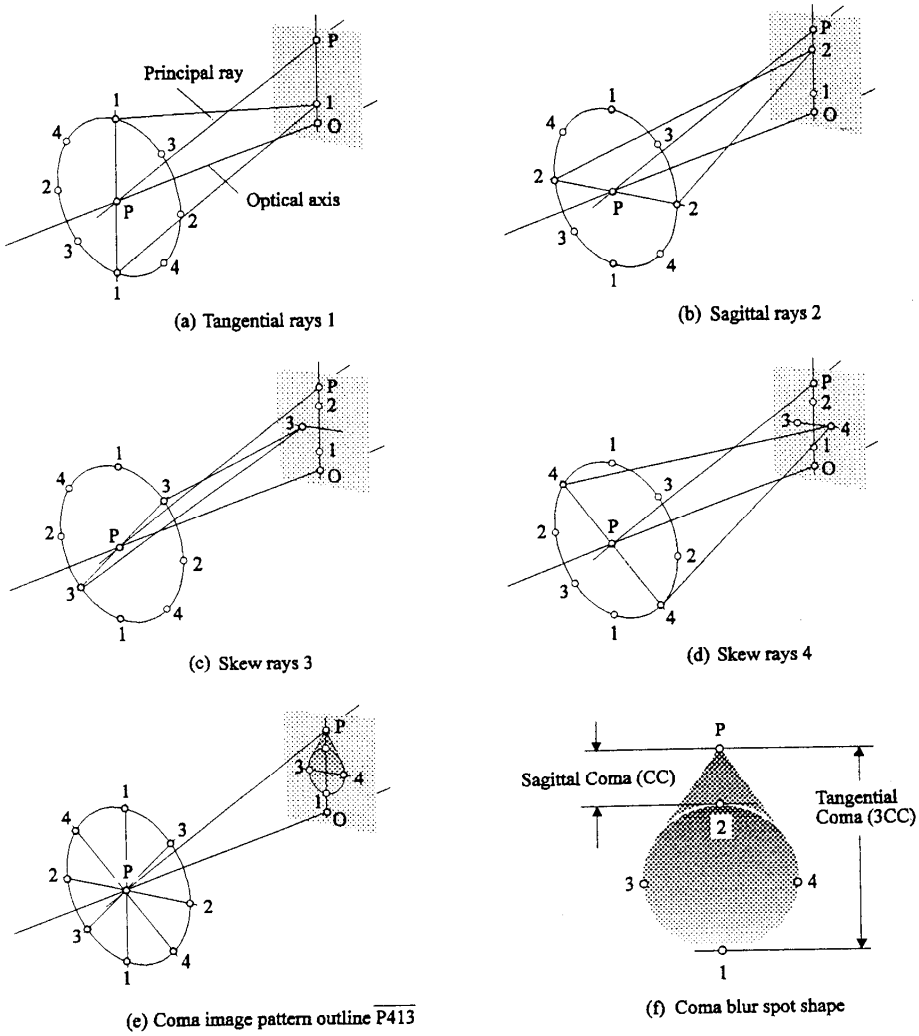

Figure (2.9): Constructions of coma blur [14]

The image pattern formed by tracing many rays of the entering bundle through the lens is shown in figure (2.11). The optical axis and principle ray of the system are identified by PO and PP, respectively. The construction of the image blur shape is presented by sequence (a) through (e). The circle marked with point pairs 1-1, 2-2, 3-3, and 4-4 is exit pupil of the lens. Rays entering the lens parallel to the principle ray, passing through these identified points are focused in image plane as point 1, 2, 3, and 4, forming the outline of the image blur that resembles the shape of a comet, hence the name coma. The plane that contains points *1* from the exit pupil and the principle ray PP is called the tangential plane. The plane perpendicular to the tangential plane, containing the principle ray and exit pupil points 2 is sagittal plane. The image pattern [figure 2.9(f)] identifies the distance P-2 as sagittal coma and P-1 as tangential coma [14].

Sagittal coma is one-third as large as tangential coma. About half of all the energy in the coma patch is concentrated in the small triangular area between P and 2, thus the sagittal coma is a somewhat better measure of the effective size of the image blur than is the tangential coma [17].

Coma varies with shape of the lens element and also with the position of any aperture or diaphragms which limit the bundle of rays forming the image [17]. In an axially symmetrical system the size of the coma patch (coma aberration) is linearly proportional to the field of view (FOV) and squarely proportional to diameter of aperture [17]. To eliminate coma from a thin lens born and wolf gave the following condition:

$$\frac{1}{R_1} = \left(\frac{2n+1}{n+1}\right)\frac{1}{u} + \left(\frac{n^2}{n^2-1}\right)\frac{1}{f} \qquad (2.5)$$

$$\frac{1}{R_2} = \left(\frac{2n+1}{n+1}\right)\frac{1}{v} + \left(\frac{n^2-n-1}{n^2-1}\right)\frac{1}{f} \qquad (2.6)$$

Where *u*= object distance, *f* = focal length, *n*= refractive index and *v* the image distance.

Let $n= 4$, $u= \infty$ (germanium lens and object at infinity):

$R_1 = 0.94f$ and $R_2 = 1.36f$ or $R_1 = 0.7R_2$

Thus, comatic aberration produced by a single lens may be reduced by suitable choice of radii of curvatures of the lens surfaces.

Spherical aberration and coma, however, vary greatly as the lens shape is changed. Figure (2.10) shows the amount of these two aberrations plotted against the curvature of the first surface of the lens. Notice that coma varies linearly with lens shape.

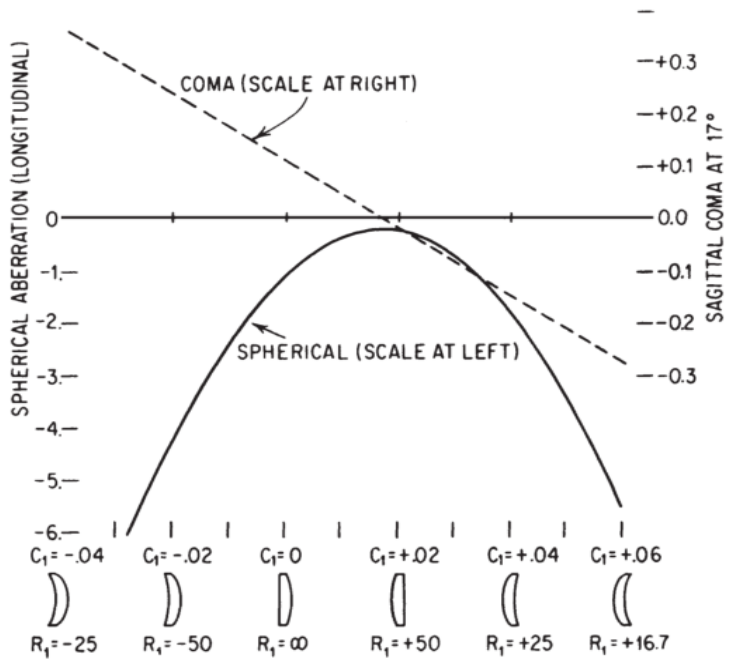

Figure (2.10): Spherical aberration and coma as function of lens shape. Dates plotted are for a 100 mm focal length (with the step at the lens) at f/10 covering ±17° field [17]

Coma and spherical aberration are differing in following respects:

1- Coma is measured laterally while spherical aberration measured longitudinally.
2- Circles formed in coma are comatic, while those in spherical aberration are centric. Coma is linearly proportional to the FOV and proportional to the square of the aperture.
3- Coma can be corrected by using aplanatic lens.

4- Moving the position of the stop can control coma [2], as illustrated in figure (2.11)

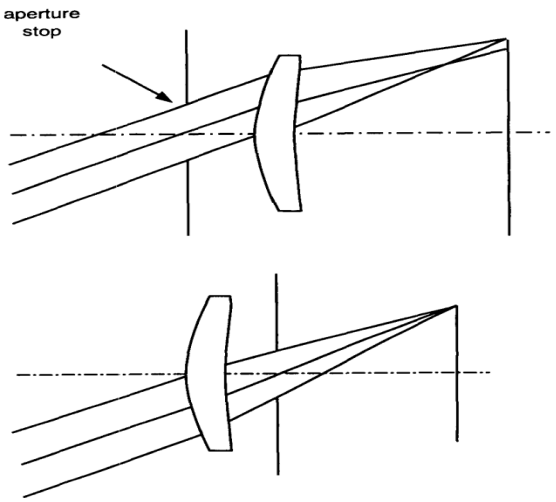

Figure (2.11): Coma with stop in front of lens and reduced coma with stop after of lens [9]

The coma can be made equal zero with almost the same bending that produces the minimum spherical aberration, when the stop in contact with the lens. If the lens has a large spherical aberration, the coma may be corrected only with the stop shifted with respect to the lens [20].

2.5.1.3 Astigmatism

Astigmatism is best described with a three-dimensional picture. Figure (2.12) identifies two planes that are perpendicular to each other. The plane that contains the object point and the optical axis is called meridional, or tangential plane. The rays in this plane form the tangential fan. The plane perpendicular to the tangential plane, containing the object point is the sagittal plane [14].

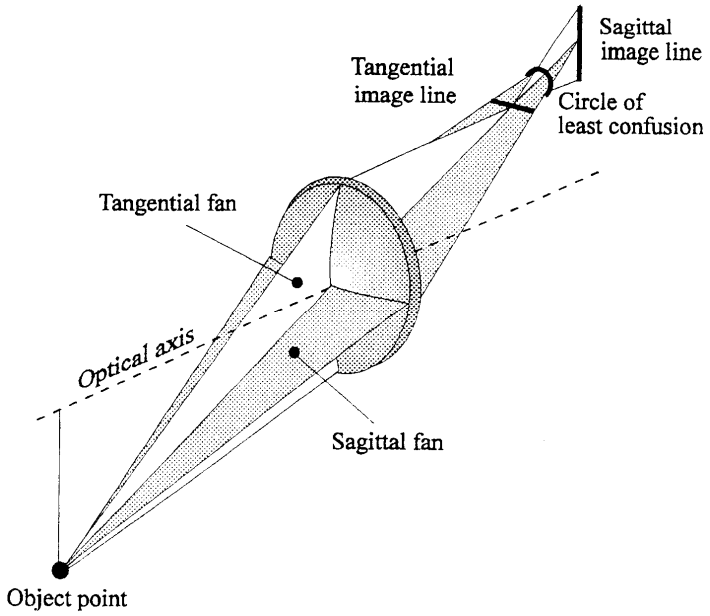

Figure (2.12): Astigmatism [14]

On the image side there is a longitudinal separation between the tangential and sagittal images. The images of an object point are formed in different planes. Because of this, the sagittal and tangential images of the object point are lines. Approximately halfway between these two image lines lies the so-called of least confusion, a blur with the smallest linear dimension as its diameter [14].

Astigmatism occurs when the tangential and sagittal (sometimes called radial) images do not coincide. As the image moves further from the axis, the amount of astigmatism gradually increases. The amount of astigmatism in a lens is a function of the power and shape of the lens and its distance from the aperture or diaphragm which limits the size of the bundle of rays passing through the lens. In the case of a simple lens or mirror whose own diameter limits the size of the ray bundle, the astigmatism is equal to the square of the distance from the axis to the image (i.e. image height) divided by the focal length of the element, i.e., $-h^2/f$ [13].

As shown in figure (2.12) if the angle of incidence of the cone of light from object point is θ, then for small angle θ, the astigmatic difference

F1-F2 (F1 is tangential image plane and F2 is sagittal image plane) is proportional to θ^2.

Astigmatism can be corrected by the use of suitable stop placed at appropriate places to limit the pencil of the rays and by using suitable combination of concave and convex lenses forming an anastigmatic combination. Therefore by bending (lens shapes) and selecting the stop's position we may only change the astigmatism [20].

2.5.1.4 Filed Curvature

Even if spherical aberration, coma, and astigmatism were absent, the image of an off-axis object point would still not lie in a plane without correction for field curvature. Assuming the first three aberrations were eliminated. The image surface would be parabolic in shape. Depending on the power of the lens, the parabola is either curved toward the lens or away from it. Positive lenses (positive-power lenses) have inward-curved image surface (toward the lens). Negative lenses (negative-power lenses) have their image surface bent in the other direction. The basic field curvature is named after Josef Max Petzval, who discovered the behavior of astigmatism relative to field curvature. The image surfaces and the Patzval surface are identified in figure (2.13) Measured parallel to the optical axis, for the single element shown, in presence of primary astigmatism the tangential image surface is three times farther away from the Patzval surface than the sagittal image surface. If astigmatism is eliminated (in absence of astigmatism), the tangential and sagittal image surfaces coincide and lie on the Patzval surface [14].

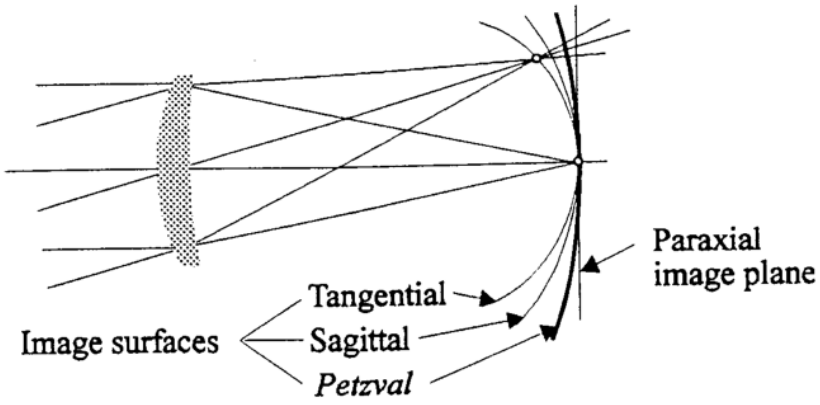

Figure (2.13): Field curvature and Patzval surface [14]

The Patzval curvature (i.e. the longitudinal departure of the Patzval surface from ideal image surface) of a thin lens element is equal to one-half the square of the image height divided by the focal length and index of the element, $-h^2/2nf$. Note that "field curvature" means the longitudinal departure of the focal surfaces from ideal image surface (which usually flat) and not the reciprocal of the radius of the image surface [13]. Therefore the curvature of Patzval image is inversely proportional to the product of the focal length of the lens and its index of refraction. When a number of lenses are used as a combination, the resulting curvature will be the sum of the individual curvatures. Therefore the Patzval curvature depends only of total power (1/f) of the lenses forming the optical system and not on the lens shapes (bending) nor on the stop position [16].

Bothe positive and negative powered lenses are often located either in the image plane or very close to it and called field lenses. In wide field of view (WFOV) and fast lenses (low f/number), a negative lens is used as field flattener to correct the field curvature. The Patzval radius of the final image plane is given by:

$$\frac{1}{r} = \frac{1}{n_1 f_1} + \frac{1}{n_2 f_2} + \cdots + \frac{1}{n_n f_n} \quad \text{Or}$$

$$r = \frac{1}{\sum n \frac{1}{n_i f_i}} \qquad (2.7)$$

For a flat image, r must be infinity.

$$\frac{1}{R} = \frac{1}{\sum nf} = \frac{1}{\infty} = 0$$

This is the Patzval condition for zero curvature. It may be noted that this condition is independent of the thickness and separation of the constituent lenses [14].

2.5.1.5 Distortion

The only aberration that does not result in image blur is distortion; it changes the shape of the object in image plane. If all other aberrations in the system, expect distortion, are corrected, an object point is imaged onto a perfect image point, which is displaced from its paraxial position. The amount of distortion can be expressed either as a lateral displacement in length unit or as a percentage of the paraxial image height. Distortion is defined as:

$$\text{distortion} = \frac{h - h_p}{h_p} \qquad (2.8)$$

Where $h\ is$ the height in the image plane and h_p is the paraxial height [3]. Third order distortion increased with cube of the field of view. A distorted image of rectilinear object is shown in figure (2.14). Distortion can be positive or pincushion distortion or alternately negative or barrel distortion [9].

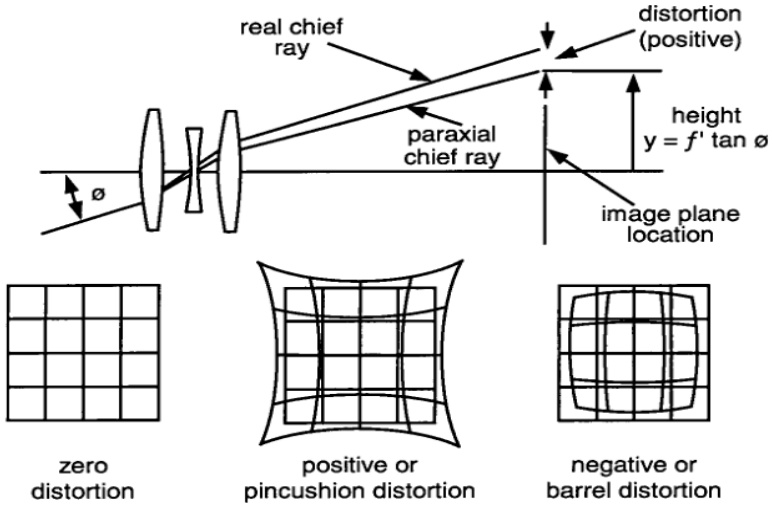

Figure (2.14): Distortion [9]

For a thin lens with the aperture stop on the lens, distortion is equal to zero. The thickness of a lens and its position relative to the aperture stop determines its contribution to the system distortion [9].

Distortion is a cosmetic-type aberration not affecting resolution; its appearance is very important, especially n visual systems [9]. For a visual system a distortion of 2 to 3% is acceptable [2].

Figure (2.15) shows where distortion comes from. In this situation, the aperture stop is located to the left of the lens, and angle of incident on the lens by ray bundle is large enough so that there is a reasonable difference between the paraxial angle of refraction and the real ray angle of refraction. As with spherical aberration, the real rays are refracted more severely than paraxial rays. In this case, this causes the real image to be pulled inward from the paraxial image thus causing negative barrel distortion [9].

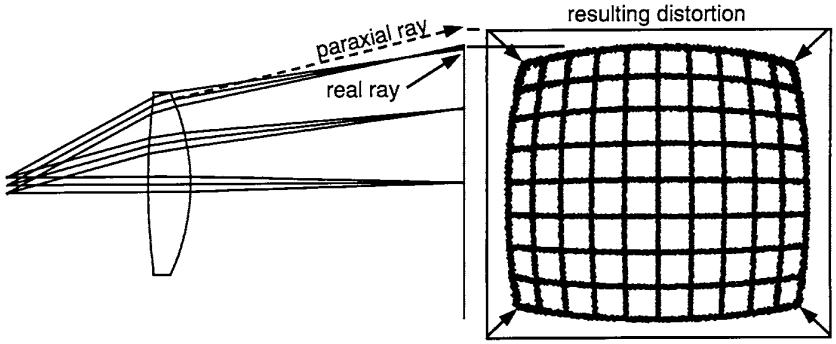

Figure (2.15): Where does distortion come from? [9]

Table (2.2) summarizes the aperture and field dependence of the primary (third order) monochromatic aberrations.

Table (2.2): Summary of primary monochromatic aberration dependence on aperture and field angle [2, 9]

Aberration	Field dependence or angle	Aperture dependence
Spherical aberration	–	Cubic
Coma	Linear	Quadratic
Astigmatism	Quadratic	Linear
Field curvature	Quadratic	Linear
Distortion	Cubic	–

2.5.1.6 Axial Chromatic Aberration

Generally chromatic aberration occur because the index of refraction (amount of ray bending) for a particular materials is a function/depends on the wavelength. It can be shown using lens makers formula given in equation (2.9), that the focal length of a lens and its corresponding image plane location changes with a change in the lens index of refraction [12].

$$\frac{1}{f} = (n_1 - n_m)\left(\frac{1}{r_1} - \frac{1}{r_2}\right) \qquad (2.9)$$

Where n_1 is refractive index of the lens, n_m is refractive index of the medium surrounding the lens (always air=1), and r_1& r_2 are curvature of the lens surfaces.

Therefore the focal length for different color (different wavelength) will be different, namely shorter wavelength have smaller focal length (the index of refraction is higher for shorter wavelength than for longer wavelength). That mean the focus for blue light is nearer to the lens than red light as shown in figure (2.16). This longitudinal variation of focus with wavelength (the difference or spread between the two focus positions) is called axial/longitudinal chromatic aberration [2].

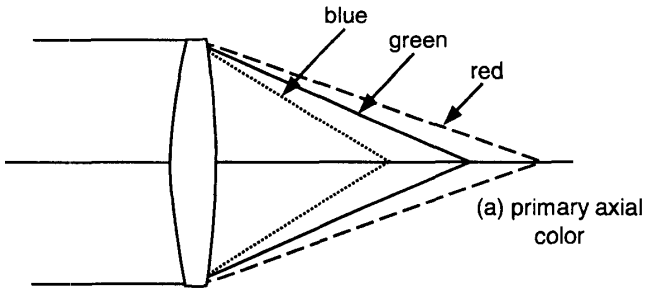

Figure (2.16): Axial chromatic aberration - red, green, blue lights are assumed for simplicity [9]

This gives the elongation of point image, which corresponds to axial chromatic aberration given by [2]:

$$f_r - f_b = \left(\frac{n_b - n_r}{n-1}\right) f = \omega f. \qquad (2.10)$$

In the absence of spherical aberration, a system with uncorrected chromatic aberration forms a bright spot surrounded with a purple halo coming from short and long wavelengths (the blue and red light) [3].

Is there a way to correct the axial color? A lens that focus an infinitely distance object as shown an example in figure (2.17). In order to bring the blue and red to focus together, a positive lens must be split into two lenses made from different material with different dispersions (dispersion is change in the index of refraction with wavelength). The first is a positive lens with low dispersion. This type of material is called crown glass. The second lens has lower optical power than the first one, so that the total power of the doublet is positive. However, the second lens is made of high-dispersion glass called a flint glass, which means that it spreads light more with color (wavelength), and it cancels most of axial chromatic aberration created by the first lens because of its negative power. This doublet is called a chromatic doublet [9].

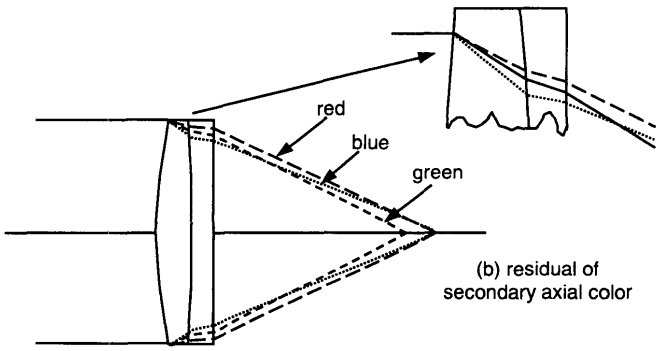

Figure (2.17): Chromatic doublet to correct axial chromatic aberration [9]

2.5.1.7 Lateral Chromatic Aberration

When a lens forms an image of an off-axis point at different heights for different wavelengths, the lens has lateral chromatic aberration. It is consequence of the difference in magnification with wavelengths. Figure (2.18) illustrates this situation [9].

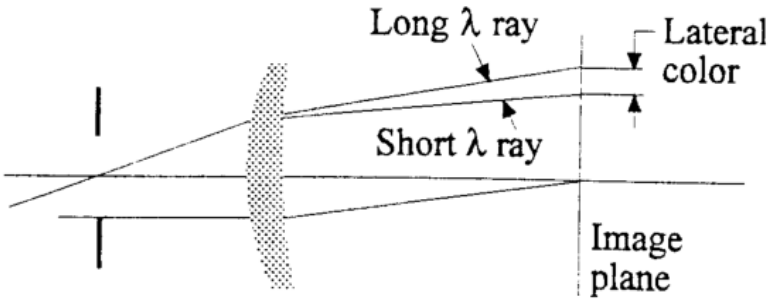

Figure (2.18): Lateral chromatic aberration or lateral color, results in different-sized images for different wavelengths [14]

The shorter wavelengths are bent refracted more severally than the longer wavelengths. Therefore, the short wave length image is formed closer to the optical axis the long wavelength image. This leads to the differential in magnification.

In a wide field of view (WFOV) optical systems, lateral color is often the aberration that is the most difficult to correct. Its correction may require the use of anomalous dispersion materials, which are often expensive, or diffractive elements, also very expensive elements because of manufacturability [9].

The seven aberrations discussed cannot be simultaneously eliminated or even minimized in a single lens. Yet when several elements are used, the aberration of one element can be balanced against those of anther. In general, the better the imagery required, the greater the number of elements needed to achieve it. Regardless of how many elements are used, the designer must concentrate on eliminating those aberrations that will be most detrimental to the intended use of the system. In most IR systems that have to cover just small instantaneous field of view (IFOV), only spherical aberration, coma, and the chromatic aberrations are of concern. In a system covering a wide field of view (WFOV), astigmatism, field curvature, and distortion must also be reduced. It not surprising, therefore, those optical systems designed to cover only a small field of view produce better images than those designed for a wide field of view [3].

Generally the lens factors those effects on the aberrations of any optical system (degrees of freedom in correct/ minimize the aberrations) are:

- Lens shape: one of the most powerful tools available to the lens designer in minimize/correct the aberration is changing the shape of an element (lens) without changing its power/ bending
- Stop position: it is obvious that, depending on its position in a lens system, a stop selects some rays from an oblique pencil and rejects others then the longitudinal stop shift changes all of oblique (off-axis) aberrations in a lens. It will not affect the axial (on-axis) aberrations provided the aperture diameter is changed as necessary to maintain a constant f/number [19].
- Aperture
- Field of view

The aperture and field may be fixed to specific values for specific design, in this case the designer play with lens shape and stop position to correct/minimize the aberration.

Table (2.3) lists the relationships between the primary aberrations and semi-diameter *y* (aperture) and the image height/field height *h* (field of view). to illustrate the use of this table, let us assume that we have a lens whose aberrations are known, we wish to determine the size of aberration if the aperture diameter increased by 50 percent and the field cover decreased by 50 percent. The new *y* will be 1.5 times the original, and the new *h* will be 0.5 times the original.

Since the longitudinal spherical aberration is shown to vary with y^2, the 1.5 times increase in aperture will cause the spherical to be $(1.5)^2$, or 2.25 times as large. Similarly transverse spherical, which varies as y^3, will be $(1.5)^3$, or 3.375 times larger (as will the image blur due to spherical).

Coma varies as y^2 and h; thus, the coma will be $(1.5)^2 \times 0.5$, or 1.125 times as large. The Petvzal curvature and astigmatism, which vary with h^2, will be reduced to $(0.5)^2$, or o.25 of their previous value, while the blurs due to astigmatism or field curvature will be $1.5(0.5)^2$, or 0.375 of their original value.

Table (2.3): Variation of primary aberrations as function of aperture and field height [18]

Aberration	Vs semi aperture (y)	Vs field height (h)
Spherical (longitudinal)	y^2	--
Spherical (transverse)	y^3	--
Coma	y^2	h
Astigmatism	--	h^2
Astigmatic line length	y^2	h
Field curvature	--	h^2
Distortion (linear)	--	h^3
Distortion (percentage)	--	h^2
Chromatic (longitudinal)	--	--
Chromatic (lateral)	--	h

The aberrations of lens also depend on the position of object and image. A lens which is well corrected for infinitely distant object, for example, may be very poorly corrected if used to image a nearby object. This is because the ray path and incident angles change as the object position change [17].

2.6 Image Quality and Performance Evaluation of the Optical System

When we think about the image quality of an image-forming optical system such as a camera lens, the first parameter that often comes to mind is resolution or resolving power. Classically, the ability of an optical system to separate two closely spaced point sources at the nominal object distance is generally considered to be the resolution.

In an imaging system, the optics, detector, electronics, and display component of imaging system all have inherent resolution. The overall

system resolution is a composite of the subsystem resolution. Generally, in well-designed systems, the electronics and display do not adversely affect the perceived image quality; therefore, it has become commonplace to infer image quality from the optics and detector performance. Imaging systems resolution depends on the optical blur diameter [caused by aberrations and the main task of optical designer is reduce/eliminate the aberrations] and the detector size (pixel size). When the system is detector limited, small changes in the blur diameter have little effect on the system resolution. The detector size limits the smallest size that can be discerned. With a large blur diameter, the resolution is limited by the optics; most infrared imaging systems fall into this category. A commonly used measure of optical resolution is the Airy disk [14]. Therefore, the quality of thermal imaging system is determined by the quality of the final image that comes from matching between the thermal detector and IR optical system.

Below is a brief explanation of the common measurements and specifications in lenses that have an impact on quality of the image:

2.6.1 Resolution and F/number

The resolution for a camera is effectively the size of the pixel. Smaller pixels mean more of them will go into building the same image, giving it sharper corners and overall better definition. When choosing a lens, however, resolution can be tricky.

Matching a resolution for a camera and lens is important. The wrong choice could waste money or provide a poor quality image. For the best possible resolution, the lens' f/number and camera’s pixel size should match (choose the lens that has an AAD around camera’s pixel size) [21].

2.6.2 Performance Evaluation

The performance characteristics of an imaging optical system can be represented in many ways. Often the final optical performance specification is in terms of modulation transfer function (MTF), rms blur diameter, encircled energy, or other image quality criteria. These criteria related to in different ways to the image quality of the system. Image quality can be thought of as resolution or how close two objects can be approach each other while still being resolved or distinguished from one another. Image quality can also be thought of as image sharpness, crispness, or contrast.

As discussed earlier, imagery is never perfect. It is limited by geometrical aberrations, diffraction, the effects of manufacturing and assembly errors, and other factors. The characterization of image quality by the methods described in the following sections will help us to assess just how our system performs with respect to its imagery.

It is important to realize that the image quality or resolution of the entire system not totally dependent on the optics (despite the very large effect compared with other subsystems of imaging system), but may include the sensor, electronics, display device and/or other system components making up the system. For example, if the eye is the sensor, it can accommodate for both defocus and field curvature, whereas a flat sensor such as thermal FPA or CCD array cannot. In the following sections we will be discussing only the optics contribution (which is greater contribution) to the image quality [9].

The following list contains some of the more common ways to measure and evaluate the image quality of an image forming systems:

- spot diagrams
- Modulation transfer function (MTF)
- Ray trace curves (transverse ray fan plot)

- Encircled energy

For the infrared, the blur spot size and the radial energy distribution in the image plane are two of great interest. They include the minimum detector element size (pixel size) required to collect a certain amount of energy. From this information, one can drive the MTF, a measure of contrast virus resolution [14].

2.6.2.1 Spot Diagrams

Due to diffraction and uncorrected aberrations, the image of an object point is never a point but a diffused disk [14]; Spot diagrams are the geometrical image blur formed by the lens when imaging a point object [9]. Thus the spot diagrams give a visual representation of the energy distribution in the image of a point object. If several spot diagrams are obtained, for different colors, the chromatic aberration may also be evaluated [16]. This is a more functionally useful form of output; however, it is sometimes difficult to distinguish the specific aberrations present. Figure (2.19) shows the spot diagrams for a Cooke triplet form of lens and shows both the transverse ray aberration curves which discuss later as well as spot diagrams for same field positions. Generally, rms spot radius or diameter is the diameter of a circle containing approximately 68% of the energy. This metric can be of great value, especially when working with pixilated sensors (FPA detector) where one often wants the image of a point object to fall within a pixel [9].

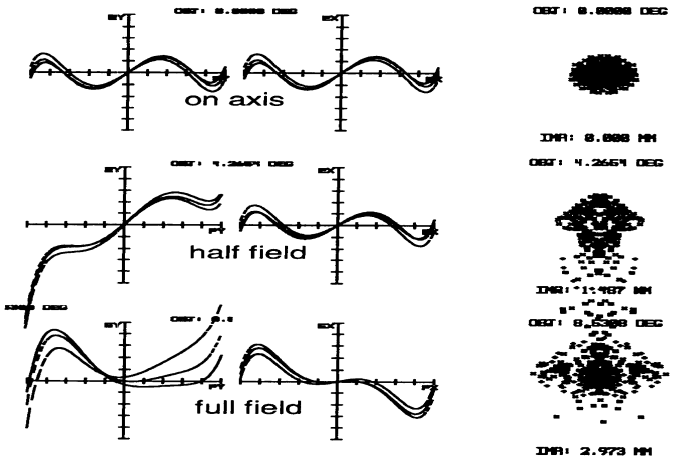

Figure (2.19): Geometrical-based Spot diagrams and transverse ray aberration curves for Cooke triplet example [9]

Note that in optical design software (as Zemax) we often come across the terms “spot radius,” “spot diameter,” “spot size,” while the designer is most interested in spot diameter, the software generally outputs spot radius. The use of the words “spot size” is fine for relative comparison (for example, “the spot size has increased by factor of 2”); however, the term can cause undo confusion when tied to a specific value. For example, “the spot size is 50 μm” does not really tell us whether this is the radius or diameter of the image blur, nor does tell us whether this is 100%of the energy or some other value such as the rms. Be careful in interpreting these forms of date from the software which are using [9].

2.6.2.2 Ray Trace Curves

Most of the methods used in computing image quality, such as the modulation transfer function MTF, spot diagrams, encircled energy, and the like, are functionally robust and represent different, yet similar representations of the net performance of the optical system as designed. However, there are two disadvantages with this metrics. First, they can sometimes take too much time to compute. This, however, is less and less of a problem as PCs have become faster and faster. Second, the real problem is that while these metric do help to show the overall net resulting image quality, they do not provide a detailed indication to the

designer of the specific aberrations present in the design over the field of view and over the spectral bandwidth. While some information can at times be derived, more often the user really cannot tell what aberrations are presented and at what magnitudes. These data are important to the designer as an aid in correcting the residual aberrations.

The solution is to generate what are called transverse ray aberration curves or simply ray trace curves. With these graphical data, a reasonably experienced designer can immediately tell just how much spherical aberration, coma, astigmatism, field curvature, axial color, lateral color, and field curvature are present. With this knowledge, the designer can often make a reliable judgment as to what to do next regarding further optimization of the lens. In spite of some fabulous advances in performance simulation and modeling, transverse ray aberration curves are still invaluable to the serious designer.

Figure (2.20) shows the basic information of the ray trace curve. This perspective figure shows a lens exit pupil with the lens imaging to an off-axis image position. First, consider tracing the chief ray to the image. The height on the image of the chief ray is our reference point, and is generally taken to be the image height. Now let us trace a ray through the top of exit pupil. This ray, which is called the upper marginal ray, hits the image higher than the chief ray for the aberration shown, which is coma. Now let us trace a ray through the bottom of the exit pupil. This ray, which is called the lower marginal ray, also hits the image higher than the chief ray, and in fact for classical third-order coma it hits the image the same distance above the chief ray as the ray from the top of the pupil. In other words, both of the rays from the top and the bottom of the exit pupil hit the image vertically displaced by same amount [9].

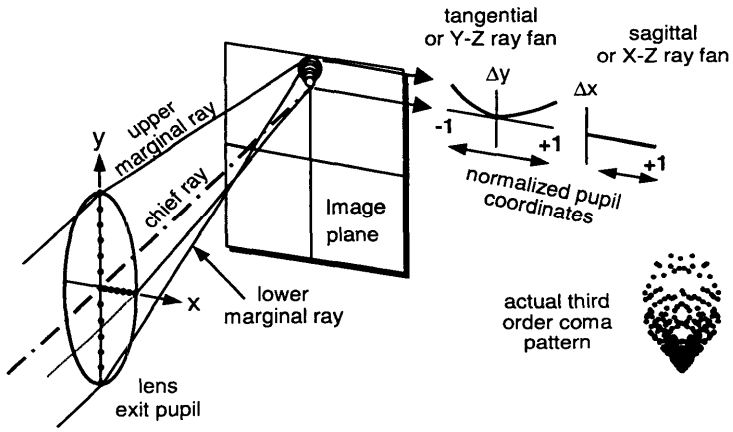

Figure (2.20): Explanation of ray trace curves [9]

We will now proceed to establish a set of coordinate axes for our ray trace curve. In the first set of coordinates (on the left in figure (2.20)), the abscissa is the normalized exit pupil radius in the *y* direction, and the ordinate is the distance above or below the chief ray on the image that our ray intersects the image plane (Δy). Thus, both the upper and lower marginal rays form the end points on the curve. We now proceed to trace rays through each of the black dots from $y = +1$ to $y = -1$, with the intersection points relative to the chief ray plotted on the curve. For third-order coma the result will be a quadratic or parabolic curve since third-order coma is quadratic with aperture.

Now we establish a second set of coordinate axes, as shown on the right in figure (2.20). Here we have the normalized *X* coordinate in the exit pupil in the abscissa, and the displacement of the ray in the *x* direction (Δx) as the ordinate. As it turns out, for third-order coma there is no *x* departure at all for these rays in the exit pupil. We will show why this is the case shortly. For now, you will see that the for third-order coma a quadratic curve in the "tangential" ray fan and zero departure for the *x* rays in the "sagittal" ray fan are the results. If any lens designer who is "worth his or her salt" sees this form of ray aberration curves with a quadratic in the tangential ray fan and virtually zero in the sagittal curve,

then he or she should conclude instantly that the lens has third-order coma.

Since these ray trace curves are so fundamentally important to the optical designer's work, a more in-depth discussion is in order. As you will see, there are here, as with many other areas of optical design, subtleties that could easily be misleading if not fully understood. Consider our coma pattern where the ray trace curves suggest zero *x* departure of the ray hitting the image, which implies or suggests zero width *x* width to the image blur. Yet we all know that coma does have width in the *x* direction. Just what is going on, and why are the data misleading?

Figure (2.21) will explain the situation. Here we trace rays around the periphery of the exit pupil from position 1 through 8. From our prior discussion, we know that the chief ray is our reference, and that ray 1 and 5 from the top and bottom of the exit pupil both hit the image high, above the chief ray. If you follow the numbers in figure (2.21), you will see how one rotation around the exit pupil results in two rotations around an ellipse in the image, and since positions 1 and 5 are both high, then positions 3 and 7 which are 180º opposed will be at the bottom of the elliptical pattern. Neither of these rays will have any *x* departure at all! Thus, ray trace curve for rays traced in the *x* directions was a horizontal line in figure (2.20). So where is the *x* spreading of the coma pattern coming from? The answer is from rays at positions 2, 4, 6, and 8, which are called *skew rays*. Since the rays making up the ray trace curves contain only the *y* (or tangential rays) and the *x* (or sagittal rays), the designers sees no indication or evidence whatsoever of the *x* spreading of the imagery. This is a real subtlety, and it is a fine example why one should never be totally dependent on only one form of image evaluation or analysis. By looking only at the ray trace curves, one could

easily conclude that such a system had virtually zero *x* spreading of the off-axis imagery, and this could make its performance ideal for some system applications. For the most part use of the ray trace curves are wonderfully helpful and revealing; however, do be aware of subtleties as pointed out earlier [9].

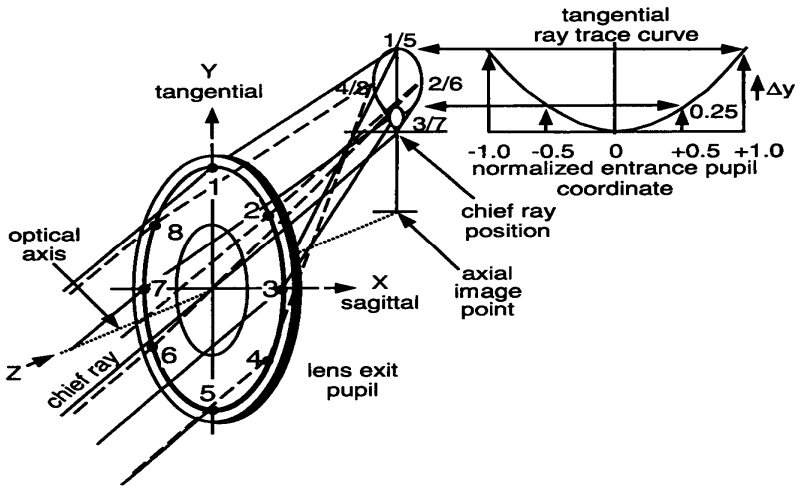

Figure (2.21): Formations of comatic image blur [9]

A further illustration of the ray trace curves, figure (2.22) shows how spherical aberration is formed and how the ray trace curves are derived. In the top of figure (2.22) the image is located at paraxial focus and it should be clear how each of the rays entering the lens from the left results in a corresponding intercept on the image plane and how this is plotted as the ray trace curve. Ray 1 strikes the image lowest and results in point *a* in the plot. Ray *2* is the next ray lower down entering the entrance pupil and it results in point *b* in the plot, and so on. Since third-order spherical aberration is cubic with aperture, the resulting curve is cubic. Note the symmetry above and below the optical axis. Now consider what happens if we relocate the image plane to the “best focus” position. Following the same logic in generating the ray trace curves, we see a much lower departure of the ray intercept points making up the curves. This is true and quit real, and it tells us that the image blur diameter when we refocus the image will be significantly reduced from

that at paraxial focus. As an exercise, what will the ray trace curve be for a perfect image where the image plane is intentionally defocused toward the lens? The answer is a straight line sloped upward to the right. So let's use this as an aid in further understanding ray trace curves. Since defocus yields a sloped but otherwise straight line, we can easily determine what any ray trace curves for any lens will look like as we go through focus by simple drawing or imagining a sloped straight line as a new coordinate axis. This is an invaluable tool as you can now immediately assess the relative improvement after refocusing a given lens. And since field curvature is a quadratic change in focus with field of view, you can with little practice assess immediately the benefits of curving your sensor if this is possible [9].

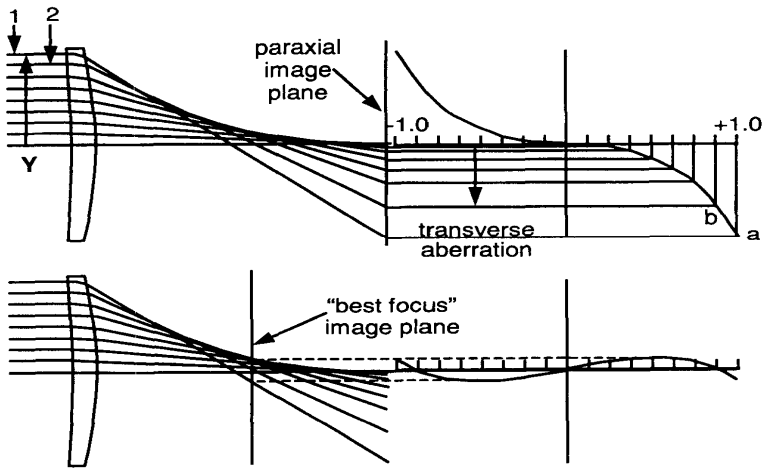

Figure (2.22): Formation of ray trace curves for spherical aberration [9]

Figure (2.23) shows ray trace curves for various typical aberrations and combinations of aberrations since:

Figure a. is pure defocus. As noted earlier, defocus will produce equal sloped straight lines in the sagittal and tangential ray fans. Recall that the tangential ray fan is in the *y-z* direction and typically oriented parallel to the field-of-view direction. The sagittal ray fan is orthogonal to the tangential ray fan, and typically, the sagittal fan is fully symmetrical which is why we sometimes show only one-half of the fan.

Figure b. shows straight lines at different slopes. This is a combination of astigmatism (which difference between the slopes of the two curves) and defocus.

Figure c. shows that if we best focus for the residual astigmatism off-axis as we might do with a curved image surface, we find the result here where an equal and opposite ray fan slope results in tangential and sagittal directions.

Figure d. is negative or under corrected third-order spherical aberration, which is, of course, a cubic with aperture.

The data in figure e. are the same third-order spherical aberration as in figure d, only we have refocused the image to a more optimum focus position to minimize the residual blur diameter.

Figure f. shows negative third-order spherical aberration, which is being balanced by positive fifth-order spherical aberration.

The data in figure g. are for pure third-order coma, which, as we know from before, is quadratic with aperture. We also know from before that the sagittal curve indicates zero images blurring in the sagittal direction. This may be misleading and is due to the nature of coma formation and the fact that the ray aberration curves show only the rays along two lines in the pupil plane.

The data in figure h. are for a combination of third-order coma and astigmatism.

Figure i. shows a combination of some negative third-order spherical aberration at the central wavelength as well as secondary axial color and spherochromatism. The secondary axial color is focus difference between the central wavelength and the common red and blue foucs, which together are focused beyond the central wavelength. The spherochromatism is the change in spherical aberration with wavelength.

Finally figure j. shows an off-axis ray trace curve with primary lateral color or color fringing along with a small amount of coma and astigmatism [9].

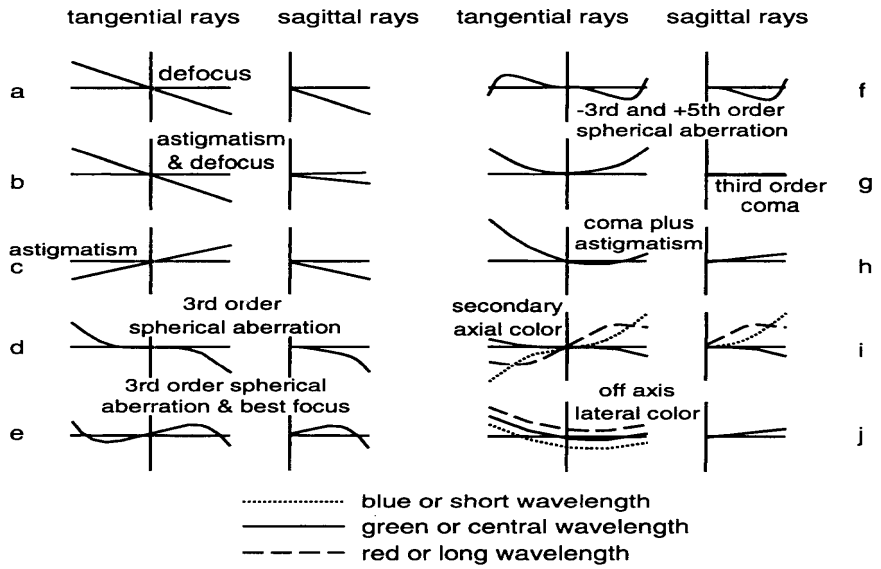

Figure (2.23): Typical transverse ray aberration curves [9]

It should be quite apparent that the ray trace curves for each of the aberrations has its own distinctive form, and this is what makes them so useful. The aberrations, in effect, add algebraically, so it is easy to tell almost immediately what aberrations are present in a given design at the different field position [9].

Transverse ray plot are generated by tracing fans of rays from a specific object point for finite object distance (or a specific field angle for an object at infinity) to a linear array of points across the entrance pupil of the lens. The curves are plots of the ray error at an evaluation plane measured from the chief ray as function of the relative ray height in the entrance pupil [figure (2.22)]. If the evaluation plane is in the image of a perfect image, there would be no ray error and the curve would be a straight line coincident with the abscissa of the plot, usually the aberration plotted along the vertical axis and entrance pupil diameter or ray height along the horizontal axis.

Aberration curves provide experienced designers with the information needed to enable them to correct different types of aberrations. Chromatic effects are much more easily classified from aberration curves also. In comparison to spot diagrams and MTF curves, the types of aberrations can be easily seen and quantified [20].

2.6.2.3 Field Plot

The ray trace curves provide evaluation for a limited number of object points – usually a point on the optical axis and several field points. The field plots present information on certain aberrations across the entire field. In these plots, the independent variable is usually the field angle and is plotted vertically and the aberration is plotted horizontally. The three field plots most often used are: distortion, field curvature, and lateral color. The first of these shows percentage distortion as a function of field angle [figure (2.24)]. The second type of plot, field curvature displays the tangential and sagittal foci as function of object or field angle [figure (2.25-a)]. In some plots the Petzval surface, the surface to which the image would collapse if there were no astigmatism over entire field. In cases of corrected field curvature [figure (2.25-b)], this plot provides an estimate of residual astigmatism between the axis and the corrected zone and an estimate of the maximum field angle at which the image possesses reasonable correction [20].

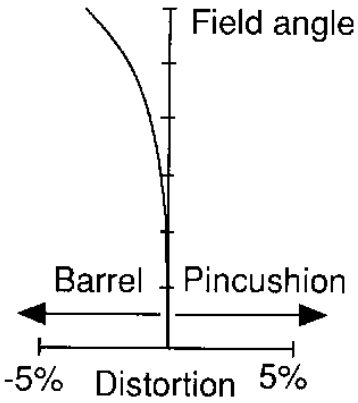

Figure (2.24): Field curve: distortion plot. The percentage distortion is plotted as a function field angle. Note that the axis of the dependent variable is the horizontal axis [20]

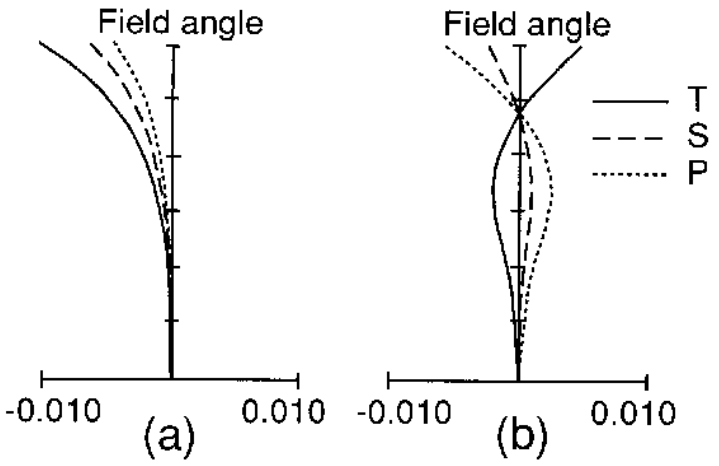

Figure (2.25): Field curve: field curvature plot. The locations of the tangential T and sagittal S foci are plotted for a full range of field angels. The tangential surface is always three times farther from the Petzval suface than from the sagittal surface. (a) An uncorrected system. (b) A corrected system [20]

The last of the field curves provides information on color error as a function of field angle [figure (2.26)]. Lateral color, the variation of magnification with wavelength, is plotted as the difference between the chief ray heights at the red and blue wavelengths as a function of field angle. This provides the designer with an estimate of the amount of color separation in the image at various points in the field. In the transverse ray error curves, lateral color is seen as a vertical displacement of the end wavelength curves from the central wavelength curve at the origin [20].

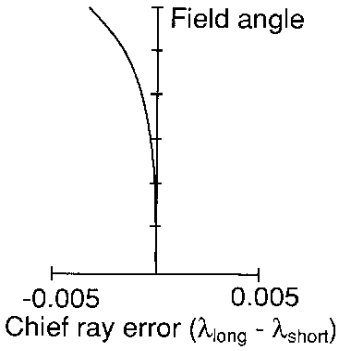

Figure (2.26): Field curve: lateral color plot, a plot of the transverse ray error between red and blue chief ray heights in the image plane for a full range of field angles. Here the distance along the horizontal axis is the color error in the image plane [20]

2.6.2.4 Encircled Energy

Encircled energy is energy percentage plotted as a function of image diameter. One good example of how we might use encircled energy is to specify an imaging optical system using a CCD or FPA sensors. Let us assume that the pixel pitch of our sensor is 7.5µm. a good reliable and simple specification is that 80% of the energy from a point object shall fall within a diameter of 7.5µm. figure (2.27) shows an encircled energy plot for our sample Cooke triplet. Eighty percent of the energy is contained within a diameter of approximately 6µm, which is a good match to the sensor. It also leaves some margin for manufacturing tolerances.

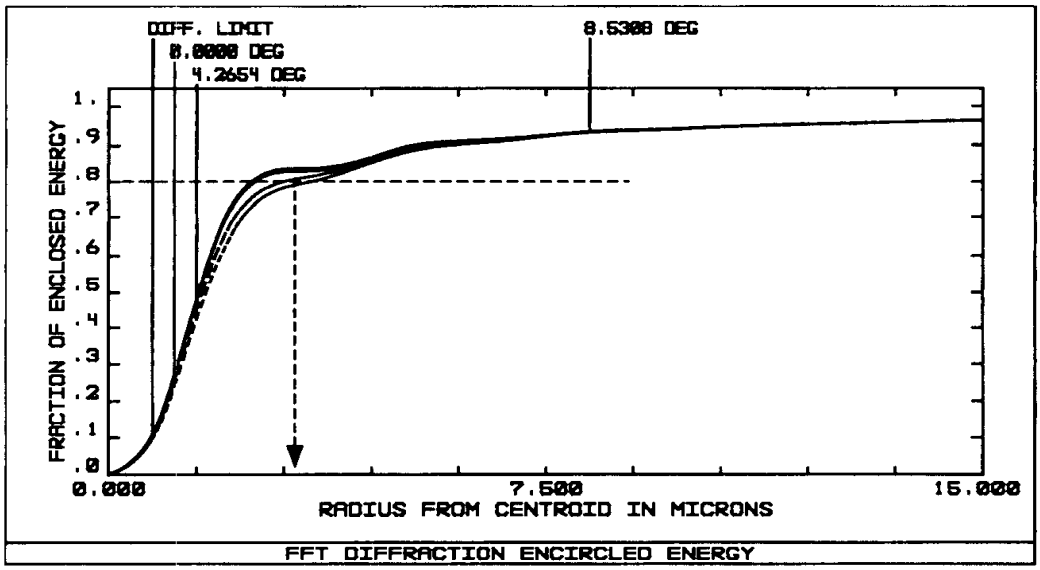

Figure (2.27): Encircled Energy for Cooke Triplet example [9]

2.6.2.5 Modulation Transfer Function (MTF)

Modulation transfer function or "MTF" is the most widely used scientific method of describing lens performance, it's as name suggests, a measure of transfer modulation (or contrast) from the subject to the image. In other words, it measures how faithfully the lens (or optical system) reproduces (or transfer) details from the object to the image produced by the lens/optical system [22].

MTF is perhaps the most comprehensive of all optical system performance criteria, especially for image forming systems [9]. The image quality of an object is a measure of the quality of a lens. With the MTF the image quality is measured as contrast against spatial frequency [10]. *{Spatial frequency" is a fancy way of saying how many line pairs per mm (lp/mm) there are in the image. The more line pairs, the higher the spatial frequency. Note that a line pair is one black line and one white line (space), so the number of line pairs per mm (counting black lines and white lines) is the same as the number of lines per mm (counting only black lines) [16]}*. The image formed by the optics always differs from the original object in that there is a general loss of detail. A point object always appears as a "blur spot" due to diffraction, aberration, manufacturing inaccuracies, and assembly and alignment errors. The image quality is dictated by the shape and size of the blur spot. A rule of thumb is that the smaller the blur spot, the better is the image. The MTF concept helps in this regards [2]. Thus the MTF plays a key role in the theoretical evaluation and optimization of an optical system, it is the primary parameter used for system design, analysis and specifications.

Figure (2.28) is representation of what is happening, we being with periodic with a periodic object or target, which is varying sinusoidally in its intensity. This target is imaged by the lens under test, and we plot the resulting intensity pattern at the image [9]. The contrast in the object

space is not the same as in image space because when a radiation passes through an optical system, it gets attenuated/ reduced. That is means the imagery will be somewhat degraded and the brights will not be as bright and the darks will not be as dark as the original pattern in object space. The degradation of the contrast by entire optical system is represented by the MTF [2].

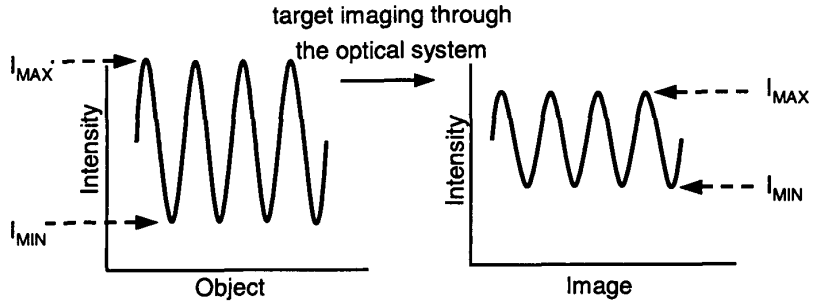

Figure (2.28): Illustration of the meaning of the Modulation Transfer Function (Simple Sinusoidal Curves before and after Modulation) [9]

Let us define some terms:

$$\text{Contrast Modulation} = \frac{I_{max}-I_{min}}{I_{max}+I_{min}}$$

$$\text{MTF} = \frac{contrast\ modulation\ in\ the\ image\ space}{contrast\ modulation\ in\ the\ object\ space} \quad \text{or}$$

$$\text{MTF} = \frac{modulation\ in\ image\ (output\ modulation)}{modulation\ in\ object\ (input\ modulation)}.$$

The plot of MTF against spatial frequency is typically used when describing the performance of lens/optical system.

Figure (2.29) shows several typical MTF curves. We show the MTF of a perfect optical system, a perfect system with central obstruction (such as cassegrain telescope), and a typical real system. The MTF of the perfect obscured system has more diffraction due to its obstraction, and thus a lower MTF.

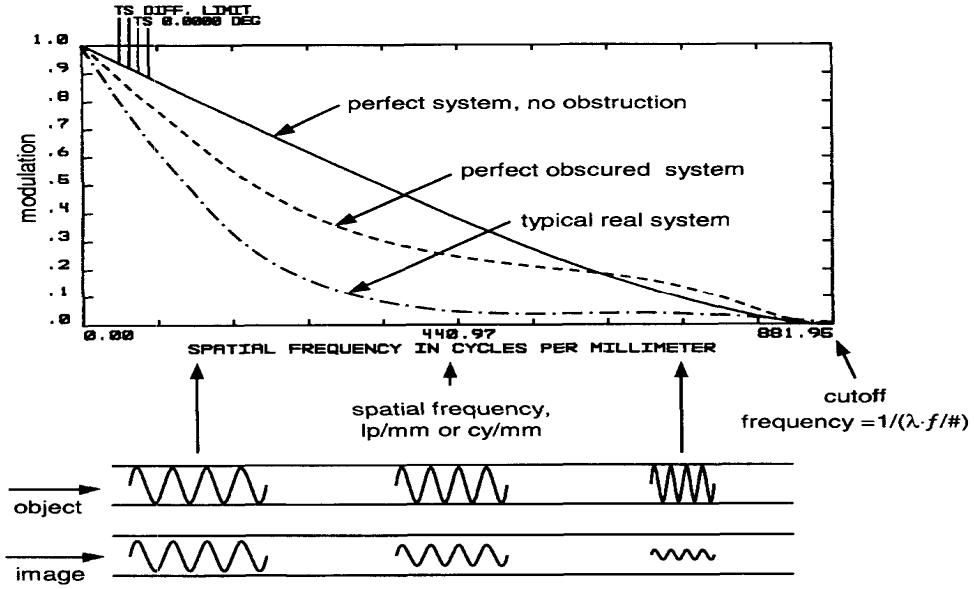

Figure (2.29): Typical MTF curves [9]

The MTF has values ranging between 0 and 1 (1 for an ideal/ perfect, free-aberration system). The spatial frequency where the MTF goes to 0 (the first time) is called the cut-off frequency; it's given by equation (2.11), this cutoff frequency called optical cutoff frequency [23].

$$\mathcal{V}_{cutoff(optics)} = \frac{1}{\lambda(f/number)} \qquad (2.11)$$

Where $\mathcal{V}_{cutoff(optics)}$ is the optical system's cut-off frequency in cycle/mm, and λ is wavelength In cases of FPA imaging system (sampling imagers/ starring array) the system cut-off frequency is defined as the smaller of the optical cutoff, detector cutoff, or Nyquist frequency (one half the sampling frequency). For starring array the Nyquist frequency is always smaller than detector and optical cutoff frequencies, and is typically also the system cut-off frequency; it's given by:

$$\mathcal{V}_c = \frac{1}{2dx} \qquad (2.12)$$

Where $\mathcal{V}_c$ is system cut-off frequency, and dx is sample width in most cases the optical cut-off frequency is well beyond the detector cut-off frequency, in this case it can be said that the imaging system is detector

limited and not optics limited. Spatial frequencies above systems cut-off frequency can be detected but not faithfully reproduced [2].

The example shown in figure (2.29) is an *f/2* lens in the visible region (λ=0.55μm), and the cut-off frequency (optical cut-off frequency) is approximately 882 line pairs/mm. for example, an *f/4* optical system has twice the Airy disk diameter and thus half the cut-off frequency of 441 line pairs/mm [9].

In most applications, the designer will be working with rotationally symmetric optical system. The MTF for a perfect diffraction limited imaging system with a circular exit pupil is shown in figure (2.30). This represents the ideal MTF against which real system must be compared.

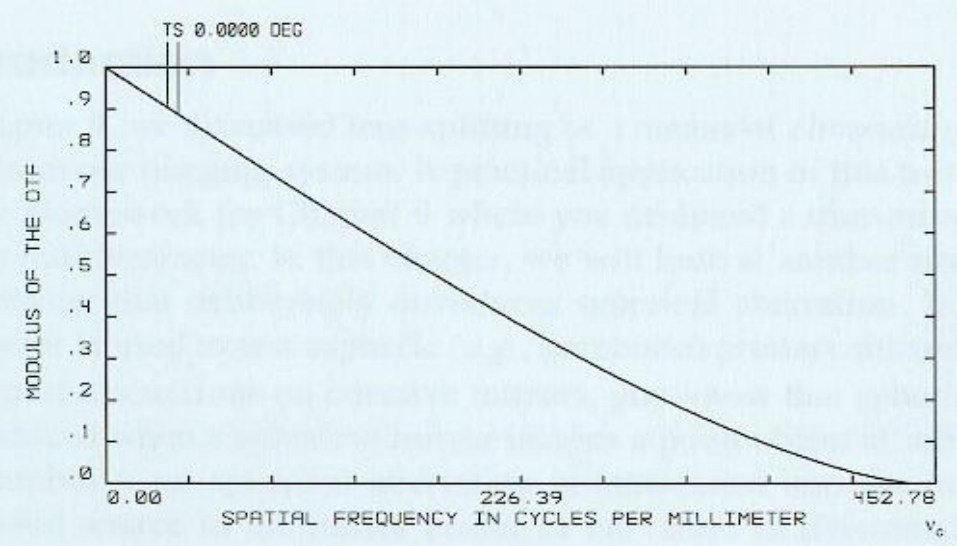

Figure (2.30): Diffraction-limited MTF for circular pupil [23]

In the case of diffraction-limited systems, modulation transfer function may provide better estimates of system performance [20].

A criterion for excellent performance in any designed optical system is to look for 50 percent MTF (≈ 0.5) at system cutoff frequency over 90 percent of the field. This criterion will give some idea of the range of the very acceptable MTF values [24].

Some important points to remember about MTFs are:

- Every optical system acts as low pass filter.

- The maximum resolved frequency in sampling imagers is the reciprocal of twice the minimum sample width (Nyquist criteria).
- MTF depends on the wavelength. For better performance we need to measure polychromatic MTF [2].
- The image quality of an object is a measure of the quality of a lens. With MTF the image quality is measured as contrast against spatial frequency [14].

2.7 Special Optical Surfaces

An aspheric surface is considered a special optical surface. It is special because it can do more than a spherical surface with regard to aberration correction. But it is also special because it is much more expensive to manufacture, especially if the surface is produced by means other than diamond turning.

Plane-parallel elements such as beam splitter and detector windows, are often ignored by the user and not considered to be optical elements, we treat them here as elements with special surface. These elements in converging or diverging light contribute to aberrations just as lens or a curved mirror does. In addition, they shift and displace image location. Knowing the behavior of plane-parallel plats allows us to correct for their aberrations contributions or take advantages of them in balancing the system's aberrations [9].

2.7.1 Aspheric Surfaces

A spherical surface is defined by only one parameter, the radius or curvature of the surface. Radius and curvature are reciprocal to one another.

Figure (2.31-a) shows a Plano-convex lens element with a spherical radius, imaging axial point from infinity. The spherical aberration is quite evident. The high angle of incident of the upper limiting ray of

approximately 45º to the surface normal causes this ray to refract very strongly and ultimately to cross the axis significantly closer to the lens than rays closer to the optical axis. A spherical surface has the property that the rate change of the surface slope is exactly the same everywhere on the surface, and thus the aberration is inevitable. Let us consider reducing the slope of the surface toward the outer periphery of the surface in order to flatten the shape in the region surrounding the outer rays. If we make the surface shape gradually flatter as we proceed outward from the optical axis, we can differentially reduce the refracting ray angle so that the net effect is to bring all of the rays to a common focus position, as shown in figure (2.31-b). Figure (2.31-c) compares the spherical surface, which is steeper at its edge, with the aspheric surface, which is flatter at its edge. While correction of spherical aberration is not only application of aspheric surfaces, it is one of major application areas.

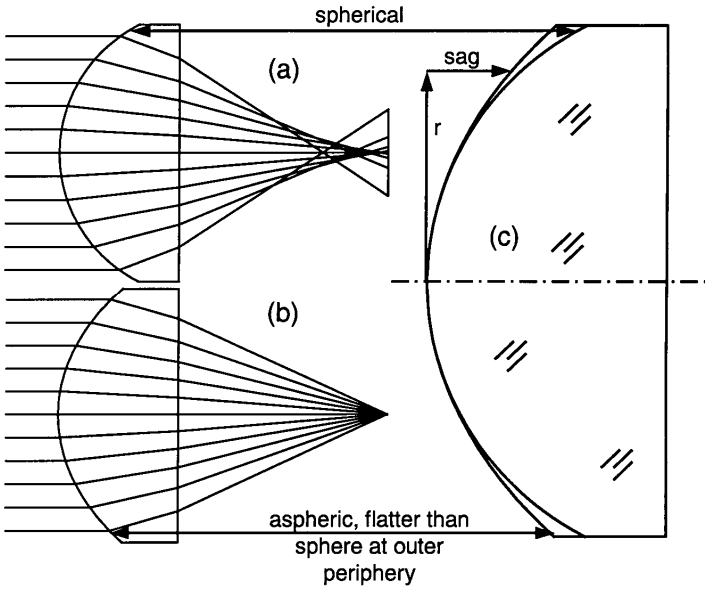

Figure (2.31): Comparison of a spherical and an aspheric lens [9]

Aspheric surfaces cannot be defined with only one curvature over the entire surface because its localized curvature changes across the surface (radius of curvature varies slightly with angle off axis). An aspheric surface is usually defined by an analytical formula, but sometimes it is given in the form of sag table for coordinate points across the surface.

The sag of surface is shown in figure (2.31). The most common form of an aspheric surface is a rotationally symmetric surface with the sag defined as a numeric equation of two parts-firstly as conic section departure from a sphere, then with further aspheric deviations according to higher polynomial terms, thus:

$$z = \frac{cr^2}{1+\sqrt{1-(1+k)c^2r^2}} + \sum a_i r^{2i} \qquad (2.13)$$

Where:

c is the base curvature of the base sphere at the optical axis or vertex (=1/radius).

k is conic constant or measure of conic shape of the surface, $k = -e^2$ (conic constant is minus the square of the eccentricity). Where: e is "eccentricity".

r is the radial coordinate measured perpendicularly from the optical axis; $r = \sqrt{x^2 + y^2}$.

$a_i r^{2i}$ are the higher –order aspheric terms (i.e. the 4^{th}, 6^{th}, 8^{th},…,etc.. order aspheric deformations respectively). Note that only even powers appear because of axial symmetry [9].

The aspheric surfaces give the optical designer more degree of freedom with which to correct aberrations. They are most often used in wide angle and zoom lenses.

2.7.1.1 Conic Surfaces

In the case where the higher-order aspheric terms in equation (2.13) are zero, the aspheric surface takes the form of a rotationally symmetric conic cross section (conic surface) with the sag defined as:

$$z = \frac{cr^2}{1+\sqrt{1-(1+k)c^2r^2}} \qquad (2.15)$$

In table (2.4), it is shown how conic surface takes on the following surface types as a function of the conic constant k in the sag equation. Or the conic constant defined type of conic surface, according to the table [9]

Table (2.4): Conic section types [19]

Shape of the surface	Eccentricity e of a plane curve	Conic constant value k
Sphere (circle)	0	0
Paraboloid	1	-1
Prolate ellipsoid (ellipse with foci on a line normal to the optical axis)	0< e < 1	-1< k < 0
Hyperboloid	> 1	< -1
Oblate ellipsoid (ellipse with foci on the optical axis)	< 0	> 0

Figure (2.32) shows nine surfaces having different conic constants but the same curvature. Most of us are generally familiar with the surface shapes described.

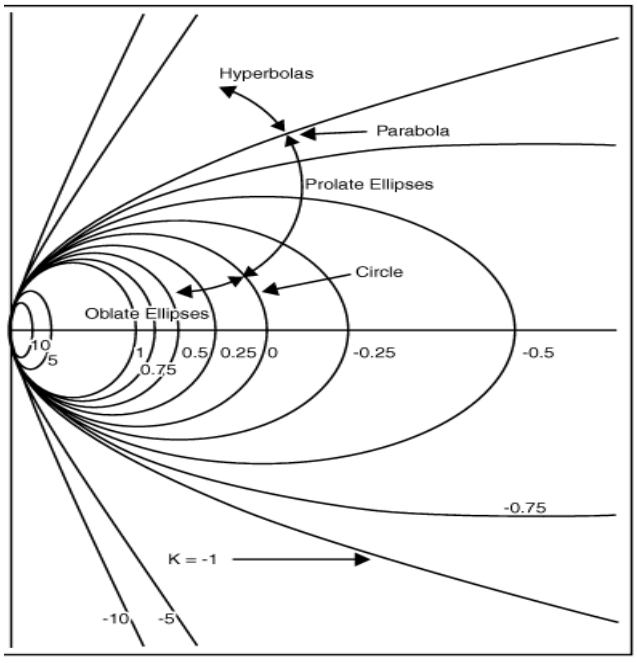

Figure (2.32): Conic surfaces with same curvature and different conic constant [23]

The primary reason for using aspheric component is to eliminate spherical aberration and other lower-order aberrations as axial chromatic aberration (especially when there is a constraint on the number of optical surfaces and incident allowed) [23]. If an aspheric surface is located at or near the aperture stop of a system, it will primarily affects or benefit spherical aberration, which is an axial aberration which, for the most part, carries across the field of view. As aspheric surfaces are located further from the stop, the can help to minimize some or all of the off-axis aberrations such as coma and astigmatism [9].

A good example of and aspheric surface used for astigmatism correction is shown in figure (2.33). In figure (2.33-a**),** we see a single-element lens with its aperture stop located far to the left of the lens. If the curved lens surface is spherical, the oblique rays create a footprint on the surface, which is larger in the plane of the figure than the orthogonal plane in/out of the figure. This trends to refract and pull the rays in the plane of the figure inward from where they would otherwise focus. We now need to ask ourselves what it would take to push the focus position outward and compensate for inward focus shift. The answer is to correct a more negatively powered surface in the plane of the figure at the outer periphery of the lens. This is shown the proper scale in figure (2.33-b) and in an exaggerated from in figure (2.33-c). This more negatively powered surface shape in the plane of the figure has virtually no effect in the orthogonal plane, hence the highly efficient correction of astigmatism by the aspheric surface [9].

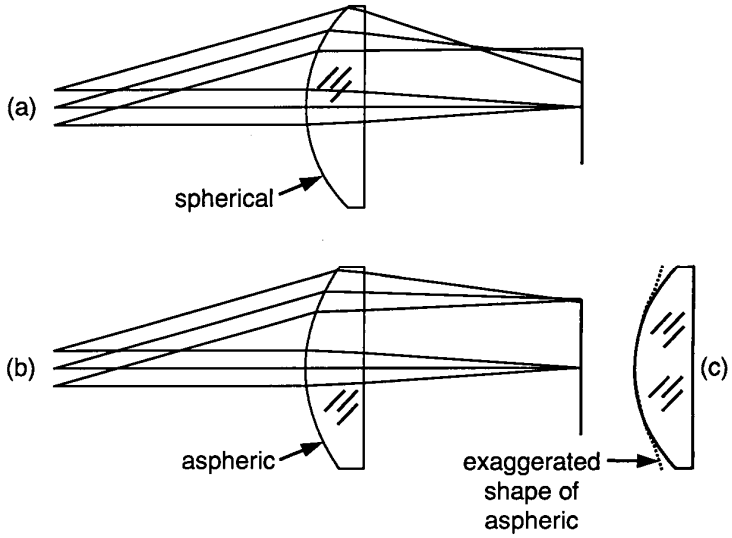

Figure (2.33): Correction of astigmatism with an aspheric surface [9]

However, most designers still prefer to use spherical rather than aspherical surfaces. The reason has more to do with fabrication issues than anything else. Aspheric are much harder to make and measure. More time and skill are required of the optician and metrologist, thereby driving up cost [the manufacturing cost for aspheres is typically 2 to 5 times that of spherical lenses with short radii [9]; but today with the advent of precise single-point diamond turning techniques, its adds little to the cost and time of fabrication to specify conics and up to 10^{th} or 12^{th} order aspherics in the reflective or refractive surface description [18]. Consequently, the use of aspherics is limited to cases where (a) there is no other way to correct the aberrations (b) a trade-off study has shown it to be cost effective in the long run. Finally, it should be noted that the use of an aspheric does not change any of first order design characteristics (cardinal points). All paraxial data remain the same [18].

There are some basic guidelines in the use of aspheric surfaces, and there are listed here:

1- Conic surfaces can be used for correcting third-order spherical aberrations and other low-order aberrations.

2- If we have a nearly flat surface, the use an r^4 and higher-order terms rather than a conic.
3- If we have at least a somewhat curved surface, then we can use the conic along with higher-order terms if required.
4- It is generally best not to use both a conic and an r^4 surface, as they are mathematically quite similar. This is because the first term of the expansion of conic is r^4. While they can both literally be used, the optimization process often tends to beat one against the other, yielding artificially large coefficients, and this may have an effect on the convergence the optimization.
5- Use aspheric beginning with lower-order terms and working upward as required. If we can stay with conic, this may make testing more manageable.
6- It is very dangerous to use a large number of aspheric surfaces, especially with higher-order terms. This is because they will beat against each other. This means that as one surface adopts a certain aspheric profile or contour, it may increase in its asphericity, with its effect cancelled by adjacent surface. For example, if the first of two closely located aspheric surfaces has significant surface departure from sphericity, the neighboring aspheric surface could very likely cancel this effect. While the lens may perform well on paper, we now need to manufacture two highly aspheric surfaces, a difficult and expensive task which may not be necessary.
7- If possible, optimize your design first using spherical surfaces, and then use the conic surface, else use aspheric coefficient in the final stages of optimization. This may help in keeping the asphericities to a more manageable level.

The common use of aspheric surfaces is in the thermal infrared where the cost of materials is extremely high. With the use of aspherics the

number of elements can be reduced to minimum, beside enhance the optical performance of IR optical systems [9].

2.7.2 Plane Parallel Plate

By definition, a plane parallel plate is flat and parallel. If this is not the case, it is a lens with convex or concave spherical cylindrical surfaces. The surfaces can also be aspheric on either or both sides. The plate can also be flat on both sides, with the surfaces not parallel to each other. In that case we have a prism. If the plate neither flat nor parallel, there is a problem.

If the plane parallel plate is inserted into an image-forming optical system, with its surface perpendicular to the optical axis (as IR detector window in case of thermal imaging camera), the image plane is shifted toward the right this relocation (longitudinal shift) occur if the plate is perpendicular to the optical axis, assuming the light is coming from left; therefore the spherical aberration is introduced [see figure (2.34)]. The amount of the spherical aberration/shift depends on the index of refraction of the material used and the thickness of it [14].

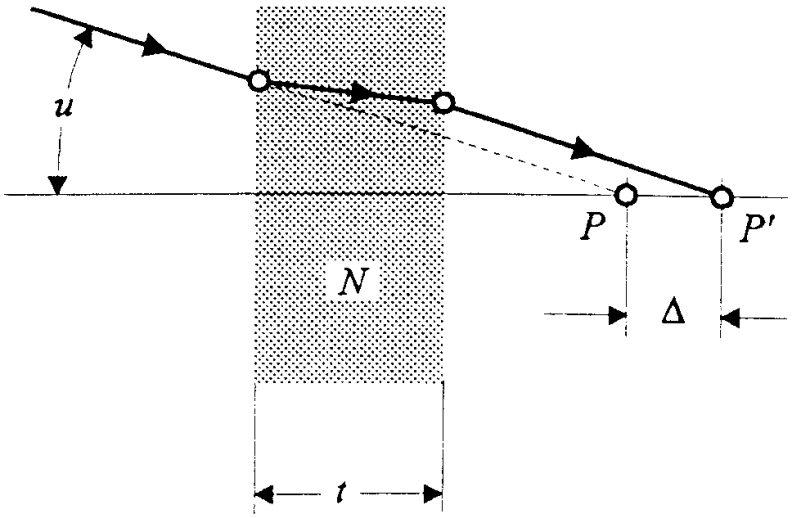

Figure (2.34): Longitudinal image shift caused by a plane-parallel plate [14]

For the paraxial region, this longitudinal displacement is:

$$\Delta_p = \frac{(N-1)}{N} t \qquad (2.16)$$

Where: *t* is the thickness of the plate with index *N*. outside the paraxial region, a more complex relationship applies:

$$\Delta_m = \left[1 - \sqrt{\frac{1-sin^2u}{N^2-sin^2u}}\right] t \;\cong\; \left[1 - \sqrt{\frac{4(f/\#)^2-1}{4N^2(f/\#)^2-1}}\right] \qquad (2.17)$$

Where *tan u =1/2(f/#)* ≈ *sin u*. while this introduces an error of about 12% for an *f/1* con, the error is already down to 3% for *f/2* and less than 1% for *f/4.*

The difference between Δ_m and Δ_p is the longitudinal spherical aberration contributed by the plane parallel-plate. It is positive value, which is referred to as overcorrected spherical aberration. The single element (single lens) already has undercorrected spherical aberration. in other words, the combination improves the situation slightly.

The second type of displacement occurs when the plate is tilted relative to the optical axis. The tilt causes the image shifted laterally, as seen in figure (2.35) [14].

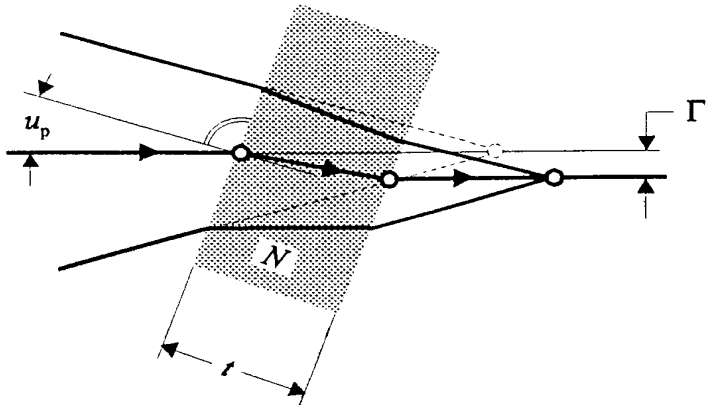

Figure (2.35): Lateral displacement of image by a tilted plane-parallel plate [14]

$$\Gamma_m = \left[1 - \sqrt{\frac{1-sin^2u_p}{N^2-sin^2u_p}}\right] t\, sinu_p \qquad (2.18)$$

Often, the beam splitter is tilted 45º relative to the optical axis the offset becomes then:

$$\Gamma_{45} = \sqrt{0.5}\left[1 - (2N^2-1)^{-1/2}\right] t \qquad (2.19)$$

This lateral displacement is about one third of the thickness (*t*) for glass with *N=1.5* and more than one half of thickness for germanium with *N=4.*

For small tilt angles (small u_p) the lateral displacement is:

$$\Gamma_s = \frac{(N-1)}{N} t\, u_p = \Delta_p u_p \qquad (2.20)$$

2.8 IR Optical Materials

While there are many glass types available for visible systems, there are only a very limited numbers of infrared transparent materials usable in thermal imager in the MWIR and LWIR bands. Some of them like halide crystal which are hyproscopic in nature and are soft may be suitable for optics as used in the laboratory condition but not at all field use [2]. The preferred IR materials with their important optical properties are shown in table (2.5).

Table (2.5): Optical properties (indices, *dn/dT*, and spectral range) of selected IR materials [25]

Material	Refractive Index		dn/dT (K^{-1})	Spectral Range
	MWIR λ=4μm	LWIR λ=10μm		
Germanium	4.0243	4.0032	0.000369	2 ~ 17μm
Silicon	3.4255	N/A	0.000160	1.2 ~ 9μm
ZnS (cleartran)	2.2523	2.2008	0.000054	0.37 ~ 14μm
ZnSe	2.4331	2.4065	0.000060	0.55 ~ 20μm
Gallium Arsenide	3.3069	3.2778	0.000148	0.9 ~ 16μm
AMTIR-1	2.5141	2.4976	0.000072	0.7 ~ 14μm
AMTIR-3	2.6200	2.6002	0.000091	1.0 ~ 14μm
AMTIR-4	2.6487	2.6353	0.000030	1.0 ~ 14μm
Sapphire	1.6753	N/A	0.000013	0.17 ~ 5.5μm

The selection of lens materials involves the consideration of many issues. A primary consideration is that of optical transmission. Many materials that transmit visible light are opaque in the IR wavelength and visa verse. The transmissions of system lenses are usually grouped into a

single system optical transmission, $\tau_{optic}(\lambda)$. The transmission of an optical system affects the amount of the flux that that propagates through the system and falls on the detector. A large transmission in the band of interest is desired. Also, the transmission is usually a strong function of wavelength, so the spectral transmission must be known along with the source spectrum and atmospheric transmission to determine the flux on the detector. The detector response is also a function of wavelength. All these spectral quantities are integrated over wavelength in order to give accurate radiometric quantities.

Lens selection must also include index of refraction considerations. If the index varies as strong function of wavelength, large chromatic aberrations occur. Sometimes a lens or lenses system is constructed from two different materials with spectral index function (dispersion) that cancel each other. Infrared lens materials usually have a higher index of refraction. Zinc selenide (ZnSe) index varies (depending on wavelength) from 2.4 to 2.7. Germanium (Ge) has an index of refraction of around 4 in midwave band.

Other material considerations are thermal properties, elastic constants, hardness, and other mechanical properties. Lens design and material selection is an extremely complicated process. Usually, a system-level engineer or scientist does not perform this level of development, as there are optical professionals that spend their lives producing optical designs. These professionals are usually consulted during the development of an IR optical system [12].

The material that has been selected for the design of this IR optical system is germanium. The salient features of germanium are discussed below.

2.8.1 Germanium (Ge)

The single crystal n-type germanium with resistivity around 4-30Ω cm is without doubt a near perfect material for IR lenses and windows for MWIR (3~5μm) and LWIR (8~12μm) regions. Recent advances in material manufacturing have eliminated the cost factor advantage of polycrystalline germanium over mono crystal. Therefore, for all practical systems, the optics industry uses single crystal germanium that has much better refractive index homogeneity as compared to polycrystalline germanium. Germanium has high mechanical strength (good hardness and hence scratch resistant) and can be made easily in any shape and size by diamond turning. Germanium crystals can be doped to control resistivity within 5-40Ω cm resistance (at 25ºC). The most suitable resistivity as an optical material is of the order 4-30Ω cm. Front element germanium suffers from frosting in cold climates. To get rid of frosting, an electric current is passed through the window/front end element. The resistivity of germanium causes a temperature rise within the material and thus provides for de-icing and defogging. Heated germanium windows are currently being produced with a thermal uniformity of ±1.5º F while maintaining a transmitted wavefront of λ/10 over an aperture of 200 mm and above, at 10.6 micron [2].

Germanium has very high refractive index (>4.003) which results in high optical power. This leads to smooth lens curvature (shallow curves with long radii) for imaging and thereby reducing germanium consumption. Moreover, a high refractive index material yields low spherical aberrations. In the LWIR band the dispersion of the refractive index as a function of wavelength is very low; therefore chromatic is also very small and often, no correction is needed. Another important parameter of germanium is that it shows a relatively high change in

refractive index with respect to temperature (i.e., $\frac{dn}{dT}$ is high). The $\frac{dn}{dT}$ of germanium is 0.000396/ºC as compared to the $\frac{dn}{dt}$ of 0.00000360/ºC for ordinary glass BK-7. This large $\frac{dn}{dT}$ calls for provisioning of athermalization, i.e. focus compensation with respect to temperature. The problem is that at 70ºC, the typical aerodynamic heating temperature, germanium lenses experience significant absorption. At 200ºC the transmittance drops to almost zero percent [2].

The maximum transmission of uncoated germanium is around 47% due to high surface reflection caused by the high refractive index. However, this transmission could be raised easily to a maximum of 98% by giving it an antireflection coating. In addition, germanium has a small thermal coefficient of expansion apart from good surface hardness and mechanical strength. The general myth that germanium blank contains 0.05% thorium or other radioactive source should be ignored as the user is not supposed to look directly through a ' germanium eye piece ' and the probability of such a dander has not been really detected so far by any researcher [2].

Electromagnetic interference (EMI) grad germanium is also produced for ship-borne applications, where radar signal can be strong enough to make nearby infrared systems ineffective. A ship-borne system's germanium windows should have resistivity of only 1-5ohm. Cm so that if the radar signal is effectively shorted out to the frame or the system's envelope, then the IR system works well without difficulty.

In brief, one can say about germanium that:

1- The n-type Ge is better than p-type because the absorption cross-section of the hole is approximately 20 times greater than the electro cross-section within 8 ~12 μm range

2- Resistivity of Ge between 4 to 30 Ω cm is considered to be ideal for infrared optical material.
3- The current popular specification that Ge blanks contain less than 0.05% thorium or other radioactive source materials can be dropped as no sign of the presence of radioactive material has been observed.
4- There is absorption at 11.7μm and a sharp sideband at the 11.9μm (lattice band) with one cm thick sample.
5- Transmittance for uncoated witness sample 0.2 inches thick cut from the same bowl as the finished blank should be: 8 -10μm >> 46%, 10 - 11μm >> 45%, 11 – 11.5μm >> 43%.

Advantages of Ge as an optical material

1- Has high refractive index and high optical power. Leads to smooth lens curvatures resulting in low Ge consumption.
2- Has low spherical aberration, low chromatic aberration; often no correction needed.
3- Results in low dispersion.
4- Has nearly all the qualities required, like strength, diamond turnability for use as lens or window material, and is free from radioactive substances. It is therefore to be the best material for infrared use.

Drawbacks of Ge as optical material

1- Is opaque in the visible region; so it is not suitable for dual bands using visible and IR.
2- High dn/dT compels introduction of athermalization techniques.
3- It is expensive with respect to other materials [2].

A rough estimation of the market share of applications of Ge is shown in figure (3.36).

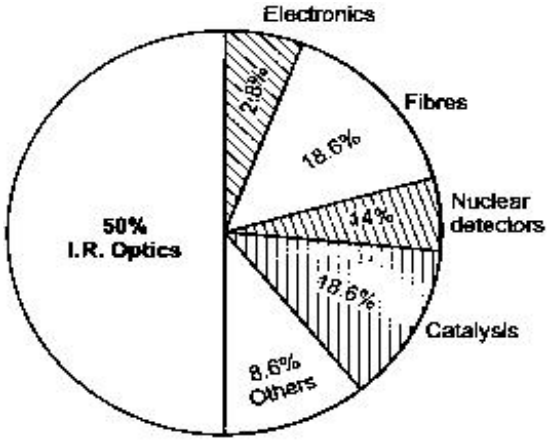

Figure (2.36): Rough estimate of market share of germanium [2]

In selection phase of optical materials to designing specific IR optical systems, the following properties of the selected materials must be taken into account in the selection process and should be examined in terms of the intended system application:

1- Spectral transmittance and its variation with temperature.
2- Index of refraction and its variation with temperature.
3- Hardness.
4- Resistance to surface attached by liquid.
5- Thermal conductivity.
6- Thermal expansion.
7- Specific heat.
8- Elastic module.
9- Softening and melting temperature.
10- RF properties.

The first two items are, of course, crucial in any application. Hardness and resistance to surface attack must be considered for protective windows and IR domes. Knowledge of the thermal coefficients and the elastic module is important when the system will exposed to high transient head load and in the design of mountings to prevent thermally induced stresses from causing the optics to fracture. Since a few materials soften at unusually low temperatures,

they should be not used in certain applications. Occasionally there is interest in dual-mode systems, that is, those combining infrared and radar and using common protective dome (IRRA dome); it is then necessary to know RF properties of the material as well [3].

DESIGN AND EXPERIMENTAL WORK

3.1 Introduction

The basic steps followed in design of high performance IR optical system for infrared thermographic camera which begins from choice of thermal detector module, identifying required basic parameters and specifications of the optical system, select some design criterion to arrive at the criteria for an optimum performance, and the design phase of high performance IR optical system at software level (ZEMAX) each of these have been clarified in this chapter. In addition to design of the simple mechanical case (objective) to integrate the IR detector module with designed and manufactured optical system which leads to the production of thermal camera. After that established PC software program to convert thermal/gray image to thermographic one and read the temperature of the object from thermal image was clarified here also.

3.2 IR Optical System Design

3.2.1 Choice of Thermal Detector

The thermal detector (which is usually based on a semiconductor material sensitive to low-energy infrared photons) is one of the most important subsystems of thermal imaging cameras is a heart of thermal imaging systems. Selection of the thermal detector is the first step or the first decision should be taken by the designer before entering into design phase of IR optical system, because it affects on the construction of the optical system which will be designed, or according to specification of it the IR optical system is built. The detector enters in accounts of design criterion of the optical system and in accounts of overall camera specification such as field of view (one of the most important basic

specifications of thermal camera), sensitivity and resolution of it. Therefore, a design of an IR optical system and thermal imager begins with specifications and availability of thermal detector.

In this work, the design of an IR optical system will depend on GUIDIR Company's production IR113 uncooled microbolometer (amorphous silicon, a-Si) focal plane array thermal imaging module [see appendix A]. The number of pixels (*384×288)* and pixel pitch (*25μm×25μm)* are most important specifications of the detector which affects on general specification of the optical system and then overall specifications of thermal camera. The optical interfaces of the detector that should take into account in the construction of the optical system are: the thickness (*1mm*) and the material (*Germanium*) of detector window (filter), and the distance between detector window and sensitive area (*3.15mm*). If any one of these are changed this leads to failure of the designed optical system.

3.2.2 The Design Criteria

In this work, for design a good IR optical system from optical, mechanical, and financial aspects, there are some criterions (goals/limitations/boundaries) must be met: Firstly, from optical point of view to constructs high performance IR optical system the design limits/criterions which must be achieved are that (performance goals): the diameter of diffraction blur (spot diagram) should be less than diameter of single pixel of detector (less than 25μm) as much as possible, and the polychromatic (for wavelengths 8, 10, and 12μm) Modulation Transfer Function (MTF) at cutoff frequency/Nyquist frequency (*Nyquist frequency = 1/2×pixel pitch = 20 lpmm*) at image should be above 0.5 and close to diffraction limit (close to ideal/free aberration system). Secondly, from mechanical point of view the criterions required in the designed IR optical system are that: light weight, small size, and short

length, and simple in structure. I mean compact design. And finally, low cost optical system from financial point of view.

Achieve these restrictions lead to design IR optical system characterized by high image quality, compact, and low cost design.

3.2.3 Basic Design Specifications (Optical Specifications)

The basic parameters/specifications required for the optical system which will design according to previous detector module [IR113] are shown in table (3.1).

Table (3.1): Basic design specifications/basic optical specifications

Wave band spectral range	8~12μm
Effective focal length (EFFL)	45mm
f/number (f#)	1.125
Field of view (FOV= HFOV×VFOV) (1)	12.8°×9.15°
Entrance pupil diameter	40 mm
Total track (TOTR) (2)	58.5 mm

Where:

(1) *The parameter FOV is depending on EFFL of the system and dimension of the detector in both horizontal and vertical directions.*

Effective focal length (EFFL) = 45mm.

Horizontal detector dimension (HDD) = horizontal number of pixels × pixel pitch

= 384 × 0.025 = 9.6 mm.

Vertical detector dimension (VDD) = vertical number of pixels × pixel pitch

= 288 × 0.025 = 7.2 mm.

Horizontal field of view (HFOV) $= 2\,tan^{-1}\left(\frac{HDD}{2\times EFFL}\right) = 2\,tan^{-1}\left(\frac{9.6}{2\times 45}\right) =$ *12.18°.*

Vertical field of view (VFOV) $= 2\,tan^{-1}\left(\frac{VDD}{2\times EFFL}\right) = 2\,tan^{-1}\left(\frac{7.2}{2\times 45}\right) =$ *9.15°.*

(2) *The parameter total track (TOTR) is a length of the optical system as measured by vertex separations between the "left most" and "right most" surfaces. The computation begins at surface 1. The thickness of each surface between surface 1 and the image surface is considered [26]. Generally this*

parameter depending on EFFL of the optical system; but is no precise relation/equation between parameters (TOTR& EFFL) as in the case of the FOV case. In this work because we are target a compact optical system as mechanical goal. For this reason and just from my previous experiences the best choice of total track is TOTR = 1.3×EFFL = 1.3×45 = 58.5 mm.

3.2.4 Design Procedure

After selecting the heart of the thermal camera (I mean the detector) and identify the basic parameters that are required and defined for the features of the optical system which will be designed/constructed. Now we can go the design/construction phase of targeted optical system.

The basic design parameters in table (3-1) meet the target requirements of an IR optical system if the design criterions that identified is section (3.2.2) are achieved. For the design, optimize, analyze, and thus construction the IR optical system for uncooled thermographic camera ZEMAX optical design program (optical design and analysis code) was selected as the main workhorse throughput this project, because it's a comprehensive software tool. It integrates all the features required to conceptualize, design, optimize, analyze, tolerance, and document virtually any optical system. It is widely used in optics industry as standard design tool. This program uses ray tracing to model refractive, reflective, and diffractive sequential and non sequential optical systems. Most optical systems and virtually all imaging systems (as in our case) are well desired by sequential surface model. It is fast, efficient, and lends itself to optimization and detailed analysis. In sequential ray tracing a ray starts at object surface (always surface number 0). The ray traced to surface 1, then to surface 2, and so on. Sequential ray tracing uses a "surface" model; each transition from one optical space to another requires a surface [26].

ZEMAX is a program which can model, analyze, and assist in the design of optical systems. The interface to ZEMAX has been designed to be easy to use, and with a little practice it can allow very rapid interactive design. Most ZEMAX features are accessed by selecting option from either dialog boxes or pull-down menus. Keyboard shortcuts are provided for quickly navigation or bypassing the menu structure. Neither the ZEMAX program nor the ZEMAX documentation will teach the designer how to design lenses or optical systems. Although the program will do many things to assist designer in designing and analyzing optical systems, you are still the designer. Technical support available to ZEMAX users includes assistance in using the program, but does not include tutoring on fundamental optical design principles. Most importantly, ZEMAX is not a substitute for good engineering practices. No design should ever be considered finished until a qualified engineer has checked the calculations performed by the software to see if the results are reasonable. This is particularly important when a design is to be fabricated and significant costs are involved. It is the engineer's responsibility to check the results of ZEMAX, not the other way around [26].

Generally, the optical design process includes a myriad of tasks that the designer must perform and consider in the process of optimizing the performance of an imaging optical system. The following are the basic steps generally followed by an experienced optical designer in performing a given design task. Needless to say, due to the inherent complexity of optical design, the processes often become far more involved and time consuming. Figure (3.1) outlines these basic steps [9].

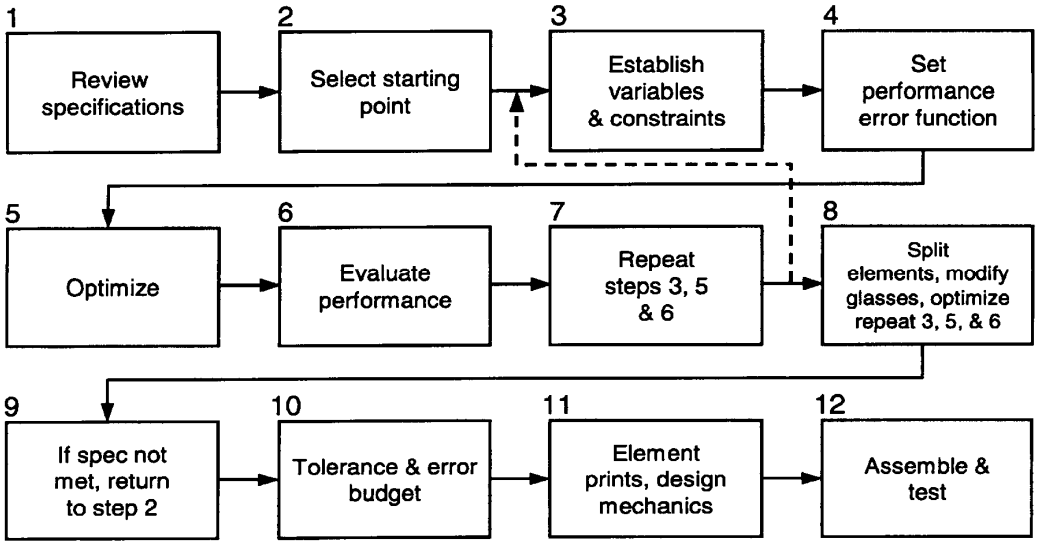

Figure (3.1): Lens design and optimization procedure [9]

To get the final design there are many critical and necessary steps in software package (ZEMAX) should be done carefully by deep and true understanding, the sequence of these steps briefly are:

- Entered the starting point into software package (ZEMAX) and setting the basic parameter of the optical system like system aperture, FOV, operating wave length, EFFL, f/number, and entered the information about lenses itself like: surface type, surface radius of curvature, element thickness and material.

  The selection of starting point is the more critical decision made by the designer. In this work the starting point was chosen from my previous work and experience in the field of design IR optical systems. In this step put in mind the starting point which should be chosen, wherever possible, be configurations which inherently capable of meeting the specifications for the design. For example EFFL, entrance pupil diameter, FOV, and f/number, etc**.**

- After entered the starting point into software and setting basic parameter, and determined the degree of freedom by establish the variable (as surfaces radius of curvature, element and air thickness, surface type, and etc.) and constraints, and set the

performance error function or create merit function (the merit function is a numerical representation of how closely an optical system meets a specified set of goals. ZEMAX uses a list of operands which individually represent different constraints or goals for the system. Operands goals such as image quality, focal length, length of system, and other/ operand within merit function define the goals which are attempting to achieve in final design. The merit function is proportional to the square root of weighted sum of the squares of the difference between the actual and target value of each operand in the list. The merit function is defined this way so a value of zero is ideal [22]. It now time to initiate optimization to achieve the final design, [in lens design the goal of optimization is to reduce the merit function as much as possible, because the smaller the final value of this function (error/merit function) the closer the optical system is to desired sate. Optimization algorithm will attempt to make the value of the merit function as small as possible. Optimization requires three steps: 1) a reasonable system which can be traced, 2) specification of the variables, and 3) a merit function [22]. All of these steps which precede the optimization process were done carefully.

- Evaluated the optical system performance by using criteria were specified for the optical system to ensure that the design criterions (optical criterions) compatible with basic optical specifications (mechanical criterions) are met. ZEMAX optical design program provides many analysis/diagnostic features either graphic or text used to evaluate the designed optical system optically and measure the optical performance of obtained optical system as: spot diagram, modulation transfer function (MTF), ray

fan plot, encircled energy, chromatic focal shift, and others. In addition to prescription data this function generates a list of all surfaces data, and summarizes the optical system. It's suitable for describing the lens/optical system prescription.

Most work of design into software confined in the last 2 steps (optimization and evaluation). Therefore, these steps are repeated (as closed loop) frequently as many times as necessary by true understanding and many adjustments and tradeoffs until the desired performance goals of the optical system are met. That means the construction of final design was done carefully.

- By following the previous steps the IR optical system was designed after many optimization cycles and many adjustments/tradeoffs to the carefully selected starting point in the design phase at the program (ZEMAX) to meet the performance goals of the IR optical system, thus the final design was constructed. The results obtained from designed IR optical system or performance of it will discuss in chapter 4.
- Performed a tolerance analysis, tolerance is very important part of the optical design; a design is not complete without tolerance analysis because no optical or mechanical part can be fabricated or aligned "perfectly". Tolerance is small errors/imperfections allowed in fabrication and assembly of the optical elements (lenses). The amount tolerance values and impact of these errors value are determined as the last step of the design processes [See analysis of tolerances text window].

By the end of tolerance analysis step the design of IR optical system was finished and will be ready to enter into manufacturing of the design stage. Therefore, the mechanical drawing of optical elements (lenses) based on tolerance analysis was done to send the designed optical

system (3 germanium lenses) to a company specializing in production of this type of lenses to do the process of industrialization.

The drawings of 1st, 2nd, and 3rd lenses that will send to a special manufacturer company to do the industrialization process of it are shown in Figure (3.2), figure (3.3), and figure (3.4) respectively.

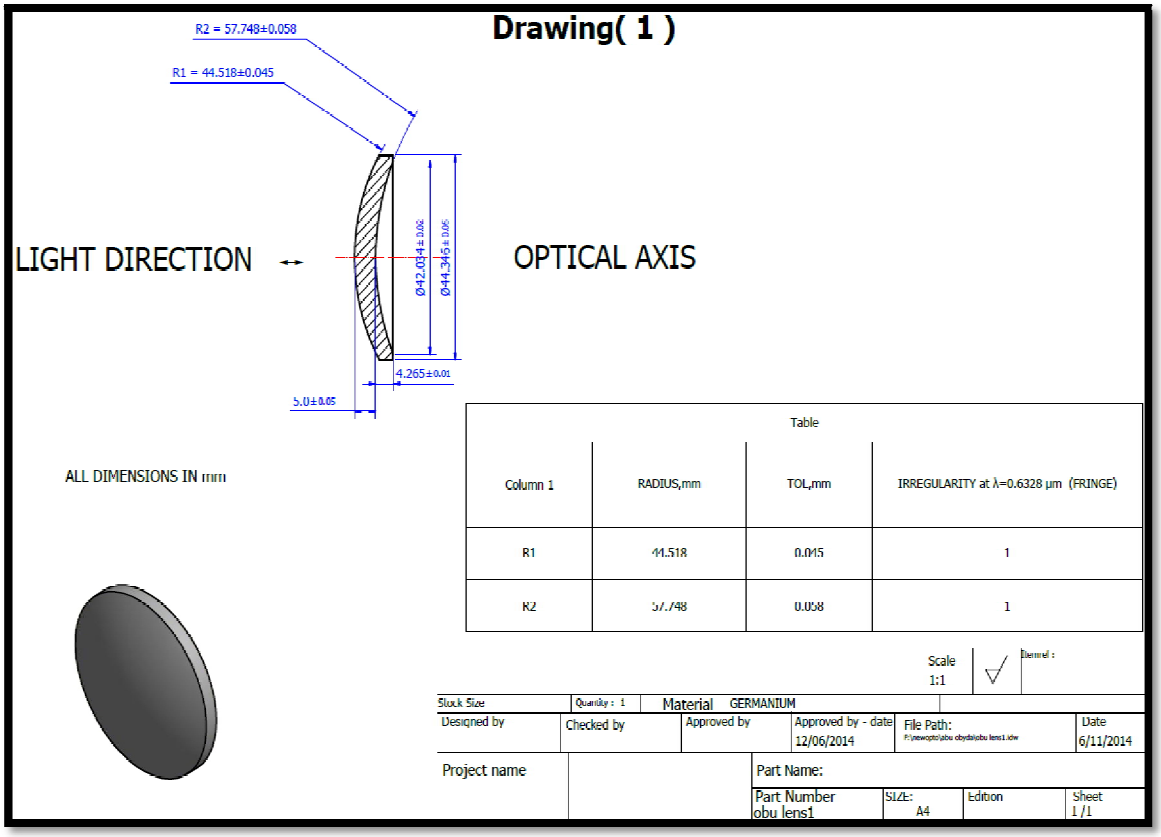

Figure (3.2): Drawing of 1st lens

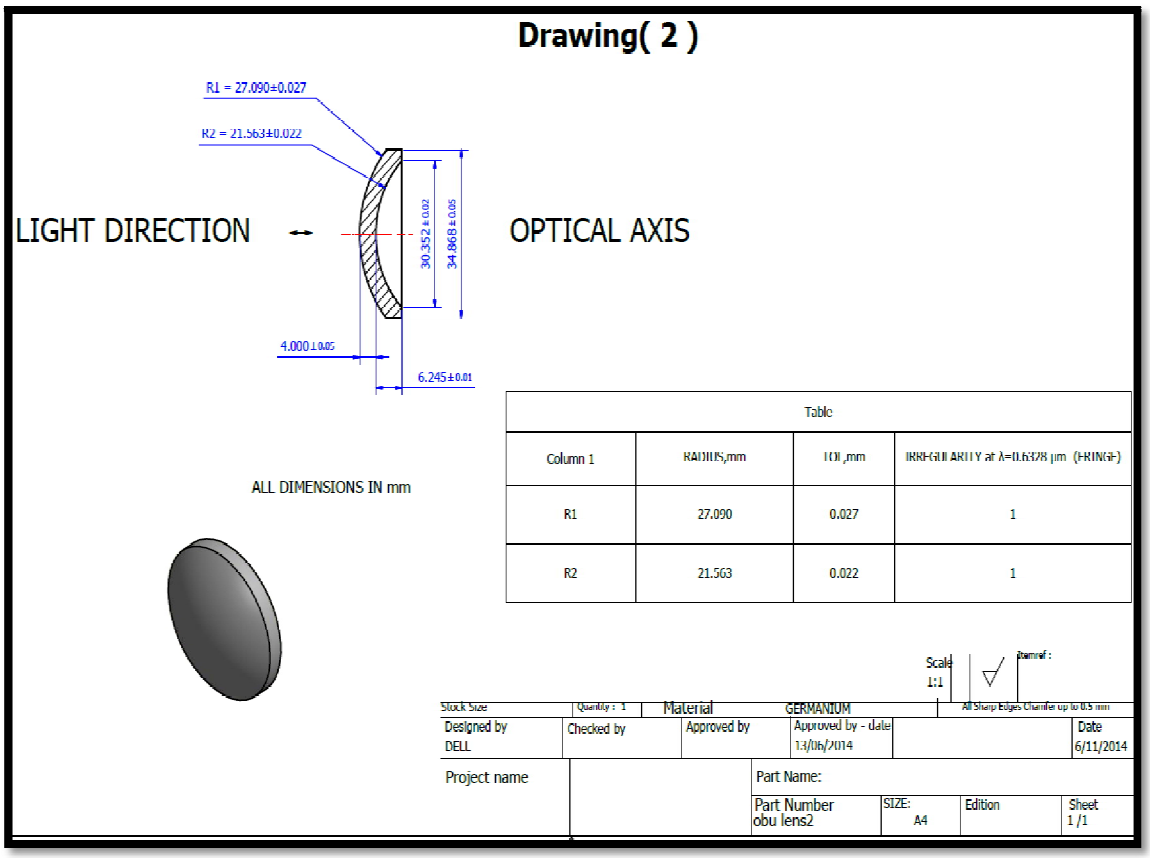

Figure (3.3): Drawing of 2nd lens

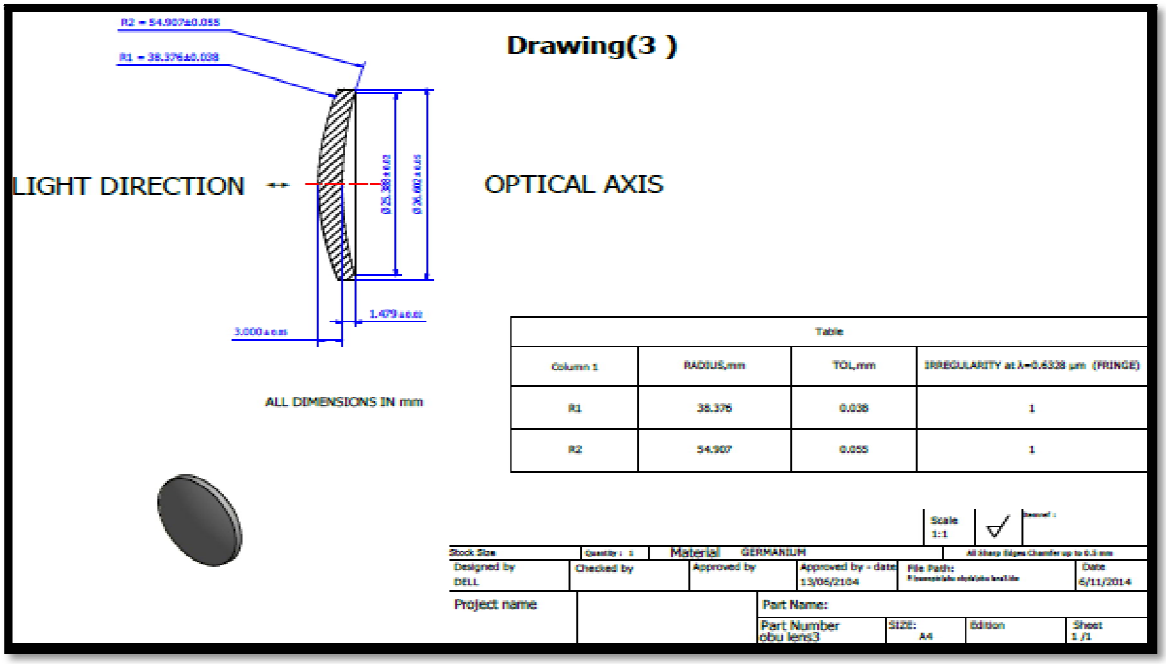

Figure (3.4): Drawing of 3rd lens

3.2.5 Defocus Treatment

Generally in all imaging systems when the object becomes close to the camera, this leads to the emergence additional type of aberration on the

final image of that object. This is type of aberration is called defocus (focus shift). It appears as a blurring (degradation in quality by reduction the sharpness and contrast) in final image. The defocus (focus shift) is a significant problem exactly in the infrared region.

The problem of defocus (focus shift) in this design was solved by mechanical passive method, because it simple method, no need any additional parts, and done manually. The basic principle behind this approach is to passively modify the axial position (longitudinal movement) of lens or lens group (focusing lens) in order to compensate the focus shift. In our design this mission is done by using the 3rd lens as focusing lens to compensate the focus shift caused by the approaching of the body to the image-forming device (thermal camera).

By ending of this task (defocus treatment) the minimum distance between the object and the camera to create a clear image (focusing image) was determined, and also the exact distance traveled by 3rd lens (focus lens) to treatment the defocus (maintain the focus fixed) was calculated [see results in table (4.4)] and was given to mechanical engineer for putting as consideration in the design of mechanical case.

3.3 Design and Manufacture of Mechanical Case

The mechanical case plays as holder (objective) to holds the 3 germanium lenses (optical system) in its proper and accurate positions, and linker carefully between the optical system and thermal detector module (IR113) in order to assemble them (germanium lenses + thermal detector module) in a single portable unit.

Design of the mechanical case (objective) was done with participation of mature mechanical engineer (designer) after giving to him all the necessary and important optical system data which will be required as important preliminary information in the design and will affect on the

construction of the mechanical case. This data and values were given to the mechanical designer with tolerances and mechanical considerations, such as:

- The diameters, radiuses of curvature, and thicknesses of lenses as shown in figure (3.2), figure (3.3), and figure (3.4) for 1^{st}, 2^{nd} and 3^{rd} lens respectively.
- The air thickness number one (air gap between 1^{st} and 2^{nd} lens) is 10 ± 0.05 mm.
- The air thickness number two (air gap between 2^{nd} and 3^{rd} lens) is 22.92 ± 0.05 mm.
- The air thickness number three (air gap between 3^{rd} lens and detector window) is 9 ± 0.05 mm.
- The distance traveled by 3^{rd} lens inside the case to accomplish the focusing task is 0.52 mm.
- The dimensions and form of the detector module inside its house are available at designer as hard unit.
- The centers of curvature of all surfaces fall on a common line, i.e., the optical axis with error in decentering ± 0.05mm in X and Y axis.
- Tolerance for lenses in the tilt is ±0.033° in X and Y axis. [see tolerance values in table (4.3)].

The mechanical designer put the previous constraints into account and use INVENTOR mechanical design program to design simple (uncomplicated as possible) mechanical case (objective). Figure (3.5) shows the drawing of the mechanical case which designed in order to hold/carry the IR optical system (3 germanium lenses) and link it with thermal detector module (IR113).[see figure (4.13)]

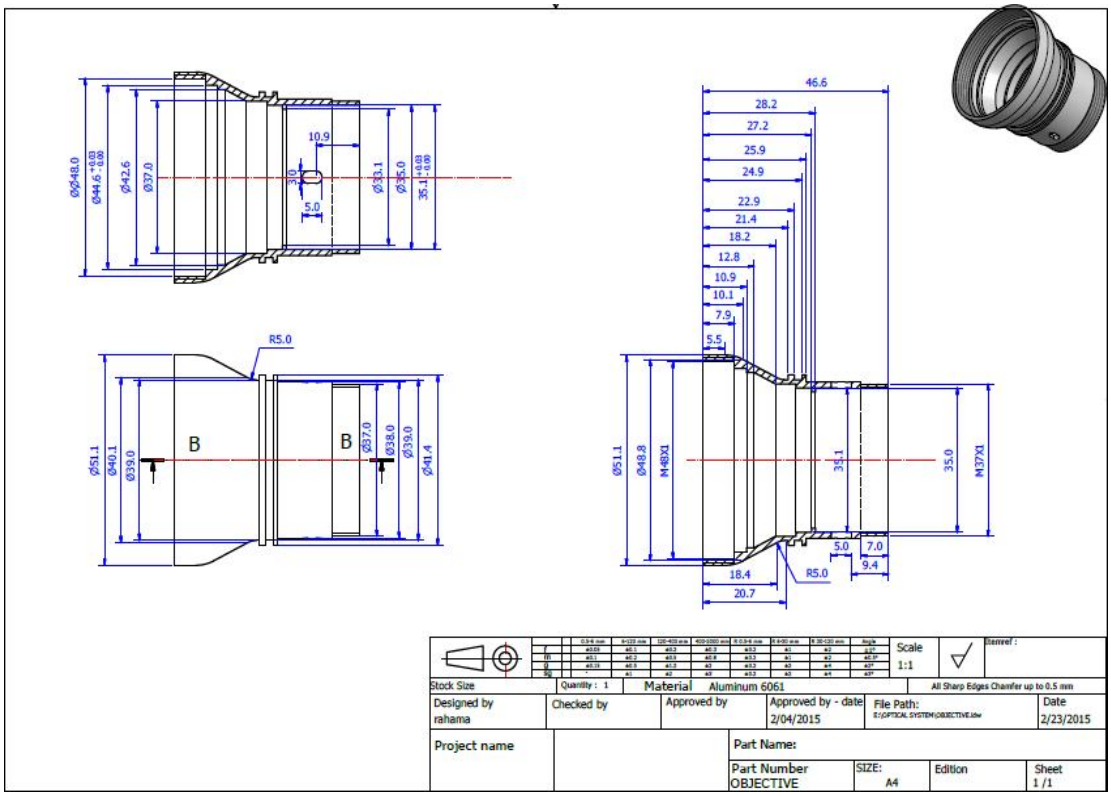

Figure (3.5): Drawing of mechanical case (objective)

The mechanical case was manufactured from Aluminum alloy (6061) in specializing mechanical company. Figure (3.6) shows the assembly drawing of the mechanical case with 3 germanium lenses (items number 2).

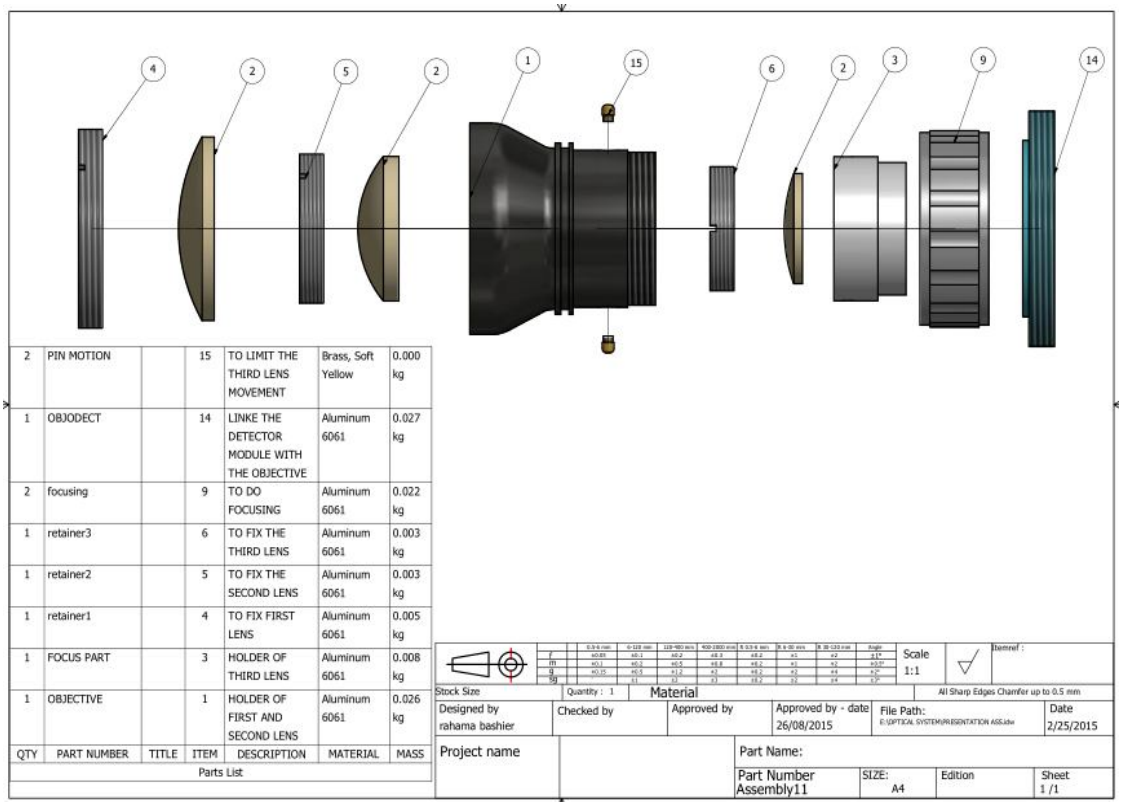

Figure (3.6): Assembly drawing

3.4 Creation of Thermal Image Processing Software

The function of this software is converting the thermal (gray/monochrome) images that will be obtained from the thermal camera which was designed to thermographic (pseudo/flash color) images in order to improve the visibility and mainly to read the object's temperature from thermographic image.

The idea of this program is based on this fact: Thermal imaging systems senses the radiation (continual emission of energy) that appears to emanate (emitted) from surface, the emitted energy depends upon the surface temperature and surface characteristics (emissivity), therefore, in reality the thermal images of high temperature objects appears more bright and intense due to it has more emission energy than cooled (low temperature) objects. The relation between intensity of the thermal image and the object temperature has been used to measure the temperature of the object from its thermal image by knowing all of

image intensity and emissivity of the object through establish of thermal images processing software and authorship an equation linking the image intensity and emissivity of the object as input values and temperature of the object. The MATLAB software was used to establishing this thermal image processing software (PC software), [see appendix C].

The steps involved to create this software program are as follows:

- Firstly, find an ideal source of infrared (can control its temperature, and it is known emissivity), these terms and more applicable to a blackbody that exists in the Minimum Resolvable Temperature Difference (MRTD) test station, see figure (3.7).

Figure (3.7): The MRTD test station and thermal camera

- Used the thermal camera which was designed and test station to capture several thermal images of the blackbody at different temperatures and known in advance.

- Applied one of MATLAB predefined color maps (jet: ranges from blue to red, and passes through the colors cyan, yellow, and orange [27].) On the thermal images that obtained from previous step in order to convert them to flash color (thermographic) images. [see results in table (4.5)]

  Table (4.5) shows the output of these steps, i.e. thermal (gray) images and its information (temperatures) in addition to thermographic (flash color) images corresponding to each case.

The next part of this program is dedicated to calculate the object temperature from its thermal image.

An image may be defined as two-dimensional function, *f(x, y)*, where *x* and *y* are spatial (plane) coordinates, and the amplitude of f at any pair of coordinates (*x, y*) is called the intensity of image at that point. The term *gray level* is used often to refer to the intensity of monochrome images. Converting an image to digital form requires that the coordinates, as well as the amplitude, be digitized. Thus when *x, y*, and the amplitude value of *f* are all finite, discrete quantities, we call the image a digital image [27]. By using these finite and discrete quantities of *x, y* and amplitude of *f*, and focusing on the amplitude (intensity or gray level) value of digital image versus temperature this program was created. This is because the intensity values are proportional with temperature.

The steps followed for completion the second part [read a temperature of the object (currently is blackbody) from its thermal image] as follows:

- The same setup that shown in figure (3.7) was used for the purpose of captured several images of blackbody also at different temperatures and known in advance.

- Entered these images in software and read the intensity (gray level) of each thermal image at specific spatial coordinate (x, y) as fixed criteria in all images. See results in table (4.6).

Of course the intensity (gray level) of these images at these specific coordinates (x, y) varies with temperature difference, and the relationship between the intensity (gray level) and the temperature of blackbody or any other body can be imaged by the thermal camera is a direct proportional relationship.

- The values of images intensity (gray levels) as independent variable Vs known temperatures of the blackbody as dependent variable which shown in table (4.6) was plotted in curve [see figure (4.15)].
- Fitted the curve and found from it a polynomial of third-degree linear equation (linear model poly3) linking between the image intensity of blackbody and the blackbody temperature for the purpose of finding the temperature of blackbody from its thermal image [see equation (4.1)].

The equation (4.1) can be used to predict and find the temperature of any other object/target (non-blackbody/gray body) which can be imaged by this thermal camera just by knowing the emissivity of this object/target (see appendix B). Of course the emissivity of any other objects less than emissivity of blackbody; I mean less than 1 always.

- By knowing the image intensity (gray level) and multiplying the equation (4.1) in the emissivity value for any other target (non-blackbody) we become able to find the temperature of that target from its thermal image. The figure (3.8) illustrates the flowchart of this thermal image processing software.

- testing of the equation that link between intensity of thermal images and temperature of objects was done by imaging different objects known in advance all of their temperature and emissivity in order to calculate their temperature from its thermal image by using of this software and compare between values of temperature which known in advance and calculated by software [see equation (4.2) and table (4.7).

The details of this software appear in flow chart of thermal image processing software, and MATLAB Code who established to the thermal image processing which show in figure (3.8) and appendix C respectively.

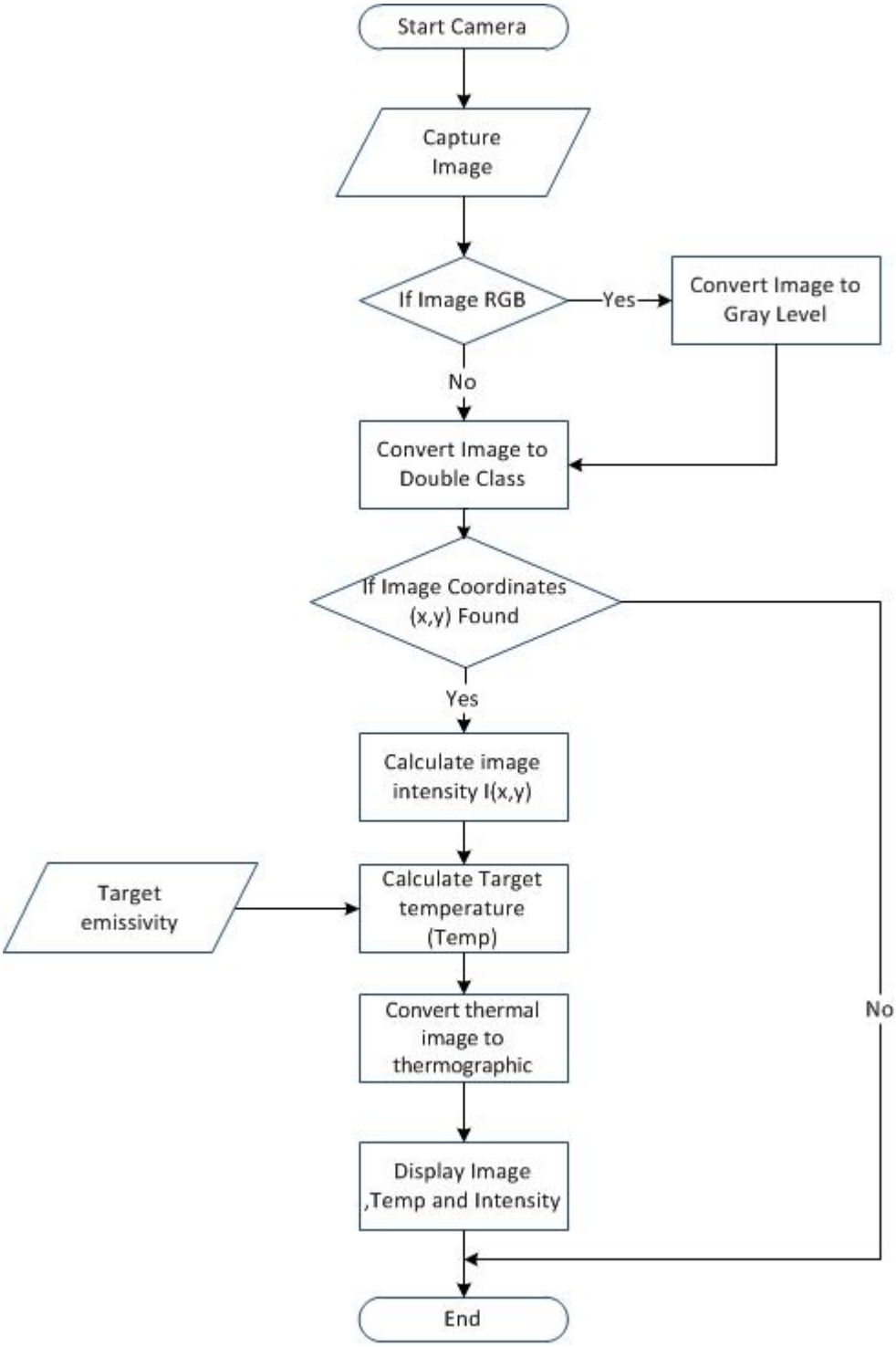

Figure (3.8): Flow chart of thermal image processing software

RESULTS AND DISCUSSION

4.1 Introduction

This chapter was specified to discuss the results which have been obtained from the work which was introduced in chapter 3. Section 4.2 deals with the detailed results of the designed which include; general specification of constructed optical system, evaluation of it, tolerance analysis, and solve of defocus treatment. Section 4.3 was customized to mechanical case and the construct of thermal camera and takes multiple images so as to ensure the quality of designed IR optical system. In section 4.4 the results which will be discussed related to thermograhic images that have been obtained from the addition of image processing software (PC program) to thermal (black &white) images in order to be converted to a thermographic (flash color image) one, and the temperatures values that have been read from thermographic images for several cases/bodies according to the apparent color on it.

4.2 IR Optical System

4.2.1 General Specifications of Constructed Optical System

The specifications of final designed and constructed IR optical system based on IR113 thermal detector module are shown in table (4.1).

Table (4.1): Final design specifications

Detector	
Detector material	UFPA microbolometer, a-si
Spectral range	8~12 µm
Resolution (number of pixels)	384×288
Pixel pitch	25 µm
Noise equivalent temperature difference (NETD)	<100mK@30°C
Thermal response time	7 ms
Fill factor	>80%
Bad pixel	<1%
Optics	
Effective focal length (EFFL)	45 mm
f/number (F#)	1.125
Field of view (FOV)	12.18°×9.15°
Focus	5m to infinity
TOTR	58.5 mm

Figures (4.1a), (4.1b), and (4.1c) show 2D, 3D, and shaded model layout diagrams of the constructed IR optical system.

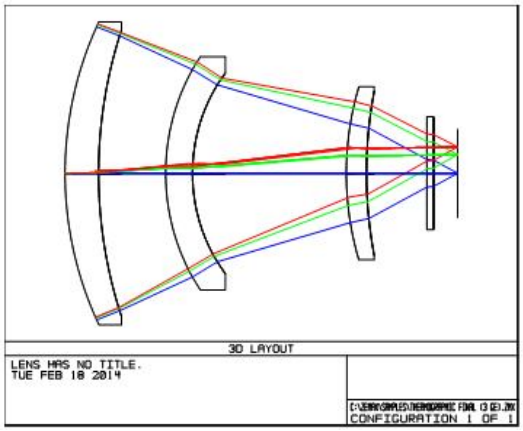

Figure (4.1a): 2D layout

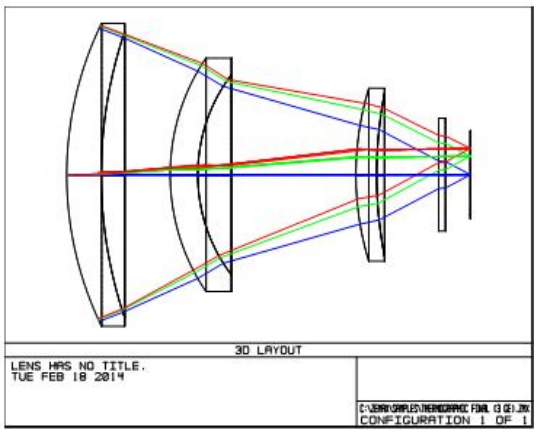

Figure (4.1b): 3D layout

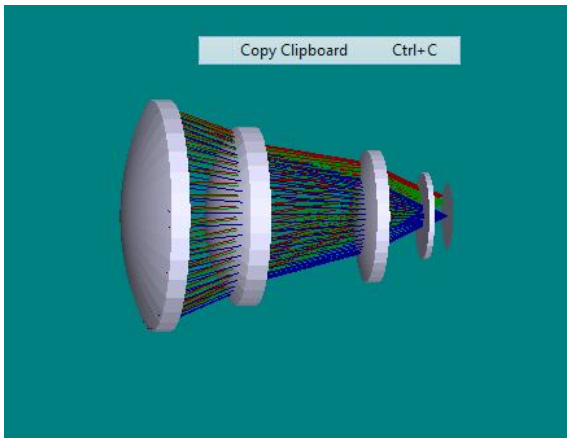

Figure (4.1c): Shaded model layout

- ✓ The designed IR optical system consists of 3 lenses made from germanium (Ge) material.
- ✓ All surfaces of lenses in this design (6 surfaces) are spherical surfaces with exception of the first surface of the lens number 1; it is a conic (simple aspheric) surface. The use of this surface contributed to make the design: better in aberration correction, this surface alone doing the mission of number of spherical surfaces in aberration correction with high efficiency, light in weight and better in transmission by decreasing the number of surfaces, and more compact design.
- ✓ The weight of overall lenses without mechanical considerations is 55.21g, and real weight is 70g because of mechanical considerations (i.e. the increase in diameters of manufactured lenses in order to be installed in the mechanical case about 2mm).
- ✓ The length of the system is very compact (TOTR =58.5mm/ 5.85cm).
- ✓ The field of view is large enough (12.18°×9.15°), this allows the camera to view or cover large area (for example covers area 2.16×1.61 m^2 at a distance of 10m).
- ✓ F/number of system is low (F# =1.125), therefore the speed of designed optical system is high. Thus its ability to capture sharp images for quick targets.

The prescription of the final design is shown in report of system prescription data text window below which generated from ZEMAX.

System/Prescription Data

File : c:\ ZEMAX\ samples\ thermographic final (3GE).ZMX
Title : lens has no title.
Data : TUE FEB 18 2014

GENERAL LENS DATA:

Surfaces	:	9
Stop	:	1
System Aperture	:	Entrance Pupil Diameter = 40
Glass Catalogs	:	Schott INFRARED
Ray Aiming	:	Off
Apodization	:	Uniform, factor = 0.00000E+000
Effective Focal Length	:	45.00001 (in air at system temperature and pressure)
Effective Focal Length	:	45.00001 (in image space)
Back Focal Length	:	3.592533
Total Track	:	58.5
Image Space F/#	:	1.125
Paraxial Working F/#	:	1.125
Stop Radius	:	20
Paraxial Magnification	:	0
Entrance Pupil Diameter	:	40
Entrance Pupil Position	:	0
Exit Pupil Diameter	:	146.5855
Exit Pupil Position	:	-164.8962
Field Type	:	Angle in degrees
Maximum Field	:	7.614
Primary Wave	:	10
Lens Units	:	Millimeters

Fields : 3
Field Type: Angle in degrees

#	X-Value	Y-Value	Weight
1	0.000000	0.000000	1.000000
2	4.300000	3.230000	1.000000
3	6.090000	4.570000	1.000000

Wavelengths : 3
Units: Microns

#	Value	Weight
1	8.000000	1.000000
2	10.000000	1.000000
3	12.000000	1.000000

SURFACE DATA DETAIL:

Surface OBJ	: STANDARD
Surface STO	: STANDARD 1ST LENS
Surface 2	: STANDARD
Surface 3	: STANDARD 2ND LENS
Surface 4	: STANDARD
Surface 5	: STANDARD 3RD LENS
Surface 6	: STANDARD
Surface 7	: STANDARD DETECTOR WINDOW
Surface 8	: STANDARD
Surface IMA	: STANDARD FPA

SOLVE AND VARIABLE DATA:

Curvature of 1	: Variable
Conic of 1	: Variable
Curvature of 2	: Variable
Thickness of 2	: Variable
Curvature of 3	: Variable
Curvature of 4	: Variable
Thickness of 4	: Variable
Curvature of 5	: Variable
Curvature of 6	: Variable
Thickness of 6	: Variable

INDEX OF REFRACTION DATA:

Surf	Glass	Temp	Pres	8.000000	10.000000	12.000000
0		20.00	1.00	1.00000000	1.00000000	1.00000000
1	GERMANIUM	20.00	1.00	4.00532048	4.00312464	4.00233954
2		20.00	1.00	1.00000000	1.00000000	1.00000000
3	GERMANIUM	20.00	1.00	4.00532048	4.00312464	4.00233954
4		20.00	1.00	1.00000000	1.00000000	1.00000000
5	GERMANIUM	20.00	1.00	4.00532048	4.00312464	4.00233954
6		20.00	1.00	1.00000000	1.00000000	1.00000000
7	GERMANIUM	20.00	1.00	4.00532048	4.00312464	4.00233954
8		20.00	1.00	1.00000000	1.00000000	1.00000000
9		20.00	1.00	1.00000000	1.00000000	1.00000000

ELEMENT VOLUME DATA:

Values are only accurate for plane and spherical surfaces. Element volumes are computed by assuming edges are squared up to the larger of the front and back radial aperture. Single elements that are duplicated in the Lens Data Editor for ray tracing purposes may be listed more than once yielding incorrect total mass estimates.

		Volume cc	Density g/cc	Mass g
Element surf 1 to 2		5.875765	5.327000	31.300203
Element surf 3 to 4		3.470024	5.327000	18.484819
Element surf 5 to 6		1.018147	5.327000	5.423669
Total Mass:				55.208691

4.2.2 Evaluation of Constructed IR Optical System

There are many analysis (diagnostic) tools, either graphic or text in ZEMAX program used to analyze and measure performance of obtained IR optical system. Most important tools in this application (IR optical system) from my point of view used to evaluate and measure the quality of this IR image forming designed optical system are:

4.2.2.1 Spot Diagram

It's very useful analysis tool, because one of the most important criterion used in creation of this design is that: the diffraction blur (spot diagram) of point source should be less than pixel pitch (25μm) and concentrate on it as much as possible.

As shown in figure (4.2) the black box surrounding the spot represents the dimension of pixel (box width= 25μm), and root mean square of spot radiuses for all selected field points (on axis= 0.00°×0.00°, 0.7FOV= 4.30°×3.23°, and full FOV= 6.09°×4.57°) are 5.928μm, 8.006μm, and 8.847μm for on axis, 0.7FOV, and full FOV points respectively. These values of RMS radius are very acceptable value. And as shown in same figure most geometry of the spot is constrain at pixel (box width), thus one of very important targeted criteria is met in this design.

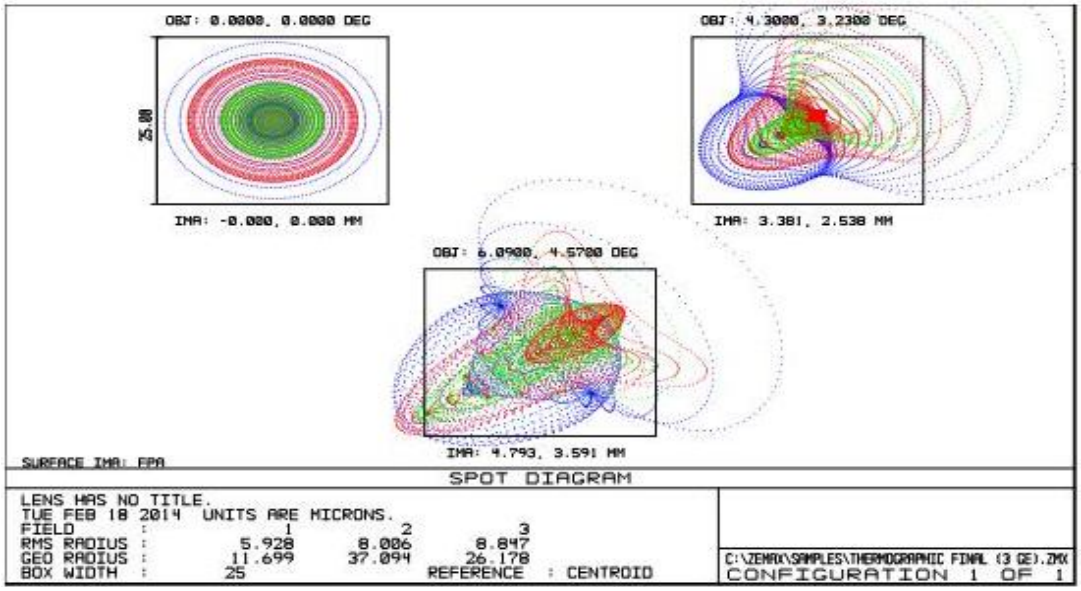

Figure (4.2): Spot diagram on 25μm pixel for on axis, 0.7FOV, and full FOV points

4.2.2.2 Modulation Transfer Function (MTF)

It's best and more comprehensive way to evaluate image forming optical systems. The MTF used as criterion in this design [see 3.2.2 design criterion]. As shown in figure (4.3) the lower value of MTF at cutoff frequency (Nyquist frequency) 20cycle/mm is 0.56 at edge of FOV, this value is greater than targeted value in design criterion (0.5). and the MTF values for on axis and 0.7FOV very close to diffraction limit (ideal/free aberration system) MTF values, so this criteria is met well in the this optical system.

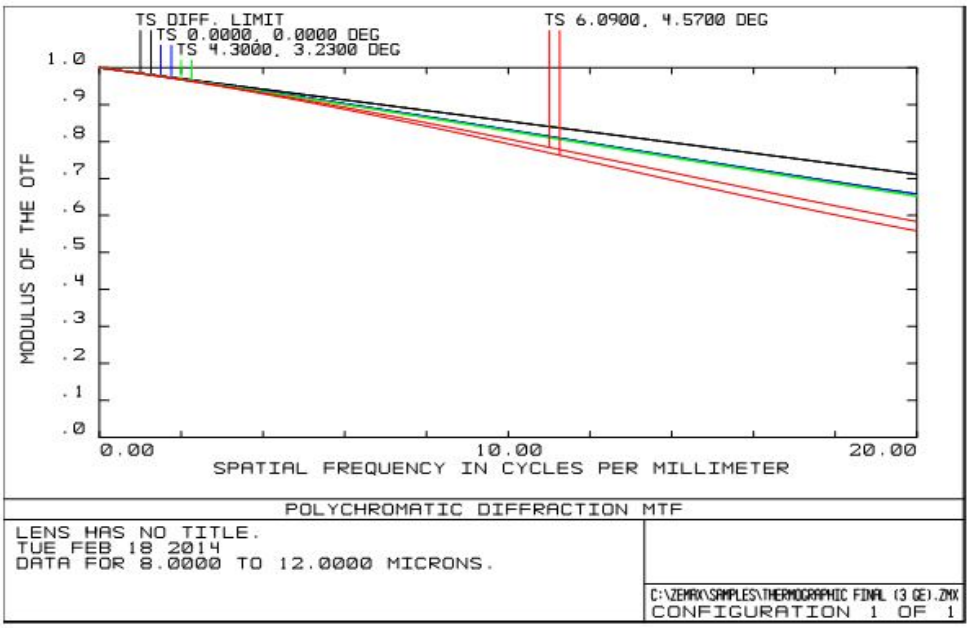

Figure (4.3): Polychrochromatic diffraction MTF curve for on axis, 0.7FOV, and full FOV points at Nyquist frequency

The targeted performance/ design criterion from optical point of view was achieved with more than excellent values, where the RMS radiuses are 5.928µm, 8.006µm, and 8.847µm at on axis, 0.7FOV, and full FOV respectively and overall spots diagram were concentrated on the pixel width at all FOV points [see figure (4.2)]. In addition to the MTF value that achieved [diffraction limit MTF at Nyquist frequency is 0.71149, on axis MTF at Nyquist frequency is 0.65805, 0.7FOV MTF at Nyquist frequency is 0.65340, and full field MTF at Nyquist frequency is

0.58340 [see figure (4.3)]. All these MTF values are greater than targeted value in design criterion (0.5).

When comparing the spot diagram and MTF (design criterion) values of designed/constructed optical system [figure (4.2) & figure (4.3)] with values of spot diagram and MTF of an IR optical system works in 3~5µm {optical design of a long range dual field of view of thermal imaging camera in 3~5µm wave band [28]}. which shown in figure (4.4) and figure (4.5).

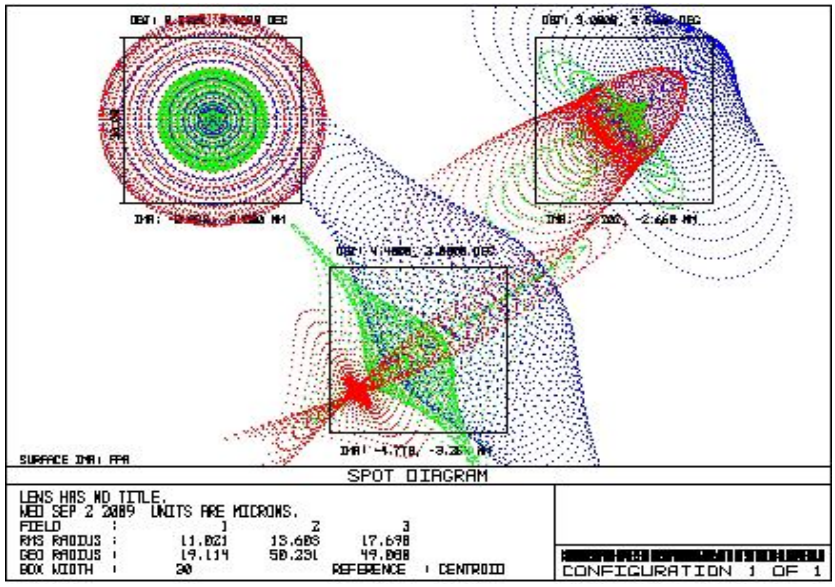

Figure (4.4): Spot diagram on 30µm pixel for wide FOV at on axis, 0.7FOV, and full FOV points [28]

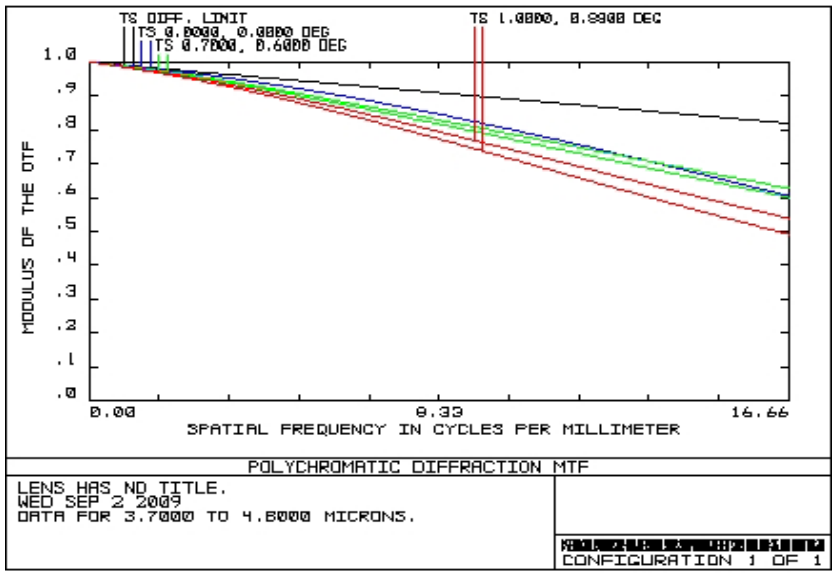

Figure (4.5): Polychrochromatic diffraction MTF curve for wide FOV in on axis, 0.7FOV, and full FOV points at Nyquist frequency [28]

The comparing of the exact results (spot diagram & MTF) of constructed optical system and optical design of a long range dual field of view of thermal imaging camera in 3~5µm wave band is shown in table (4.2)

Table (4.2): Comparing between spot radius& MTF values for designed and long range dual field of view of thermal imaging camera in 3~5µm wave band optical systems

	RMS spot radius /µm			**Polychromatic MTF at Nyquist frequency**		
	On axis	0.7 FOV	Full FOV	On axis	0.7 FOV	Full FOV
Designed optical system	5.928	8.006	8.847	0.65805	0.65340	0.58348
Optical design of a long range dual field of view of thermal imaging camera in 3~5µm wave band.	11.021	13.603	17.698	0.62740	0.59039	0.43329

As shown in table (4.2): the RMS spot radii values for designed optical system at all FOV points is better (less) than RMS spot radii values in optical design of a long range dual field of view of thermal imaging camera in 3~5µm wave band. And the concentration of overall spot within 25µm pixel pitch is better than the concentration of spot within 30µm pixel pitch as shown in figure (4.2) & figure (4.4).

The MTF values at Nyquist frequency obtained from designed optical system in all FOV points are also better (more) than MTF values of optical design of a long range dual field of view of thermal imaging camera in 3~5µm wave band at all FOV points, and more close to diffraction limit (free aberration) case in designed optical system than optical design of a long range dual field of view of thermal imaging camera in 3~5µm wave band as shown in figure (4.3) & figure (4.5).

In above comparison keep in mind that: the pixel pitch of the detector in our design is 25µm, and in optical design of a long range dual field of view of thermal imaging camera in 3~5µm wave band is 30µm. the increase in pixel pitch leads to increase the cut off (Nyquist) frequency.

From previous comparisons shown in figures (4.2, 4.3, 4.4, and 4.5) and summarized in table (4.2) in terms of spot diagram and MTF (my design criterion). It is clear that the designed optical system is higher performance, and higher image quality than optical design of a long range dual field of view of thermal imaging camera in 3~5µm wave band.

Other analysis (diagnostic) tools provides by ZEMAX program used to analyze and measure performance of obtained IR optical system:

4.2.2.3 Transverse Ray Fan Plot (Ray Aberration)

This is one of the most important analysis tools in ZEMAX, transverse ray aberration plot is commonly used as tool to assessed the resolution of the optical system [for more information see ray trace curves chapter 2]. A given ray passes through the entrance pupil at a particular height P ($-1<P<1$) and intercepts the image plane at a separation Δh from the chief ray is illustrated by transverse ray fan plots. In ZEMAX Transverse ray-intercept fan plots (ray fan plots) present the transverse ray height errors (ray aberration) Δh (Y-axis) at image plane as function of pupil zone height P (X-axis). These data present separately for the tangential (meridional) fan and the sagittal fan. Therefore, a transverse aberration plot shows the variation in blur size at the detector for a cross-section of rays across an input beam. Figure (4.6) shows ray fan plot of this designed system

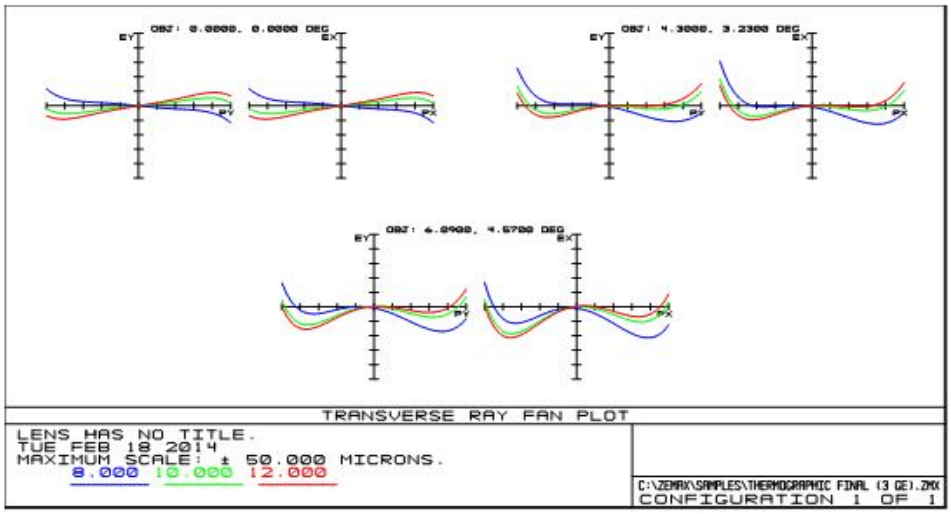

Figure (4.6): Ray fan plot for 8, 10, and 12µm at on-axis, 0.7FOV, full FOV

Figure (4.6) shown ray aberrations (vertical axis) as a function of pupil coordinate (horizontal axis), these plots are generated by tracing fans of rays from a specific field angle (on-axis: 0.000°, 0.0000°; 0.7FOV: 4.3000°, 3.2300°; and full FOV: 6.0900°, 4.5700°) to a linear array of points across the image plane (her is thermal detector module) of the system. The data being plotted is the difference between the ray intercept coordinate and the chief ray intercept coordinate. Y-axis is aberration data measured in image plane local coordinates, tangential data (tangential fan) is Y aberration as function of P_y and sagittal data (sagittal fan) is X aberration as function of P_x at on-axis, 0.7FOV, and full FOV for selected wavelengths (8, 10, and 12µm). Each aberration has a characteristic appearance in ray fan plot. As shown in figure (4.6) generally the magnitude of bullring (values of combination aberration) is relatively low, and the accurately concentration/focus most of this blur within pixel is possible.

4.2.2.4 Encircled Energy

This is percentage of total energy enclosed as function of distance from the image centroid at the image of point source. This analysis tool shows the energy percentage of blur spot as function of blur radius. Figure (4.7) shows the encircled energy of designed optical system

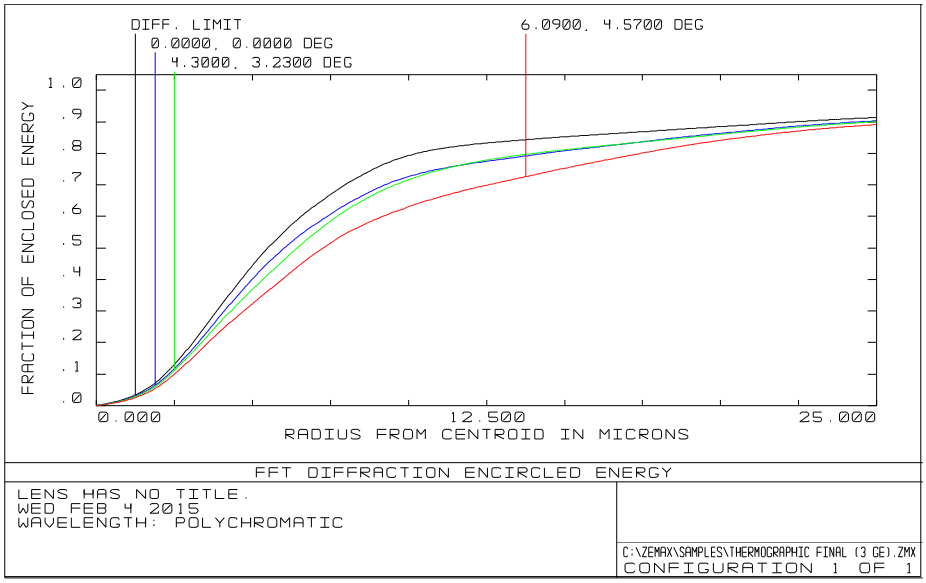

Figure (4.7): Encircled energy

This analysis tool uses to specify an imaging optical system using FPA sensors. The pixel pitch of our sensor is 25µm. in this design a good reliable specification is that ≥0.8 fraction of enclosed/encircled energy from a point object shall fall within a diameter of 25µm (pixel pitch). As shown in Figure (4.7) the fraction of enclosed/encircled energy (y-axis) at diameter of 25µm (x-axis) for all field points is: 0.9034% at on-axis, 0.9005% at 0.7FOV, and 0.8914% at full FOV. This achieved result is excellent and matching well with our FPA detector.

4.2.2.5 Chromatic Focal Shift (Chromatic Aberration)

Because the refractive indexes of optical materials are changes with wavelength, then the focal length (focus distance) of any optical system is function of wavelength. This plot (chromatic focal shift) shows the shift in back focal length with respect to primary wavelength, in other words, the shift in image space required to reach focus for the primary wavelength is computed. Figure (4.8) shows the chromatic focal shift plot of designed optical system.

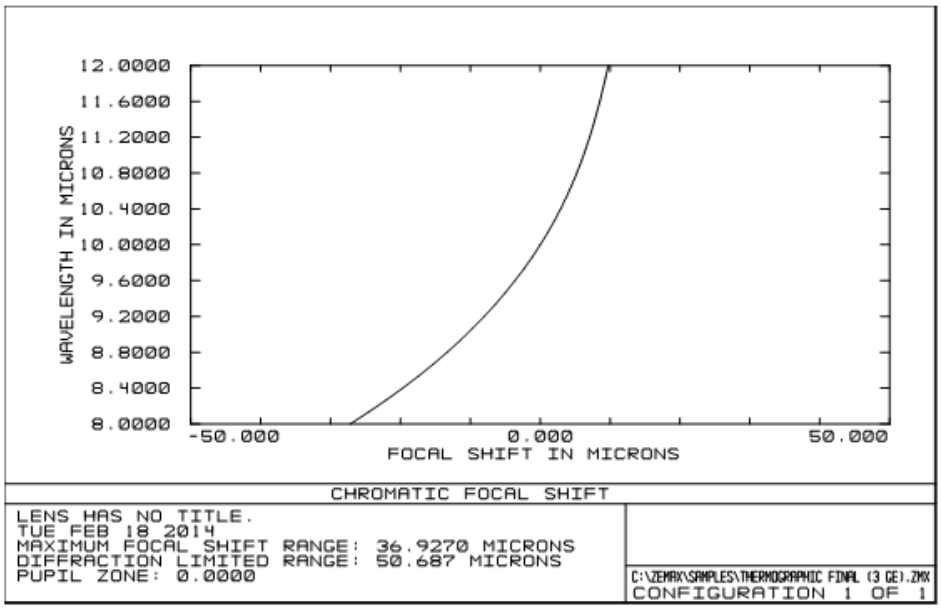

Figure (4.8): Chromatic focal shift

The shift between primary wavelength (10µm) and shortest wavelength (8µm) is 27.19603µm, and between primary wavelength and longest wavelength (12µm) is 9.73098µm. this is very acceptable values because it is compatible with pixel pitch of the detector (25µm), in other words, the most of wavelengths in LWIR band (8~12µm) are concentrated within 25µm.

4.2.2.6 Lateral Color

This field plot provides information on color error as a function of field angle. Figure (4.9) shows the difference between the chief ray heights at shortest (8µm) and longest (12µm) wavelengths as a function of field angle. For this reason the lateral color aberration is defined briefly as variation in magnification with wavelength.

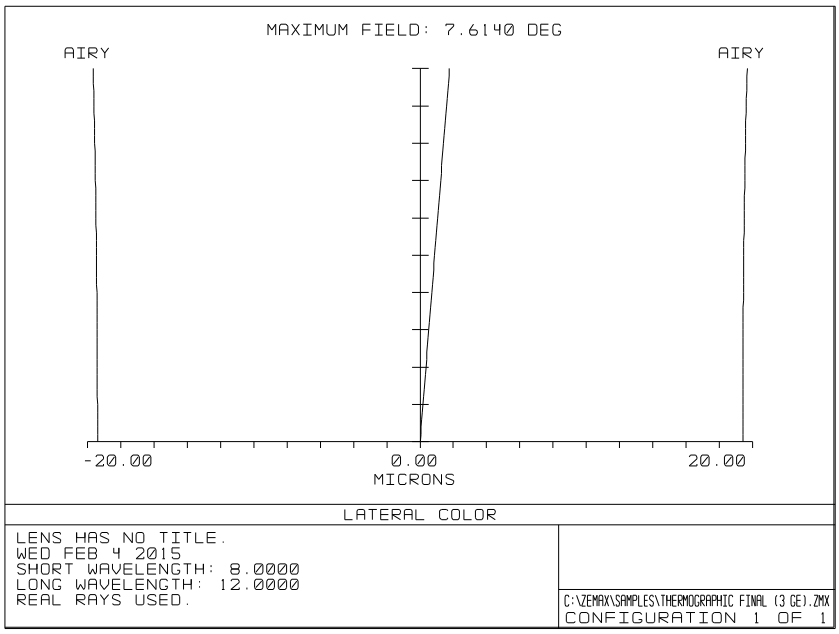

Figure (4.9): Lateral color

From figure (4.9) the maximum value of lateral color is 1.7683µm which obtained from/edge of diagonal field is 1.7683µm. This is very low value when compared with pixel pitch of the detector (25µm), therefore this perfect and more than acceptable value.

According to previous results and analytics:

- ✓ The constructed/designed IR optical system met all required specifications and more from optical point of view (quality of final image).

On other hand, the advantage of this design from mechanical point of view is:

- ✓ Light weight. The weight of constructed system after addition of mechanical consideration is 70 g.
- ✓ Simple in structure. Consist from 3 lenses (6 surfaces) and 5 spherical surfaces in addition to only one aspheric surface (1^{st} surface is conic surface).
- ✓ Short length/compact design. The total track of the system (the length of the optical system as measured by vertex separation

between the “left most” and “right most” surface / the distance between 1st surface and image surface) is 58.5mm.

These mechanical features by default have a positive impact affect on the production cost of designed optical system by reduce the raw material cost and manufacturing cost to elements that contribute on building the IR optical system.

4.2.3 Tolerance Analysis

It is final design task must be accomplished in the design process; it precedes the manufacturing stage directly. Tolerance values have a considerable impact on fabrication method, cost, and performance and ultimately it sets by the designer.

The tolerances available for analysis include variation in construction parameters such as curvature, thickness, aspheric constant, index of refraction and irregularity of surface shape. ZEMAX also supports analysis of decentration of surfaces and lens groups, tilts of surfaces or lens groups about any arbitrary point.

The values which were chosen for fabrication errors (surface tolerances) and assembly/alignment errors (element tolerances) effects on system performance of this design are shown on table (4.3).

Table (4.3): Tolerance values

1st : Surfaces tolerance (manufacturing tolerance)		
Name	*Description*	*Value*
TRAD	Tolerance on radius of curvature of surface no1 (44.514mm)	±0.045mm
	Tolerance on radius of curvature of surface no2 (57.748mm)	±0.058mm
	Tolerance on radius of curvature of surface no3 (27.090mm)	±0.027mm
	Tolerance on radius of curvature of surface no4 (21.563mm)	±0.022mm
	Tolerance on radius of curvature of surface no5 (38.376mm)	±0.038mm
	Tolerance on radius of curvature of surface no6 (54.907mm)	±0.055mm
TTHI	Tolerance on thickness 1 [thickness of lens no 1 (5mm)]	±0.05mm
	Tolerance on thickness 3 [thickness of lens no 2 (4mm)]	±0.05mm
	Tolerance on thickness 5 [thickness of lens no 3 (3mm)]	±0.05mm
TCON	Tolerance on conic of surface no1 (-0.132)	±0.003
TSDX	Tolerance on all surfaces decentering in X	±0.05mm
TSDY	Tolerance on all surfaces decentering in Y	±0.05mm
TSTX	Tolerance on all surfaces tilt in X (degree)	±0.033°
TSTY	Tolerance on all surfaces tilt in Y (degree)	±0.033°
TIRR	Tolerance on all surfaces irregularity (fringes)	1 fring
TIND	Tolerance on all surfaces index of refraction	±0.001
2nd : Elements tolerance (assembly tolerance)		
TEDX	Tolerance on all elements decentering in X	±0.05mm
TEDY	Tolerance on all elements decentering in Y	±0.05mm
TETX	Tolerance on all elements tilt in X (degree)	±0.033°
TETY	Tolerance on all elements tilt in Y (degree)	±0.033°
TTHI	Tolerance on thickness 2 [air gap between lenses 1& 2 (10mm)]	±0.05mm
	Tolerance on thickness 4 [air gap between lenses 2& 3 (22.92mm)]	±0.05mm
	Tolerance on thickness 6 [air gap between lenses 3& detector (9mm)]	±0.05mm

By applying the above selected tolerance values on designed optical system at the level of software ZEMAX as a final stage in optical design processes, the analysis of tolerances text window below from ZEMAX shows the influence of these tolerance values which were selected on the efficiency of the final design, i.e. the output of tolerance analysis stage.

```
                    Analysis of Tolerances
File : C:\ZEMAX\Samples\thermographic final (3 GE).ZMX
Title: Lens has no title.
Date : MON FEB 3 2014
Units are Millimeters.
Mnemonics:
TRAD: Tolerance on radius of curvature.
TCUR: Tolerance on curvature (inverse length).
TFRN: Tolerance on curvature in fringes.
TTHI: Tolerance on thickness.
TCON: Tolerance on conic.
TSDX: Tolerance on surface decentering in x.
TSDY: Tolerance on surface decentering in y.
TSTX: Tolerance on surface tilt in x (degrees).
```

TSTY: Tolerance on surface tilt in y (degrees).
TIRX: Tolerance on surface total indicator runout in x.
TIRY: Tolerance on surface total indicator runout in y.
TIRR: Tolerance on irregularity (fringes).
TEXI: Tolerance on extended Zernike irregularity.
TIND: Tolerance on Nd index of refraction.
TABB: Tolerance on Abbe number.
TPAR: Tolerance on parameter.
TEDV: Tolerance on extra data value.
TMCO: Tolerance on multi-configuration value.
TEDX: Tolerance on element decentering in x.
TEDY: Tolerance on element decentering in y.
TETX: Tolerance on element tilt in x (degrees).
TETY: Tolerance on element tilt in y (degrees).
TETZ: Tolerance on element tilt in z (degrees).
TUDX: Tolerance on user surface decentering in x.
TUDY: Tolerance on user surface decentering in y.
TUTX: Tolerance on user surface tilt (degrees) around the x-axis.
TUTY: Tolerance on user surface tilt (degrees) around the y-axis.
TUTZ: Tolerance on user surface tilt (degrees) around the z-axis.
Compensator: Thickness 6, Min = -1.0000, Max = 1.0000
Criteria : RMS Spot Radius in Millimeters
Mode : Sensitivities
Sampling : 10
Optimization Cycles : Automatic mode
Nominal Criteria : 0.00767034
Test Wavelength : 0.6328

Sensitivity Analysis: (the **change** in **criteria -spot radius-** from nominal as function of parameter perturb. Each individual parameter is changed according to normal probability distribution between its minimum and maximum values)

		Minimum			Maximum		
Type	**Value**	**Criteria**	**Change**	**Value**	**Criteria**	**Change**	
Conic tolerance on surface 1							
TCON 1	-0.003000	0.007868	0.000197	0.003000	0.008987	0.001317	
Thickness 6:		9.02940E+000			8.97001E+000		
Radius tolerance on surface 1							
TRAD 1	-0.045000	0.007867	0.000197	0.045000	0.008041	0.000371	
Thickness 6:		8.85827E+000			9.14124E+00		
Radius tolerance on surface 2							
TRAD 2	-0.058000	0.007763	0.000093	0.058000	0.007753	0.000082	
Thickness 6:		9.09270E+000			8.90705E+000		
Radius tolerance on surface 3							
TRAD 3	-0.027000	0.007758	0.000088	0.027000	0.007915	0.000245	
Thickness 6:		8.88282E+000			9.11687E+000		
Radius tolerance on surface 4							
TRAD 4	-0.022000	0.007934	0.000264	0.022000	0.007796	0.000126	
Thickness 6:		9.11257E+000			8.88760E+000		
Radius tolerance on surface 5							
TRAD 5	-0.038000	0.007731	0.000061	0.038000	0.007629	-0.000042	
Thickness 6:		8.98289E+000			9.01652E+000		
Radius tolerance on surface 6							
TRAD 6	-0.055000	0.007640	-0.000030	0.055000	0.007709	0.000039	
Thickness 6:		9.00991E+000			8.98953E+000		
Fringe tolerance on surface 7							
TFRN 7	-1.000000	0.007672	0.000002	1.000000	0.007669	-0.000001	
Thickness 6:		9.00034E+000			8.99907E+000		
Fringe tolerance on surface 8							
TFRN 8	-1.000000	0.007669	-0.000002	1.000000	0.007672	0.000002	
Thickness 6:		8.99912E+000			9.00029E+000		
Thickness tolerance on surface 1							
TTHI 1 2	-0.050000	0.007714	0.000044	0.050000	0.007742	0.000072	
Thickness 6:		9.07934E+000			8.92038E+000		
Thickness tolerance on surface 2							
TTHI 2 4	-0.050000	0.007726	0.000056	0.050000	0.007658	-0.000013	
Thickness 6:		9.02170E+000			8.97775E+000		
Thickness tolerance on surface 3							
TTHI 3 4	-0.050000	0.008634	0.000964	0.050000	0.008240	0.000570	
Thickness 6:		9.23547E+000			8.76619E+000		
Thickness tolerance on surface 4							
TTHI 4 6	-0.050000	0.007770	0.000099	0.050000	0.007602	-0.000068	
Thickness 6:		9.01531E+000			8.98407E+000		
Thickness tolerance on surface 5							
TTHI 5 6	-0.050000	0.007630	-0.000040	0.050000	0.007720	0.000050	
Thickness 6:		9.03735E+000			8.96215E+000		
Thickness tolerance on surface 6							
TTHI 6 8	-0.050000	0.007670	-0.000000	0.050000	0.007670	-0.000000	
Thickness 6:		8.94970E+000			9.04970E+000		
Thickness tolerance on surface 7							
TTHI 7 8	-0.050000	0.007695	0.000025	0.050000	0.007647	-0.000023	
Thickness 6:		8.96137E+000			9.03804E+000		
Decenter X tolerance on surfaces 1 through 2							
TEDX 1 2	-0.050000	0.008115	0.000445	0.050000	0.008115	0.000445	
Thickness 6:		8.99975E+000			8.99975E+000		
Decenter Y tolerance on surfaces 1 through 2							
TEDY 1 2	-0.050000	0.008115	0.000445	0.050000	0.008115	0.000445	

```
 Thickness   6:             8.99975E+000                          8.99975E+000
Tilt X tolerance on surfaces 1 through 2 (degrees)
TETX 1  2  -0.033000    0.007737    0.000067    0.033000    0.007737    0.000067
 Thickness   6:             8.99970E+000                          8.99970E+000
Tilt Y tolerance on surfaces 1 through 2 (degrees)
TETY 1  2  -0.033000    0.007737    0.000067    0.033000    0.007737    0.000067
 Thickness   6:             8.99970E+000                          8.99970E+000
Decenter X tolerance on surfaces 3 through 4
TEDX 3  4  -0.050000    0.007759    0.000089    0.050000    0.007759    0.000089
 Thickness   6:             8.99972E+000                          8.99972E+000
Decenter Y tolerance on surfaces 3 through 4
TEDY 3  4  -0.050000    0.007759    0.000089    0.050000    0.007759    0.000089
 Thickness   6:             8.99972E+000                          8.99972E+000
Tilt X tolerance on surfaces 3 through 4 (degrees)
TETX 3  4  -0.033000    0.007676    0.000006    0.033000    0.007676    0.000006
 Thickness   6:             8.99971E+000                          8.99971E+000
Tilt Y tolerance on surfaces 3 through 4 (degrees)
TETY 3  4  -0.033000    0.007676    0.000006    0.033000    0.007676    0.000006
 Thickness   6:             8.99971E+000                          8.99971E+000
Decenter X tolerance on surfaces 5 through 6
TEDX 5  6  -0.050000    0.007824    0.000154    0.050000    0.007824    0.000154
 Thickness   6:             8.99971E+000                          8.99971E+000
Decenter Y tolerance on surfaces 5 through 6
TEDY 5  6  -0.050000    0.007824    0.000154    0.050000    0.007824    0.000154
 Thickness   6:             8.99971E+000                          8.99971E+000
Tilt X tolerance on surfaces 5 through 6 (degrees)
TETX 5  6  -0.033000    0.007689    0.000019    0.033000    0.007689    0.000019
 Thickness   6:             8.99970E+000                          8.99970E+000
Tilt Y tolerance on surfaces 5 through 6 (degrees)
TETY 5  6  -0.033000    0.007689    0.000019    0.033000    0.007689    0.000019
 Thickness   6:             8.99970E+000                          8.99970E+000
Decenter X tolerance on surfaces 7 through 8
TEDX 7  8  -0.050000    0.007670   -0.000000    0.050000    0.007670   -0.000000
 Thickness   6:             8.99970E+000                          8.99970E+000
Decenter Y tolerance on surfaces 7 through 8
TEDY 7  8  -0.050000    0.007670   -0.000000    0.050000    0.007670   -0.000000
 Thickness   6:             8.99970E+000                          8.99970E+000
Tilt X tolerance on surfaces 7 through 8 (degrees)
TETX 7  8  -0.033000    0.007670    0.000000    0.033000    0.007670    0.000000
 Thickness   6:             8.99970E+000                          8.99970E+000
Tilt Y tolerance on surfaces 7 through 8 (degrees)
TETY 7  8  -0.033000    0.007670    0.000000    0.033000    0.007670    0.000000
 Thickness   6:             8.99970E+000                          8.99970E+000
Decenter X tolerance on surface 1
TSDX   1   -0.050000    0.009140    0.001470    0.050000    0.009140    0.001470
 Thickness   6:             9.00003E+000                          9.00003E+000
Decenter Y tolerance on surface 1
TSDY   1   -0.050000    0.009140    0.001470    0.050000    0.009140    0.001470
 Thickness   6:             9.00003E+000                          9.00003E+000
Tilt X tolerance on surface (degrees) 1
TSTX   1   -0.033000    0.008252    0.000582    0.033000    0.008252    0.000582
 Thickness   6:             8.99977E+000                          8.99977E+000
Tilt Y tolerance on surface (degrees) 1
TSTY   1   -0.033000    0.008252    0.000582    0.033000    0.008252    0.000582
 Thickness   6:             8.99977E+000                          8.99977E+000
Decenter X tolerance on surface 2
TSDX   2   -0.050000    0.008320    0.000650    0.050000    0.008320    0.000650
 Thickness   6:             8.99979E+000                          8.99979E+000
Decenter Y tolerance on surface 2
TSDY   2   -0.050000    0.008320    0.000650    0.050000    0.008320    0.000650
 Thickness   6:             8.99979E+000                          8.99979E+000
Tilt X tolerance on surface (degrees) 2
TSTX   2   -0.033000    0.007965    0.000294    0.033000    0.007965    0.000294
 Thickness   6:             8.99976E+000                          8.99976E+000
Tilt Y tolerance on surface (degrees) 2
TSTY   2   -0.033000    0.007965    0.000294    0.033000    0.007965    0.000294
 Thickness   6:             8.99976E+000                          8.99976E+000
Decenter X tolerance on surface 3
TSDX   3   -0.050000    0.009212    0.001541    0.050000    0.009212    0.001541
 Thickness   6:             9.00025E+000                          9.00025E+000
Decenter Y tolerance on surface 3
TSDY   3   -0.050000    0.009212    0.001541    0.050000    0.009212    0.001541
 Thickness   6:             9.00025E+000                          9.00025E+000
Tilt X tolerance on surface (degrees) 3
TSTX   3   -0.033000    0.007834    0.000163    0.033000    0.007834    0.000163
 Thickness   6:             8.99974E+000                          8.99974E+000
Tilt Y tolerance on surface (degrees) 3
TSTY   3   -0.033000    0.007834    0.000163    0.033000    0.007834    0.000163
 Thickness   6:             8.99974E+000                          8.99974E+000
Decenter X tolerance on surface 4
TSDX   4   -0.050000    0.009679    0.002009    0.050000    0.009679    0.002009
 Thickness   6:             9.00021E+000                          9.00021E+000
Decenter Y tolerance on surface 4
TSDY   4   -0.050000    0.009679    0.002009    0.050000    0.009679    0.002009
 Thickness   6:             9.00021E+000                          9.00021E+000
Tilt X tolerance on surface (degrees) 4
TSTX   4   -0.033000    0.007809    0.000139    0.033000    0.007809    0.000139
```

```
 Thickness   6:             8.99975E+000                          8.99975E+000
Tilt Y tolerance on surface (degrees) 4
TSTY   4   -0.033000    0.007809    0.000139    0.033000    0.007809    0.000139
 Thickness   6:             8.99975E+000                          8.99975E+000
Decenter X tolerance on surface 5
TSDX   5   -0.050000    0.009045    0.001375    0.050000    0.009045    0.001375
 Thickness   6:             8.99949E+000                          8.99949E+000
Decenter Y tolerance on surface 5
TSDY   5   -0.050000    0.009045    0.001375    0.050000    0.009045    0.001375
 Thickness   6:             8.99949E+000                          8.99949E+000
Tilt X tolerance on surface (degrees) 5
TSTX   5   -0.033000    0.007958    0.000287    0.033000    0.007958    0.000287
 Thickness   6:             8.99966E+000                          8.99966E+000
Tilt Y tolerance on surface (degrees) 5
TSTY   5   -0.033000    0.007958    0.000287    0.033000    0.007958    0.000287
 Thickness   6:             8.99966E+000                          8.99966E+000
Decenter X tolerance on surface 6
TSDX   6   -0.050000    0.008442    0.000772    0.050000    0.008442    0.000772
 Thickness   6:             8.99957E+000                          8.99957E+000
Decenter Y tolerance on surface 6
TSDY   6   -0.050000    0.008442    0.000772    0.050000    0.008442    0.000772
 Thickness   6:             8.99957E+000                          8.99957E+000
Tilt X tolerance on surface (degrees) 6
TSTX   6   -0.033000    0.007988    0.000318    0.033000    0.007988    0.000318
 Thickness   6:             8.99965E+000                          8.99965E+000
Tilt Y tolerance on surface (degrees) 6
TSTY   6   -0.033000    0.007988    0.000318    0.033000    0.007988    0.000318
 Thickness   6:             8.99965E+000                          8.99965E+000
Decenter X tolerance on surface 7
TSDX   7   -0.050000    0.007670   -0.000000    0.050000    0.007670   -0.000000
 Thickness   6:             8.99970E+000                          8.99970E+000
Decenter Y tolerance on surface 7
TSDY   7   -0.050000    0.007670   -0.000000    0.050000    0.007670   -0.000000
 Thickness   6:             8.99970E+000                          8.99970E+000
Tilt X tolerance on surface (degrees) 7
TSTX   7   -0.033000    0.007719    0.000049    0.033000    0.007719    0.000049
 Thickness   6:             8.99969E+000                          8.99969E+000
Tilt Y tolerance on surface (degrees) 7
TSTY   7   -0.033000    0.007719    0.000049    0.033000    0.007719    0.000049
 Thickness   6:             8.99969E+000                          8.99969E+000
Decenter X tolerance on surface 8
TSDX   8   -0.050000    0.007670   -0.000000    0.050000    0.007670   -0.000000
 Thickness   6:             8.99970E+000                          8.99970E+000
Decenter Y tolerance on surface 8
TSDY   8   -0.050000    0.007670   -0.000000    0.050000    0.007670   -0.000000
 Thickness   6:             8.99970E+000                          8.99970E+000
Tilt X tolerance on surface (degrees) 8
TSTX   8   -0.033000    0.007718    0.000047    0.033000    0.007718    0.000047
 Thickness   6:             8.99969E+000                          8.99969E+000
Tilt Y tolerance on surface (degrees) 8
TSTY   8   -0.033000    0.007718    0.000047    0.033000    0.007718    0.000047
 Thickness   6:             8.99969E+000                          8.99969E+000
Irregularity of surface 1 in fringes
TIRR   1   -1.000000    0.007637   -0.000033    1.000000    0.007804    0.000134
 Thickness   6:             9.00730E+000                          8.99212E+000
Irregularity of surface 2 in fringes
TIRR   2   -1.000000    0.007836    0.000165    1.000000    0.007621   -0.000050
 Thickness   6:             8.99188E+000                          9.00753E+000
Irregularity of surface 3 in fringes
TIRR   3   -1.000000    0.007650   -0.000020    1.000000    0.007740    0.000069
 Thickness   6:             9.00476E+000                          8.99465E+000
Irregularity of surface 4 in fringes
TIRR   4   -1.000000    0.007731    0.000061    1.000000    0.007653   -0.000017
 Thickness   6:             8.99492E+000                          9.00449E+000
Irregularity of surface 5 in fringes
TIRR   5   -1.000000    0.007675    0.000004    1.000000    0.007681    0.000010
 Thickness   6:             9.00162E+000                          8.99779E+000
Irregularity of surface 6 in fringes
TIRR   6   -1.000000    0.007682    0.000012    1.000000    0.007675    0.000004
 Thickness   6:             8.99783E+000                          9.00158E+000
Irregularity of surface 7 in fringes
TIRR   7   -1.000000    0.007668   -0.000002    1.000000    0.007675    0.000005
 Thickness   6:             9.00022E+000                          8.99919E+000
Irregularity of surface 8 in fringes
TIRR   8   -1.000000    0.007675    0.000005    1.000000    0.007668   -0.000002
 Thickness   6:             8.99922E+000                          9.00018E+000
Index tolerance on surface 1
TIND   1   -0.001000    0.007688    0.000018    0.001000    0.007656   -0.000014
 Thickness   6:             9.01289E+000                          8.98653E+000
Index tolerance on surface 3
TIND   3   -0.001000    0.007668   -0.000002    0.001000    0.007672    0.000002
 Thickness   6:             8.99728E+000                          9.00213E+000
Index tolerance on surface 5
TIND   5   -0.001000    0.007665   -0.000005    0.001000    0.007676    0.000006
 Thickness   6:             9.00152E+000                          8.99789E+000
```

Worst offenders: (list of operands -20 operands- from most to least affect on criterion)

Type			Value	Criteria	Change
TSDY	4		0.050000	0.009679	0.002009
TSDX	4		0.050000	0.009679	0.002009
TSDY	4		-0.050000	0.009679	0.002009
TSDX	4		-0.050000	0.009679	0.002009
TSDY	3		-0.050000	0.009212	0.001541
TSDX	3		-0.050000	0.009212	0.001541
TSDY	3		0.050000	0.009212	0.001541
TSDX	3		0.050000	0.009212	0.001541
TSDX	1		-0.050000	0.009140	0.001470
TSDY	1		-0.050000	0.009140	0.001470
TSDY	1		0.050000	0.009140	0.001470
TSDX	1		0.050000	0.009140	0.001470
TSDX	5		0.050000	0.009045	0.001375
TSDY	5		0.050000	0.009045	0.001375
TSDY	5		-0.050000	0.009045	0.001375
TSDX	5		-0.050000	0.009045	0.001375
TCON	1		0.003000	0.008987	0.001317
TTHI	3	4	-0.050000	0.008634	0.000964
TSDX	6		-0.050000	0.008442	0.000772
TSDY	6		-0.050000	0.008442	0.000772

Monte Carlo Analysis: (simulates the effect of all perturbations simultaneously on criteria change from nominal/considering all of the tolerances simultaneously. Each Monte Carlo sample (trail) is, in effect, a simulated fabricated system)
Number of trials: 40
Initial Statistics: Normal Distribution

Trial	Criteria	Change	
1	0.014887	0.007217	
Thickness	6:		9.06090E+000
2	0.010280	0.002609	
Thickness	6:		8.89386E+000
3	0.009095	0.001424	
Thickness	6:		9.22680E+000
4	0.009450	0.001780	
Thickness	6:		9.19300E+000
5	0.011091	0.003421	
Thickness	6:		9.02425E+000
6	0.012404	0.004734	
Thickness	6:		9.01052E+000
7	0.010025	0.002354	
Thickness	6:		8.99012E+000
8	0.008252	0.000582	
Thickness	6:		8.96005E+000
9	0.012788	0.005118	
Thickness	6:		9.23314E+000
10	0.009019	0.001348	
Thickness	6:		8.84471E+000
11	0.009355	0.001684	
Thickness	6:		9.02196E+000
12	0.009499	0.001828	
Thickness	6:		9.21801E+000
13	0.010724	0.003054	
Thickness	6:		8.98474E+000
14	0.013004	0.005334	
Thickness	6:		8.84988E+000
15	0.010180	0.002509	
Thickness	6:		9.16904E+000
16	0.014025	0.006355	
Thickness	6:		8.83573E+000
17	0.010408	0.002737	
Thickness	6:		9.19584E+000
18	0.010571	0.002901	
Thickness	6:		9.13835E+000
19	0.012140	0.004470	
Thickness	6:		9.15901E+000
20	0.009049	0.001379	
Thickness	6:		9.12266E+000
21	0.010555	0.002884	
Thickness	6:		8.91016E+000
22	0.010734	0.003063	
Thickness	6:		9.12564E+000
23	0.008702	0.001032	
Thickness	6:		8.99393E+000
24	0.010615	0.002945	
Thickness	6:		8.78907E+000
25	0.010545	0.002875	
Thickness	6:		8.89687E+000
26	0.012535	0.004865	
Thickness	6:		8.99125E+000
27	0.011184	0.003514	
Thickness	6:		9.16028E+000
28	0.012499	0.004829	
Thickness	6:		9.21306E+000
29	0.011075	0.003405	
Thickness	6:		9.03868E+000
30	0.014420	0.006750	

```
Thickness   6:                      9.18617E+000
31    0.011849    0.004178
Thickness   6:                      9.28769E+000
32    0.015989    0.008318
Thickness   6:                      9.13739E+000
33    0.009694    0.002023
Thickness   6:                      9.16146E+000
34    0.009260    0.001590
Thickness   6:                      8.83889E+000
35    0.009820    0.002150
Thickness   6:                      8.77109E+000
36    0.012353    0.004682
Thickness   6:                      9.01940E+000
37    0.010578    0.002908
Thickness   6:                      8.81111E+000
38    0.012545    0.004875
Thickness   6:                      9.06775E+000
39    0.010718    0.003048
Thickness   6:                      8.84552E+000
40    0.011535    0.003865
Thickness   6:                      9.25148E+000
90% <= 0.013004 (the amount of criteria if 90% of selected perturbations occurred together)
50% <= 0.010615 (the amount of criteria if 50% of selected perturbations occurred together)
10% <= 0.009049 (the amount of criteria if 10% of selected perturbations occurred together)
End of Run.
```

The output of sensitivity analysis and Monte Carlo analysis for 40 trails is shown in analysis of tolerances text window. The sensitivity analysis is shown first, in this step ZEMAX will perturb each parameter individually and record the amount of change in the criteria (spot radius), with each tolerance operand listed with change in criterion for its maximum and minimum values. After the sensitivity analysis comes the Monte Carlo analysis, the Monte Carlo analysis simulates the effect of all perturbations simultaneously; for each Monte Carlo cycle (here 40 trails) all of the parameters which have specified tolerances are randomly set using the defined range of the parameter. The value of Mote Carlo analysis is estimating the performance of the lenses considering all of tolerances simultaneously.

As shown in the end of text, the Monte Carlo results show that:

- ✓ 10% of Monte Carlo lenses have an RMS spot radius equal to 0.009049mm (9.049μm). [That is means, if 10% of selected perturbations occurred simultaneously, the change in criteria (RMS spot radius) from 0.00767034mm (7.67034μm) to 0.009049mm (9.049μm)].
- ✓ 50% of Monte Carlo lenses have an RMS spot radius equal to 0.010615mm (10.615μm). [That is means, if 50% of selected

perturbations occurred, the change in criterion (RMS spot radius) from 0.00767034mm (7.67034µm) to 0.010615mm (10.615µm)].

- ✓ And 90% of Monte Carlo lenses have an RMS spot radius equal to 0.013004mm (13.004µm). [That is means, if 90% of selected perturbations occurred simultaneously, the change in criterion (RMS spot radius) from 0.00767034mm (7.67034µm) to 0.013004mm (13.004µm)].

According to the results above, the selected amounts to tolerances are very reasonable, because the impact of it on optical system performance (quality of final image) is so good. This is evident from the comparison between obtained RMS spot radiuses (9.049, 10.615, and 13.004µm) and detector pixel pitch (25µm). Therefore the selected values of tolerances are reasonable values in impact on the performance of designed optical system.

The level/class of tolerances here is combination between commercial and precision levels, thus there are no difficulty in manufacturing the lenses (surfaces) at a reasonable cost with this values of tolerance that shown in table (4.3).

Finally, based on this analysis (tolerance analysis) the drawing of designed optical system/lenses that will be send to Manufacturer Company to produce it could be clarified as shown in figure (3.2), figure (3.3) and figure (3.4).

The design of an IR optical system was done successfully with the completion of the manufacturing it. Figure (4.10) shown real image for the IR optical system (3 germanium lenses) which was designed after manufacturing it. Figure (4.11) shows the real image also for IR 113 thermal detector module [for more details see the appendix A].

Figure (4.10): Real picture of IR optical system (3 germanium lenses) after manufacturing

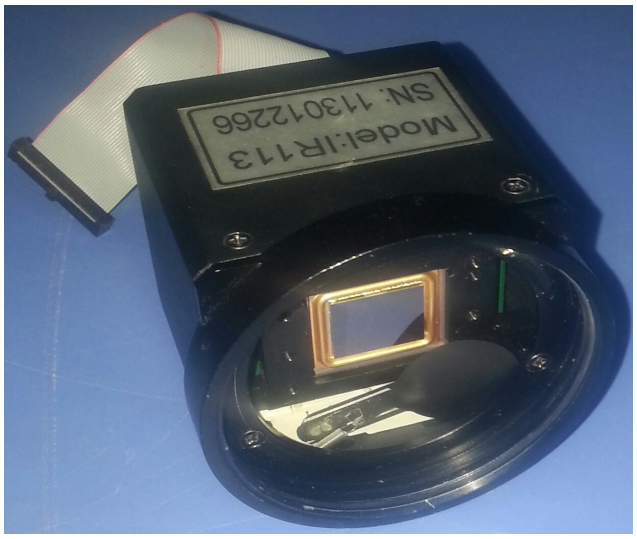

Figure (4.11): Thermal detector module (IR113) inside his mechanical case

4.2.4 Solve a Problem of Defocus

The focus shift (defocus) is a significant problem exactly in IR regions.

The problem of focus shift (defocus) in this design was solved mechanically by longitudinal movement of 3rd lens (focus lens) towards 2nd lens about 0.52mm, this lens (3rd lens) is used as focusing lens to fix the focus point at FPA when the target becomes close/near to the camera and make the system able to get clear image (focusing image) when the distance between the camera and the target (object) become about 5m (5000mm). The conclusion of defocus calculation illustrated in table (4.4).

Table (4.4): Conclusion of defocus calculation

Target (object) distance /m	**Distance traveled by the 3rd lens /mm**	Distance between 2nd and 3rd lens /mm	Distance between 3rd lens and detector /mm	**RMS spot radius/ µm**		
				On-axis	0.707 FOV	Full FOV
Infinity	0	22.92	9	5.928	8.006	8.847
5	0.52	22.40	9.52	11.732	13.421	13.581

- ✓ From the calculations that done at software (ZEMAX) and abbreviated in table (4.4) the optical system become able to images the target (any object according to the application at field) and get clear (focusing) image even when it becomes at distance 5 meters (as lower focus distance) from the camera.
- ✓ In addition to the effect of approaching objects from camera on focus shift the change in temperature also has effect on focus shift (defocus). But in this design the effect of change in temperature is ineffective this is because the optical system and overall camera working in a moderate environment (the change in temperature not high) and the impact of this small change in temperature on focus shift can be overcome by longitudinal movement of 3rd lens.

4.3 The Mechanical Case

As we mentioned earlier the purpose of this mechanical case is to assemble (carry and align) the designed and manufactured IR optical system (3 germanium lenses which illustrated in figure (4.10)) with IR113 thermal detector (figure (4.11)).

The characteristics of this mechanical case (objective) are:

- ✓ It is a simple in structure and fulfills the purpose of its creation.
- ✓ It is made from material (6160 Aluminum alloy) has excellent mechanical properties in terms of hardness, durability, and

susceptibility to manufacturing, for this reasons it is most popular material for mechanical structure and mounting the optical component of thermal imagers.

- ✓ Its light in weight (about 95 grams) because of low density of 6061 Aluminum alloy. And this contributes to reducing the weight of the thermal camera as whole system.

The importance of this mechanical case represented in: verification from the efficiency of IR optical system and its compatibility with thermal detector by carry, align and hold the optical system with detector module in order to building the thermal camera and gutting the thermal images (testing). In addition make them (IR optical system + thermal detector module/ thermal camera) as a single and portable unit (assembly stage).

Figure (4.12) shows real image of IR optical system after assembly inside the mechanical case in addition to IR113 module in our case before link them together.

Figure (4.12): Assembly of the optical system (3 lenses) on mechanical case, and thermal detector module (IR 113)

The integration which occurs between the IR optical system (3 germanium lenses) and thermal detector module (IR113) by using this

mechanical case leads to the end of the construction of the handheld thermal camera as illustrated in figure (4.13).

Figure (4.13): The thermal camera [Intended thermal camera here: the integration between the designed and fabricated IR optical system (lenses) and the detector module (IR113) which was selected by using the designed and manufactured mechanical case]

As shown in figure (4.13) and from mechanical point of view this thermal camera featuring by compact design. i.e. , small size and light weight.

Figures (4.14) show the output of the thermal camera [real thermal (gray) images for several cases taken by this thermal camera].

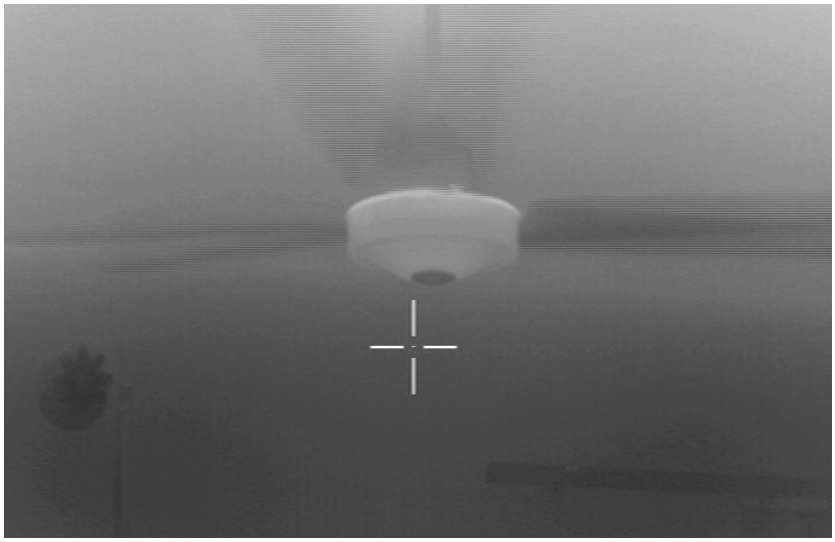

Figure (4.14.a): Thermal image Power one selling fan and power off wall lamp at distances 4 and 4.7m respectively

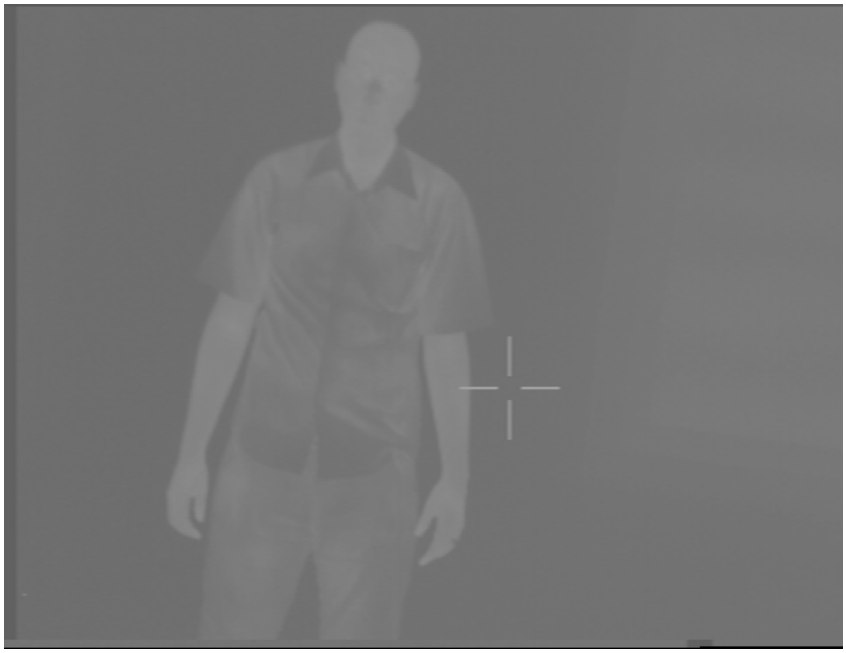

Figure (4.14-b): Person at distance 5.7 m in a total darkroom

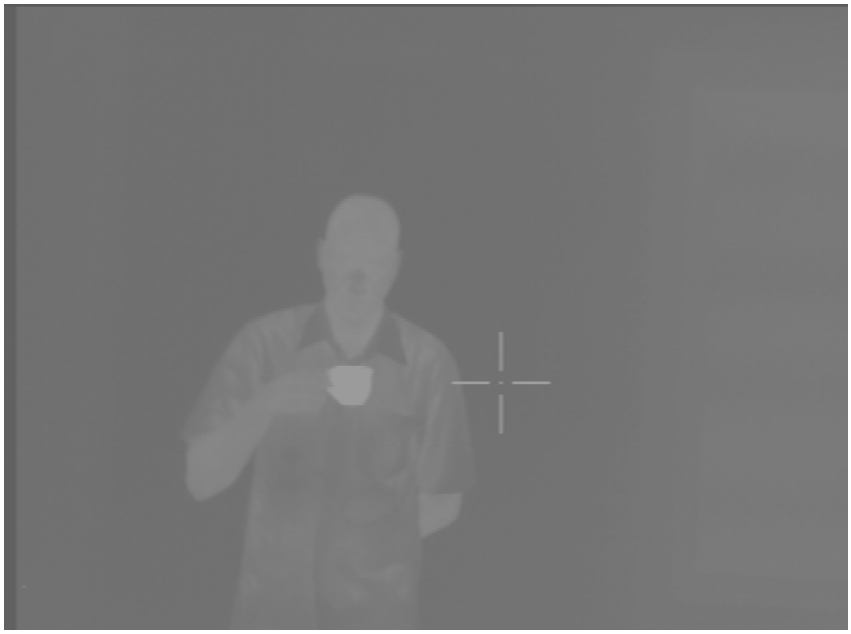

Figure (4.14.c): Same person in a total darkroom carrying a cup of tea

The images in Figures (4.14) represent a real assessment of the designed IR optical system and its integration with thermal detector module in order to produce the thermal camera. From this images can be seen that:

- ✓ These images represent areal and practical assessment of the quality of designed optical system and its integration with thermal detector module through designed mechanical case.

- ✓ The quality of the images is very good (keep in mind that the thermal images not as real - visible- images it just temperature profiling of the surfaces/objects).
- ✓ The camera has ability to image the targets from close distances for the camera with acceptable quality as a result of solving the defocus problem.
- ✓ The distribution of the heat on the objects is very clear and the distinguishing between hot and cold points from the thermal images is very easy. (White means hot and black means cold).
- ✓ The camera covers wide/ large area as result of wide FOV (12.18°×9.14°). (At distance 20m the camera has ability to cover area = 4.32m×3.22m).

Until here the design of thermal camera by the required specifications was accomplished successfully by creating good IR optical system and mechanical case, the images that shown in figures (4.14) are clear representation to accomplish of this mission.

The rest of this chapter was specified to PC software in order to convert the thermal image to thermographic image and thus the completion of the design of the thermographic camera. Note that from hardware point of view the thermal camera components or subsystems are the same components of the thermographic camera, just The difference between them comes from this software that converts the image from thermal (gray) to thermographic (flash color) image, then (thermographic camera= thermal camera+ software program).

4.4 Thermal Image Processing Software

The purpose of this MATLAB program is convert the thermal gray image to flash color (thermographic) image in order to improve visibility and to read the amount temperature to any point on the surface of object from its theromgraphic image.

4.4.1 Convert of Thermal Gray Image to Pseudo/Flash Color (Thermographic) Image

The existing of color to gray (thermal) image for purpose of emphasizes temperature differences and made the image clearer.

Table (4.5) shows the temperature reading from of blackbody and it surrounding (environment), difference temperature between them (ΔT), and IR/thermal images of blackbody and corresponding thermographic images after apply the jet color map in order to convert them (IR images) to thermographic images.

Table (4.5): Readings of blackbody temperatures from test station in addition to its thermal and thermographic images

No	Environment Temperature	**Blackbody Temperature**	Difference Temperature (ΔT°C)	**Thermal** (left) and **thermographic** (right) **images** of blackbody
1	32.02	**33.51**	0.49	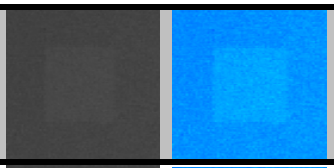
2	33.07	**34.07**	1	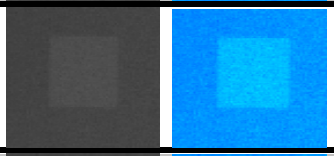
3	33.10	**34.60**	1.5	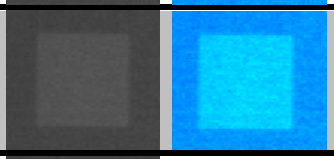
4	33.13	**35.13**	2	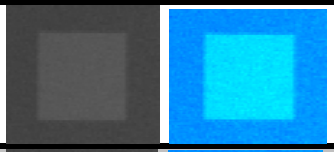
5	33.16	**35.66**	2.5	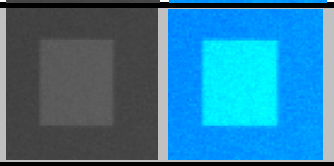
6	33.20	**37.20**	4	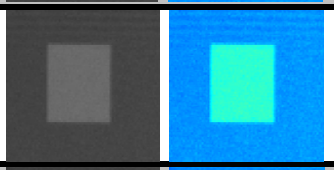
7	33.23	**41.23**	8	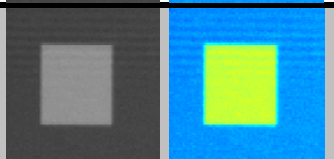
8	33.26	**45.26**	12	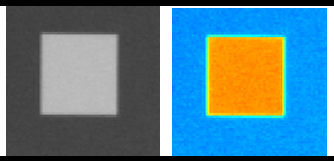
9	33.30	**49.30**	16	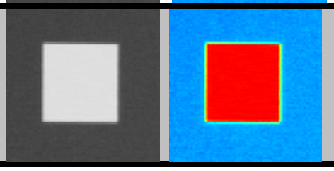

Form images that shown in right of table (4.5) can note the follows:

- ✓ The transformation of thermal (gray) images to thermographic (pseudocolor) was done successfully by replaced the gray levels of thermal image to arbitrary colors.
- ✓ As shown in right of table (4.5) the visibility of IR images ware improved after transformation the thermal images to thermographic because the human eye is better at distinguishing between different shades of color than between gray scale color.
- ✓ These pseudocolor mappings are used frequently to make small changes in gray level visible to human eye to highlight important gray-scale regions.
- ✓ The flash/pseudo colors that appears in thermographic images [see right of table (4.5)] are representation for or indictor to amount of object (blackbody) temperature and difference between object and background. As noted at lower temperature of blackbody the thermographic image appears as blue color image, the color and degree of it changes with increasing of temperature until even access to the red color at higher temperature of blackbody.
- ✓ This software program [see appendix C] is implemented on PC (PC software), this makes the camera works either thermal or thermographic camera depending on the desired application as additional degree of freedom in the area of their applications of this camera.

In general the addition of this program to thermal camera (gray images) leads to an improve image quality and to enhancement the subjective perception of details in scene (in our case the details is amount of temperature), and then creates thermographic camera.

4.4.2 Reading of Temperature From Thermographic Image

Based on intensity of gray image (RGB value) of thermal image at fixed point in all images [specific coordinate (x, y)] as fixed criteria in the thermal images of blackbody at different temperature that shown in table (4.6), and by plotting the intensity vs. temperature in MATLAB the third degree equation to measure the amount of temperature of blackbody was found (see equation (4.1)).

Table (4.6): Blackbody temperatures and corresponding images intensity

Blackbody Temperature/°C	Image Intensity
24.09	0.3922
24.84	0.4000
26.07	0.4078
27.08	0.4196
28.07	0.4275
29.04	0.4353
30.03	0.4431
31.01	0.4510
31.92	0.4627
32.92	0.4706
33.93	0.4784
34.93	0.4902
35.93	0.4980
36.94	0.5098
37.94	0.5137
38.95	0.5255
39.95	0.5373
40.96	0.5412
41.96	0.5529
42.96	0.5608
43.98	0.5725
45.00	0.5804
45.99	0.5922

Drawing of table (4.6) values as curve and fitting of this curve on MATLAB software is shown in figure (4.15).

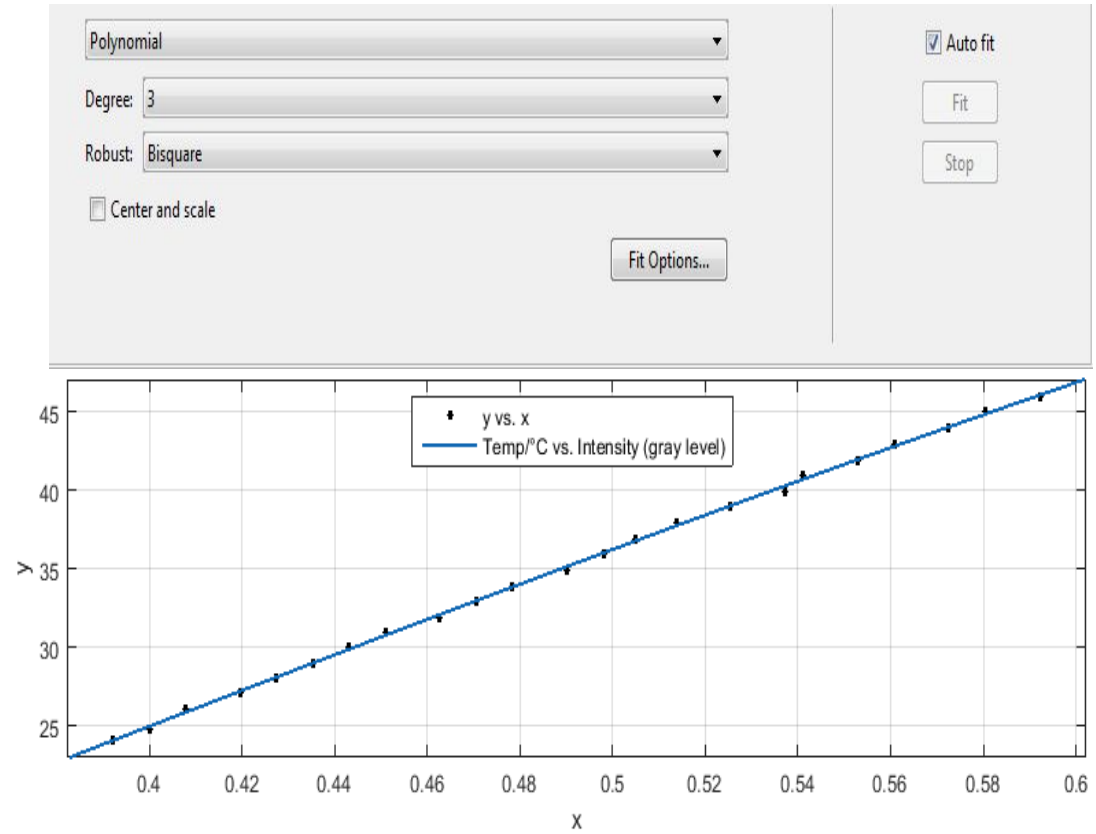

Figure (4.15): Curve fitting of blackbody Temperature Vs Image Intensity (gray level)

The polynomial of third-degree (poly3) linear equation (4.1) was generated from curve which is shown in figure (4.15) for the purpose of finding the temperature of blackbody from its thermal image

$$\text{Temp}(A) = P_1 \times A^3 + P_2 \times A^2 + P_3 \times A + P_4 \qquad (4.1)$$

Where:

A is intensity (gray level) of double class thermal image, and the coefficients:

$$P_1 = -63.95,\ P_2 = 64.03,\ P_3 = 94.14, \text{ and } P_4 = -20.55.$$

The equation (4.1) can be used to fined the temperature of any object (other than a blackbody) just by multiplying the emissivity value (ε) [see appendix B] of this object in same equation

$$\text{Temp}(A) = \varepsilon\,(P_1 \times A^3 + P_2 \times A^2 + P_3 \times A + P_4) \qquad (4.2)$$

The equation (4.2) for its generality is the formula that used in software by knowing the emissivity of the object under test.

Table (4.7) shows the known in advance blackbody temperatures together with temperatures that have been calculated by software in order to check the software efficiency.

Table (4.7): Readings of blackbody temperatures

Blackbody Temp/°C from test station	Blackbody Temp/°C from software
30.88	31.27
31.89	32.14
32.90	33.02
33.91	34.32
34.92	35.18
35.93	36.04
36.94	37.32
37.96	38.17
38.97	39.01
39.98	40.27
41.00	41.10
42.02	42.34

Table (4.8) shows the temperatures of several persons taken by FLUCK temperature meter (FLUCK meter Temp) and corresponding temperature to each case that been calculated from its thermal image by the software.

In this case the object is human (gray body) and non-blackbody that means the emissivity of human skin 0.98 will be taken into accounts instead emissivity of blackbody.

Table (4.8): Readings of several people's temperatures

Person No	FLUCK meter Temp/°C	Software Temp/°C
1	28.60	28.91
2	27.50	27.41
3	36.40	36.57
4	28.20	28.32
5	36.40	36.57
6	37.40	37.63
7	32.20	32.36

- ✓ Principle of reading the objects temperature from its thermal images been successfully.
- ✓ The temperatures that have been read from thermal images and shown in tables (4.7) and (4.8) for the blackbody and several persons respectively are acceptable readings and compatible with the applications of this type of camera.
- ✓ The small differences (fraction) in the readings in both tables maybe as follows:
    - The meters of temperatures (FLUCK and blackbody meters) not accurate and need some calibration.
    - In both cases have been used only theoretical values for emissivity i.e. 1 and 0.98 for blackbody and human skin, and as we know the emissivity is vary with/depending on characteristics of surfaces and temperature of it.

4.5 Conclusion

- ☑ The IR optical system which works in LWIR (8~12µm) and is characterized by high performance, simplicity of structure, and light weight was designed. And then manufactured at a reasonable cost.

- ☑ Efficient and simple uncooled thermal camera was obtained from compatibility between IR113 thermal detector module and IR optical system which was designed.

- ☑ MATLAB PC thermal image processing software was created. Add this software to the created thermal camera and converted it to uncooled thermographic camera done successfully.

- ☑ Implementation of thermal image processing software at computer (PC software) makes this camera works either thermal or thermographic camera depending on desired application as additional degree of freedom in the area of their applications of this camera. This represents an additional degree of freedom in the area of camera applications.

- ☑ This design suitable for thermal imaging system in many civilian and paramilitary applications.

4.6 Future Work

- ⊙ The improvement in thermal image processing software is an extended work, and depends on availability of: real or exact values of emissivity for objects under test, and high accurate temperature meters suitable for work as references for calibration. In addition to the establishment special and distinct colormap instead of jet colormap, (jet is one of MATLAB predefined colormaps).

- ⊙ Modify the IR optical system to working in two windows (LWIR 8~12µm and MWIR 3~5µm) together leads to Enhancement of camera performance. Achievement of this step linked to the availability of a special and distinct thermal detector and works in the two windows at same time (dual bands detector).

REFERENCES

1- S. P. Garnial. (2005), "*Infrared thermoraphy: A versatile technology for condition monitoring and energy conversation*", National Productivity Council, Kanpur, India.

2- R N SINGH. (2009), "*THERMAL IMAGING TECHNOLOGY design and applications*", Universities Press (India) Private Limited, Hyderabad.

3- RICHARD D. HUDSON, JR. (September 1969), "*Infrared system engineering*", WILEY-INTERSCIENCE, John Wiley& Sons, Inc.

4- Jamieson J.A., McFee R. H., Plass G. N., Gurb R. H., and Richards R. G. (1963), "*Infrared physics and enginerring*", McGraw Hill.

5- Wolf W. L., (ed.). (1965), "*Military Infrared Handbook*", Superintendent of documents, U.S. Govt. Printing office.

6- Holter M.R. et.al (1962), "*Fundamental of Infrared Technology*", Macmillan.

7- Miroshinkov M.M. (1992), "*Sov. J. Opt. Technology*".

8- Gerald C. Holst. (2000), "*COMMON APPROACH TO THERMAL IMAGING*", SPIE Optical Engineering Press, Washington USA.

9- Robert E. Fischer, Biljana Tadic-Galeb& Paul R. Yoder. (2008), "*Optical System Design*", 2nd Ed, McGraw-Hill Companies, Inc, New Yourk.

10- FLIR systems and Infrared Training Center (ITC). (2011), "*THERMAL IMAGING GUIDEBOOK FOR INDUSTRIAL APPLICATIONS an informative guide for the use of thermal imaging cameras in industrial applications*", FLIR systems AB.

11- Arnold Daniels. (2007), "*Field Guide to Infrared systems*", SPIE Field Guides Volume FG09, SPIE PRESS- the international society for optical engineering P.O Box 10, Bellingham, Washington, USA.

12- Ronald G. Diggers, Paul Cox, Timothy Edwaerd. (1999), "*Introduction to Infrared and Electro-Optical systems*", Artech House, INC. Boston - London.

13- Ikbal Singh. (2009), "*DESIGN OF INFRARED OPTICAL SYSTEM*", International Conference on Optics and Photonics, India.

14- Max J. Riedl. (1995), "*OPTICAL DESIGN FUNDENMENTALS FOR INFRARED SYSTEMS*", SPIE OPTICAL ENGINREEING PRESS-The international society for optical enginreeing PO Box 10, Bellingham, Washington, USA.

15- Bruce H. Walker. (2008), "*Optical Engineering Fundamentals*", 2nd edition, SPEE PRESS, Bellingham, Washington USA.

16- Daniel Malacara, Zacarias Malacara. (2004), "*Handbook of Optical Design*", 2nd edition, Marcel Dekker, Inc. New York.

17- Warren J. Smith. (2000), "*Modern Optical Engineering the Design of Optical Systems*", 3rd edition, McGraw-Hill Companies, Inc.

18- Allen mann. (2009), "*INFRARED OPTICS AND ZOOM LENSES*", 2nd edition, SPIE PRESS, Bellingham, Washington USA.

19- RUDOLF KINGSLAKE, R. BARRY JOHNSON. (2010), "*Lens Design Fundamentals*", 2nd edition, Elsevier Inc and SPEE PRESS, Bellingham, Washington USA.

20- Michael Bass, Eric W. Van Stryland, David R. Williams, William L. Wolfe. (1995), "*HANDBOOK OF OPTICS volume1 fundamentals, techniques, and design*", McGRAW-HILL, INC.

21- Prepared by: Channel Systems Inc. (July 2009), "*FUNDAMENTALS OF SELECTING A LENS*" Channel Systems.

22- Bob Atkins. (April 2007), "*Modulation transfer function – what is it and why does it matter*", [online] available from: http://photo.net/learn/optics/mtf/. [Accessed 22nd march 2014].

23- Joseph M. Geary. (2002), "*INTRODUCTION TO LENS DESIGN With Practical ZEMAX Examples*", Willmann-Bell, Inc.

24- Warren J. Smith, Genesee Optics Software, Inc. (1992), "*Modern Lens Design A Resource Manual*", McGraw-Hill, Inc.

25- Jay Vizgaitis. (December 14, 2006), "*Selecting Infrared Optical Materials*", University of Arizona, Optics 521.

26- *ZEMAX optical design program, User's Guide*. (June, 2009), ZEMAX Development Corporation.

27- Rafeal C. Gonzalez, Richard E. Woods, Steven L. Eddins. (2004), "*Digital image processing USING MATLAB*", Pearson Education, Inc.

28- Ramin khoei. (2009), "Optical *System Design of a Long Range Dual Field of View Thermal Imaging Camera in 3~5μm Wave Band*", Proc. of SPIE, International Conference on Optical Instruments and Technology: Optical Systems and Modern Optoelectronic Instruments, Vol. 7506 75061M-1, ed. Y. Wang, Y. Sheng and K. Tatsuno.

Appendix A: Uncooled Thermal Imaging Module Specifications

GUIDE

GUIDIR® IR113/118

Uncooled Thermal Imaging Module

IR113/118 is designed for original equipment manufacturer (OEM). It can be easily integrated into infrared systems. IR113/118 produces 384x288 pixels high quality thermal images. Favoring from a lightweight, small size, low power consumption design, it is an ideal choice for customer secondary development and system integration.

Features and Benefits

- Plug-and-play OEM module
- Lightweight and compact
- Low power consumption
- High quality thermal image
- Standard interface for easy integration
- Flexible for customization
- Various lens optional

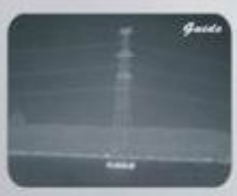

Applications

- *Industrial thermography*
- *Predictive maintenance*
- *Medical diagnosis*
- *Security application*
- *System integration*
- *Research & development*

Specifications

	IR113	IR118
Detector		
Detector Material	UFPA microbolometer, Asi	
Spectral Range	8~14μm	
Pixels	384×288	
Pitch	25μm×25μm	
NETD	<100mk@30℃	
Thermal Response Time	7ms	
Fill Factor	>80%	
Bad Pixel	<1%	
Image Presentation		
Video Output	PAL/NTSC	
Frame Frequency	50Hz /60Hz	
Adjust	Auto/Manual brightness & contrast adjustment	
Electronic Zoom	×2, x4 interpolating	
Polarity	B&W, B&W inverse (pseudo color optional)	B&W, B&W inverse
Video recording	N/A	live video recording on board
Storage media	N/A	2GB SD card, can be extended to 4GB
Storage contents	N/A	images and videos
Interfaces		
Command and Control	RS232/RS422/RS485	
Video Output	RCA/BNC alternative	
USB2.0	transfer digital live video to PC (optional)	transfer saved images & videos to PC
Power System		
Power Supply	110/220VAC adapter	
Power Dissipation	<3.5W	≤3W
Environmental Parameters		
Operating Temperature	-20℃~+50℃(-40℃~+60℃optional)	
Storage Temperature	-40℃~+60℃	
Physical Characteristics		
Weight	0.09kg	0.07kg
Size	47.2mm×42.1mm×44mm	39mm×39mm×44mm

GUIDE

Address: No. 26 Shucheng Rd., Wuhan, P.R.China
Zip Code: 430070
Tel: 027-87671925 / 87671991 / 87671983
Fax: 027-87671927
E-mail: overseas@guide-infrared.com
Website: www.guide-infrared.com

Appendix B: Emissivity

Most radiation sources are not blackbodies. Some of the energy incident upon them may be reflected or transmitted. A factor can be added to them so that they can also be applied to sources that are not blackbodies. This factor called emissivity ϵ, is given by the ratio of the radiant emittance of the source W'_{gb} to the radiant emittance of a blackbody W'_{bb} at same temperature

$$\epsilon = \frac{W'_{gb}}{W'_{bb}}$$

Thus emissivity is a numeric whose value lies between the limits of zero for non-radiating source and unity for a blackbody. It is convenient measure of the degree to which a source approximates a blackbody.

Emissivity is a function of the type of material and its surface finish and it can vary with wavelength and with temperature of material.

Three types of sources can be distinguished by the way that the spectral emissivity varies:

1. A blackbody or Planckian radiator, for which $\epsilon = 1$.
2. A gray body, for which $\epsilon = constant$ (but less than unity)
3. A selective radiator, for which ϵ varies with wavelength [6].

The table below gives values of the emissivity (total normal) of a wide variety of materials

Emissivity (total normal) of various common materials [6]

Material	Temperature (°C)	Emissivity
Metals and their Oxides		
Aluminum:		
Vacuum deposited	100	0.04
Polished sheet	100	0.05
Sheets as received	100	0.09
Anodized sheet, chromic acid process	100	0.55
Brass:		
High polished	100	0.03
Rubbed with 80-grit emery	20	0.2
Oxidized	100	0.61
Copper:		

Polished	100	0.05
Heavily oxidized	20	0.78
Gold: highly polished	100	0.02
Iron:		
Cast, polished	40	0.21
Cast, oxidized	100	0.64
Sheet, heavily rusted	20	0.69
Magnesium: polished	20	0.07
Nickel:		
Electroplated, polished	20	0.05
Electroplated, no polish	20	0.11
Oxidized	200	0.37
Silver: polished	100	0.03
Stainless Steel:		
Type 18-8, buffed	20	0.16
Type 18-8, oxidized at 800ºC	60	0.85
Steel:		
Polished	100	0.07
Oxidized	200	0.79
Tin: commercial tin-plated sheet iron	100	0.07
Other Materials		
Brick: red common	20	0.93
Carbon:		
Candle soot	20	0.95
Graphite, field surface	20	0.98
Concrete	20	0.92
Glass: polished plate	20	0.94
Lacquer:		
White	100	0.92
Matte black	100	0.97
Oil, lubricating (thin film on nickel base):		
Nickel base alone	20	0.05
Film thickness of 0.001, 0.002, 0,005 in.	20	0.27, 0.46, 0.72
Thick coating	20	0.82
Paint, oil: average of 16 colors	100	0.94
Paper: white bond	20	0.93
Plaster: rough coat	20	0.91
Sand	20	0.90
Skin, human	32	0.98
Soil:		
Dray	20	0.92
Saturated with water	20	0.95
Water:		
Distilled	20	0.96
Ice, smooth	-10	0.96
Frost crystal	-10	0.98
Snow	-10	0.85
Wood: planed oak	20	0.90

For metals, emissivity is low, but it increase with temperature and may increase tenfold or more with the formation of an oxide layer on the surface. For nonmetals, emissivity is high, usually more than 0.8, and it decreases with increasing temperature [6].

Appendix C: MATLAB Code who established to the Thermal Image Processing

```
function varargout = MyCamera2(varargin)
% MYCAMERA2 MATLAB code for MyCamera2.fig
%  MYCAMERA2, by itself, creates a new MYCAMERA2 or
% raises the existing singleton*.
% H = MYCAMERA2 returns the handle to a new MYCAMERA2 or
% the handle to the existing singleton*.
%     MYCAMERA2('CALLBACK',hObject,eventData,handles,...)
% calls the local function named CALLBACK in MYCAMERA2.M
% with the given input arguments.
%   MYCAMERA2('Property','Value',...)   creates   a   new
MYCAMERA2 or raises the existing singleton*.
%  Starting  from  the  left,  property  value  pairs  are
% applied  to  the  GUI  before  MyCamera2_OpeningFcn  gets
% called.
% An unrecognized property name or invalid value makes %
% property application stop.
% All inputs are passed to MyCamera2_OpeningFcn via
% varargin.
% *See GUI Options on GUIDE's Tools menu.
%   Choose   "GUI   allows   only   one   instance   to   run
%(singleton)".
% See also: GUIDE, GUIDATA, GUIHANDLES
% Edit  the  above  text  to  modify  the  response  to  help %
MyCamera2
% Last Modified by GUIDE v2.5 30-Sep-2015 13:06:42
% Begin initialization code - DO NOT EDIT
gui_Singleton = 1;
gui_State = struct('gui_Name',       mfilename, ...
                   'gui_Singleton',  gui_Singleton, ...
                   'gui_OpeningFcn',
@MyCamera2_OpeningFcn, ...
                   'gui_OutputFcn',
@MyCamera2_OutputFcn, ...
                   'gui_LayoutFcn',  [] , ...
                   'gui_Callback',   []);
if nargin && ischar(varargin{1})
    gui_State.gui_Callback = str2func(varargin{1});
end
if nargout
    [varargout{1:nargout}] = gui_mainfcn(gui_State,
varargin{:});
else
   gui_mainfcn(gui_State, varargin{:});
end
% End initialization code - DO NOT EDIT
% --- Executes just before MyCamera2 is made visible.
function MyCamera2_OpeningFcn(hObject, eventdata,
handles, varargin)
```

```
% This function has no output args, see OutputFcn.
% hObject    handle to figure
% eventdata  reserved - to be defined in a future
% version of MATLAB
% handles    structure with handles and user data (see
% GUIDATA)
% varargin   command line arguments to MyCamera2 (see
% VARARGIN)
% Create video object
% Putting the object into manual trigger mode and then
% starting the object will make GETSNAPSHOT return
% faster
% since the connection to the camera will already have
% been established.
handles.video = videoinput('winvideo',2,'UYVY_720x576');
triggerconfig(handles.video,'manual');
handles.video.FramesPerTrigger = Inf; % Capture frames
% until we manually stop it
% Choose default command line output for MyCamera2
handles.output = hObject;
% Update handles structure
guidata(hObject, handles);
% UIWAIT makes MyCamera2 wait for user response (see
% UIRESUME)
 uiwait(handles.MyCameraGUI);
% --- Outputs from this function are returned to the
% command line.
function varargout = MyCamera2_OutputFcn(hObject,
eventdata, handles)
% varargout  cell array for returning output args (see
% VARARGOUT);
% hObject    handle to figure
% eventdata  reserved - to be defined in a future
% version of MATLAB
% handles    structure with handles and user data (see
% GUIDATA)
handles.output = hObject;
% Get default command line output from handles structure
varargout{1} = handles.output;
% --- Executes when user attempts to close MyCameraGUI.
function MyCameraGUI_CloseRequestFcn(hObject, eventdata,
handles)
% hObject    handle to MyCameraGUI (see GCBO)
% eventdata  reserved - to be defined in a future
% version of MATLAB
% handles    structure with handles and user data (see
% GUIDATA)
% Hint: delete(hObject) closes the figure
delete(hObject);
%delete(hObject);
delete(imaqfind);
```

```
% --- Executes on button press in startStopCamera.
function startStopCamera_Callback(hObject, eventdata,
handles)
global x_x y_y
% hObject    handle to startStopCamera (see GCBO)
% eventdata  reserved - to be defined in a future
% version of MATLAB
% handles    structure with handles and user data (see
% GUIDATA)
% Start/Stop Camera
if strcmp(get(handles.startStopCamera,'String'),'Start
Camera')
 % Camera is off. Change button string and start camera.
  set(handles.startStopCamera,'String','Stop Camera')
  start(handles.video)

while(strcmp(get(handles.startStopCamera,'String'),'Stop
Camera'))
 frame=(getsnapshot(handles.video));% index image
 I0=(rgb2gray( frame));
 I=im2double(I0);
 I2 = ind2rgb(I0, jet(255));
if((y_y>=1)&&(x_x>=1)&&(y_y<=576)&&(x_x<=720))
A=I(y_y,x_x);% intensity image
       p1 =      -63.95  ;
       p2 =       64.03  ;
       p3 =       94.14  ;
       p4 =      -20.55  ;
temp =  p1*A^3 + p2*A^2 + p3*A + p4;%water emissivity
% =0.95, human skin = 0.98 and BB emissivity = 1
temp=round(temp*100)/100;
 A=round(A*100)/100;
 set(handles.editTemp, 'string', [num2str(temp)]); %
update text for x temp
 set(handles.editInt, 'string', [num2str(A)]); % update
text for y loc
% else
% set(handles.editTemp, 'string', [num2str(0)]);
% update text for x temp
% set(handles.editInt, 'string', [num2str(0)]);
% update text for y loc
    end
% axes(handles.Video_axes1)
% figure(2),
% stop(handles.video)
% [x0 y0]=ginput(1)
% F=frame(x0,y0)
imshow(I0)
   drawnow
 set(handles.startAcquisition,'Enable','on');
 set(handles.captureImage,'Enable','on');
```

```
      end
else
% Camera is on. Stop camera and change button string.
   set(handles.startStopCamera,'String','Start Camera')
   stop(handles.video)
   set(handles.startAcquisition,'Enable','off');
   set(handles.captureImage,'Enable','off');
end

% --- Executes on button press in captureImage.
function captureImage_Callback(hObject, eventdata,
handles)
global x_x y_y
% hObject    handle to captureImage (see GCBO)
% eventdata  reserved - to be defined in a future
% version of MATLAB
% handles    structure with handles and user data (see
% GUIDATA)
%R=imread('2.bmp');%get(get(handles.cameraAxes,'children
% '),'cdata'); % The current displayed frame
% fprintf('capture\n')
% if(y_y>=1)&&(x_x>=1)&&(y_y<=576)&&(x_x<=768)
 frame =
get(get(handles.cameraAxes,'children'),'cdata'); % The
% current displayed frame
 imwrite(frame,'E:\images\x1.bmp','bmp');
% --- Executes on button press in startAcquisition.
function startAcquisition_Callback(hObject, eventdata,
handles)
% hObject    handle to startAcquisition (see GCBO)
% eventdata  reserved - to be defined in a future
% version of MATLAB
% handles    structure with handles and user data (see
% GUIDATA)
% Start/Stop acquisition
if strcmp(get(handles.startAcquisition,'String'),'Start
Acquisition')
% Camera is not acquiring. Change button string and
% start acquisition.
set(handles.startAcquisition,'String','Stop
Acquisition');
trigger(handles.video);
else
% Camera is acquiring. Stop acquisition, save video
% data,
% and change button string.
stop(handles.video);
disp('Saving captured video...');
videodata = getdata(handles.video)save('testvideo.mat',
'videodata');
disp('Video saved to file ''testvideo.mat''');
```

```
start(handles.video); % Restart the camera
set(handles.startAcquisition,'String','Start
Acquisition');
end
function editTemp_Callback(hObject, eventdata, handles)
% hObject    handle to editTemp (see GCBO)
% eventdata  reserved - to be defined in a future
% version of MATLAB
% handles    structure with handles and user data (see
% GUIDATA)
% Hints: get(hObject,'String') returns contents of
% editTemp as text
% str2double(get(hObject,'String')) returns contents of
% editTemp as a double
% --- Executes during object creation, after setting all
% properties.
function editTemp_CreateFcn(hObject, eventdata, handles)
% hObject    handle to editTemp (see GCBO)
% eventdata  reserved - to be defined in a future
% version of MATLAB
% handles    empty - handles not created until after all
% CreateFcns called
% Hint: edit controls usually have a white background on
% Windows.
% See ISPC and COMPUTER.
if ispc && isequal(get(hObject,'BackgroundColor'),
get(0,'defaultUicontrolBackgroundColor'))
set(hObject,'BackgroundColor','white');
end
function editInt_Callback(hObject, eventdata, handles)
% hObject    handle to editInt (see GCBO)
% eventdata  reserved - to be defined in a future
% version of MATLAB
% handles    structure with handles and user data (see
% GUIDATA)
% Hints: get(hObject,'String') returns contents of
% editInt as text
% str2double(get(hObject,'String')) returns contents of
% editInt as a double
% --- Executes during object creation, after setting all
% properties.
function editInt_CreateFcn(hObject, eventdata, handles)
% hObject    handle to editInt (see GCBO)
% eventdata  reserved - to be defined in a future
% version of MATLAB
% handles    empty - handles not created until after all
% CreateFcns called
% Hint: edit controls usually have a white background on
% Windows.
% See ISPC and COMPUTER.
```

```
if ispc && isequal(get(hObject,'BackgroundColor'),
get(0,'defaultUicontrolBackgroundColor'))
set(hObject,'BackgroundColor','white');
end
% --- Executes on mouse motion over figure - except
% title and menu.
function MyCameraGUI_WindowButtonMotionFcn(hObject,
eventdata, handles)
global I y_y x_x x y
% hObject    handle to MyCameraGUI (see GCBO)
% eventdata  reserved - to be defined in a future
% version of MATLAB
% handles    structure with handles and user data (see
% GUIDATA)
 pos = get(hObject, 'currentpoint'); % get mouse
% location on figure
 x = pos(1); y = pos(2); % assign locations to x and y
 a=633-y;
y_y=(a+1);
 x_x=x-50;
% --- Executes on mouse press over axes background.
function cameraAxes_ButtonDownFcn(hObject, eventdata,
handles)
% hObject    handle to cameraAxes (see GCBO)
% eventdata  reserved - to be defined in a future
% version of MATLAB
% handles    structure with handles and user data (see
% GUIDATA)
if handles.first_select
handles.x = [handles.x mouse_pos_axes(1,1)];
handles.y = [handles.y mouse_pos_axes(1,2)];
  else
handles.x = mouse_pos_axes(1,1);
handles.y = mouse_pos_axes(1,2);
handles.first_select = 1;
 end
% --- Executes during object creation, after setting all
% properties.
function cameraAxes_CreateFcn(hObject, eventdata,
handles)
% hObject    handle to cameraAxes (see GCBO)
% eventdata  reserved - to be defined in a future
% version of MATLAB
% handles    empty - handles not created until after all
% CreateFcns called
% Hint: place code in OpeningFcn to populate cameraAxes
```